Sensing properties of MtrB-MtrA of *Corynebacterium glutamicum*: a two-component system involved in the osmo- and chill stress response

Inaugural-Dissertation

zur

Erlangung des Doktorgrades

der Mathematisch-Naturwissenschaftlichen Fakultät

der Universität zu Köln

vorgelegt von

Nina Möker

aus Berlin

Köln, Mai 2006

Berichterstatter:

Prof. Dr. Reinhard Krämer
Prof. Dr. Karin Schnetz

Tag der Disputation: 30.06.2006

Seltsam?

Aber so steht es geschrieben...

Sensing properties of MtrB-MtrA of *Corynebacterium glutamicum*: a two-component system involved in the osmo- and chill stress response

Being an immobile Gram-positive soil bacterium, *Corynebacterium glutamicum* has to cope with dramatic changes of environmental conditions like an altered osmolarity or temperature. It was recently shown that the MtrB-MtrA two-component system of this bacterium mediates the expression regulation of osmo- and chill stress-related genes in response to increased medium osmolarity or decreased environmental temperature. The response regulator of this system, MtrA, was shown to act as an activator of the genes *proP*, *betP*, and *lcoP* as well as a repressor of the *mscL* gene. These results led to the question, which physico-chemical stimuli are recognized by MtrB, in order to mediate the expression regulation of genes in response to changes of the environmental osmolarity and temperature.

To avoid the high complexity of the cellular system, an *in vitro* system was established for the detailed analyses of the sensory properties of MtrB. Using *E. coli* liposomes enriched with MtrB, the basic characteristics of the bacterial two-component system could be detected. These include the autokinase activity of membrane-bound MtrB, the phosphoryl group transfer to soluble MtrA, and the MtrB-catalyzed dephosphorylation of MtrA-P.

By use of the artificial membrane system the influence of a systematic variation of signals related to osmo- and chill stress conditions could be performed. The autokinase activity of MtrB turned out to be stimulated by the presence of numerous osmolytes including sugars, amino acids, compatible solutes, and high molecular weight PEGs. In addition, the histidine kinase was shown to be strongly activated by exposure to low temperature. By fusion of proteoliposomes made from *E. coli* lipid with synthetic POPG, the sensory properties of MtrB furthermore turned out to significantly depend on the composition of the membrane surrounding.

In order to identify the sensing domain of MtrB, various truncated derivatives of the protein were constructed. In contrast to most bacterial histidine kinases, which are thought to carry their sensory function within the extracytoplasmic loop, MtrB was shown to sense independently of this external domain.

Taken together, the data of this work led to the model that MtrB senses environmental hyperosmotic stress either as an increased osmolarity of the cytoplasm, or as altered membrane properties. Environmental chill conditions are suggested to be sensed as an altered physical state of the membrane.

Sensorische Eigenschaften von MtrB-MtrA von *Corynebacterium glutamicum*: Vermittlung der Osmo- und Kältestress-Antwort durch ein Zwei-Komponenten System

Corynebacterium glutamicum ist als immobiles, Gram-positives Bodenbakterium Stress-Situationen durch plötzliche Änderungen seines Habitats, wie zum Beispiel Schwankungen in der externen Osmolarität und Temperatur, ausgesetzt. Es konnte kürzlich gezeigt werden, dass das Zwei-Komponenten System MtrB-MtrA als Reaktion auf erhöhte Osmolarität im Nährmedium, sowie auf erniedrigte Umgebungstemperatur, die Expressionsregulation von Genen vermittelt, die eine wichtige Rolle in der Osmo- und Kältestress-Antwort von *C. glutamicum* spielen. Dabei agiert der Antwort-Regulator MtrA sowohl als Aktivator der Gene *proP*, *betP* und *locP*, als auch als Repressor des *mscL*-Gens. Dies führte zu der Frage, welche physico-chemischen Reize als Indikatoren für eine veränderte Osmolarität bzw. Temperatur der Umgebung von MtrB genutzt werden, um als Reaktion die Expressionsregulation spezifischer Gene zu vermitteln. Um die Reizwahrnehmung detailliert zu untersuchen, wurde ein *in vitro* System aufgebaut. In diesen, mit MtrB angereicherten, *E. coli*-Liposomen konnten die Basiseigenschaften von Zwei-Komponenten Systemen *in vitro* imitiert werden. Dies beinhaltete die Autokinase-Aktivität von Membran-gebundenem MtrB, den Transfer der Phosphoryl-Gruppe auf den gereinigten Antwort-Regulator MtrA, sowie die von MtrB katalysierte Dephosphorylierung von MtrA-P.

Mit dem Proteoliposomen-System konnte die Auswirkung vielfältiger, bei osmotischem und Kälte-Stress auftretender Signale analysiert werden. Die Autokinase-Aktivität von MtrB wurde durch die Anwesenheit zahlreicher Osmolyte wie Zucker, Aminosäuren, kompatible Solute und hochmolekulare PEGs deutlich stimuliert. Darüber hinaus konnte eine deutliche Aktivierung von MtrB durch erniedrigte Temperaturen gezeigt werden. Fusion von Proteoliposomen, die aus *E. coli*-Lipid bestanden, mit synthetischem POPG ergab ferner, dass die Sensoreigenschaften von MtrB von der Membranzusammensetzung deutlich beeinflusst werden.

Des weiteren konnte mit Hilfe von verkürzten Varianten dieses Proteins die periplasmatische Schleife, welche häufig bei den bakteriellen Sensor-Kinasen die Signal-Wahrnehmung vermittelt, als sensorische Domäne für MtrB ausgeschlossen werden.

Zusammengefasst führen diese Daten zu dem Modell, dass MtrB hyperosmotischen externen Stress entweder als erhöhte Osmolarität des Cytoplasmas, oder als veränderte Membraneigenschaft wahrnimmt. Die Wahrnehmung von Kälte wird vermutlich durch die unter diesen Bedingungen veränderte Membranphase vermittelt.

Contents

Contents

Contents

Contents

Abbreviations

AHT	Anhydrotetracycline
Ap^R	Resistance towards ampicilin
ADP	Adenosine diphosphate
ATP	Adenosine triphosphate
BHI	Brain heart infusion
bp	Base pairs
BSA	Bovine serum albumin
C	Carbon
CSPD	Disodium 3-(4-metho xyspiro {1,2-dioxetane-3,2-(5-chloro)triciclo [3.3.1.13,7]decan}-4-yl)phenyl phosphat
DIG	Digoxigenin
DTT	Dithiothreitol
EDTA	Ethylendiaminetetraacetic acid
et al.	*et alii* ("and others")
g	Gravitational acceleration (9.81 m^2/s)
IPTG	Isopropyl-1-thio-β-D-galactosid
kb	kilo base pairs
kDa	kilo Dalton
K_m	Michaelis-Menten constant
Km^R	Resistance towards kanamycin
KP_i	Potassium phosphate buffer
LB	Luria-Bertani
MM	Minimal medium
MOPS	3-[N-morpholino]propansufonic acid
OD_{600}	Optical density at 600 nm
orf	Open reading frame
PAGE	Polyacrylamide gel electrophoresis
PCR	Polymerase chain reaction
PVDF	Polyvinylidine difluoride
RT	Poom temperature
RT-PCR	Reverse transcription polymerase chain reaction
SDS	Sodium dodecylsulphate
TAE	Tris-Acetate-EDTA
TCA	Trichloroacetic acid
TE	Tris-EDTA
TEMED	N,N,N',N'-tetramethyl-ethylendiamine
Tris	2-amino-hydroxymethylpropane-1,3-diol

1.   Introduction

Living cells, including pro- and eukaryotes, have to cope with stress situations caused by changes of environmental conditions. These include, in addition to variation of the pH, nitrogen limitation, nutrient deprivation, phosphate limitation, and others, changes of the external osmolarity and temperature. Microorganisms have developed various strategies to rapidly adapt to environmental challenges, which is the prerequisite for colonization of different habitats. The cellular response to external stress requires (I) sensing of environmental changes and (II) signal transduction resulting in the regulation of gene expression as well as the activity regulation of specific proteins.

1.1   *Corynebacterium glutamicum*

Corynebacterium glutamicum is an immobile Gram-positive bacterium which inhabits the surface layers of the soil. It was first described 1957 as glutamate-producing strain *Micrococcus glutamicus* (Kinoshita *et al*., 1957). *C. glutamicum* is an aerobic and non-sporulating bacterium belonging to the irregularly shaped rods (Fig. 1) referred to as coryneform bacteria. Having a complex mycolic acid-containing cell wall and high G+C-content of the DNA, *C. glutamicum*, like the mycobacteria, belongs to the suborder *Corynebacterineae* of the mycolic acid-containing actinomycetes. This species is of increasing interest as a non-pathogenic model organism to investigate specific topics that are common to its pathogenic relatives *C. diphtheriae*, *Mycobacterium tuberculosis*, and *M. leprae*. Many of the genes present in the completely sequenced *C. glutamicum* genome (3.3 Mb, Ikeda and Nakagawa, 2003; Kalinowski *et al*., 2003) are highly conserved within the *Corynebacterineae* species. In addition, *C. glutamicum* gained high biotechnological relevance as large-scale industrial producer of amino acids. Mainly L-glutamate (1,500,000 tons per year), and L-lysine (550,000 tons per year), as well as smaller amounts of tryptophan, glutamine, alanine, isoleucine, nucleotides, and vitamins are produced by the use of different *C. glutamicum* strains (Leuchtenberger, 1996; Hermann, 2003).

Fig. 1: Scanning electron micrograph of *C. glutamicum* WT (Möker, 2002).

1.2   Osmotic stress

Microorganisms are constantly exposed to environmental challenges. Especially bacteria of the upper soil layers, like *C. glutamicum* or *Bacillus subtilis*, must cope with dramatic changes of the osmolarity in their habitat. These can occur for example after rain or periods of sunshine, resulting in either hypo-, or hyperosmotic stress, respectively (Wood, 1999). Such conditions would cause an increase (hypoosmotic stress) or a decrease (hyperosmotic stress) of the cell turgor and therefore endanger the survival of the bacterium.

In living cells, the cytoplasmic membrane serves as selectively permeable barrier separating the interior from the extralumenal space, which allows water to freely diffuse across the phospholipid bilayer, whereas macromolecules and ionic or polar substances cannot pass by diffusion. The water diffusion, or osmosis, occurs from compartments of high to those of low water potential. In bacterial cells, the water potential (Ψ_w) and hence the occurrence of osmosis, is affected by the physical pressure of the cell wall as well as the osmotic pressure derived from solutes; it is defined by the osmotic potential (Ψ_π) and the turgor potential (Ψ_p) as follows:

$$\Psi_w = \Psi_\pi + \Psi_p$$

The osmotic potential Ψ_π of a given solution is in proportion with the concentration of solutes. The elevated concentration of solutes in the microbial cytoplasm generally results in a decreased water potential compared to the surroundings. Consequently, water influx occurs causing a hydrostatic pressure on the cell wall, which increases until an equilibrium with the physical pressure exerted from the cell wall on the cytoplasmic fluid is reached. This hydrostatic pressure, the so-called cell turgor, is exerted from the cytoplasmic membrane on the cell wall and averages in Gram-negative bacteria 3 to 5 atm (Csonka and Epstein, 1996), whereas up to 20 atm are reached in Gram-positive bacteria (Whatmore and Reed, 1990). For bacterial and plant cells it is highly important to keep the cell volume and the turgor pressure at a constant level. If the turgor pressure is increased, the cell may burst, whereas a decreased turgor pressure can negatively affect cell metabolism and -division (Kempf and Bremer, 1998). The osmotic pressure Π of a solution is defined as follows

$$\Pi = - (RT / V_w) \ln a_w$$

R = Gas constant, T = Absolute Temperature, a_w = water activity, V_w = partial molar volume of water

and can be described by the term osmolarity. This indicates the sum of the concentrations of all osmotically active particles (c_i) of a solution:

$$\text{osmolarity} = \Sigma\ c_i \approx \Pi\ /\ RT$$

Since the osmolarity of a solution cannot be determined experimentally, the osmotic pressure is described by the osmolality of a solution, i.e. by the concentration of osmotically active particles in relation to one kilogram of solvent (osm/kg).

$$\text{osmolality} = \Pi\ /\ RT$$

1.2.1 Osmoregulation in response to hypoosmotic environmental conditions

If the osmolarity of the environment is suddenly decreased, a microbial cell is exposed to hypoosmotic stress, and the altered gradient between the internal osmolarity of the cytoplasm and the surrounding results in an influx of water. As a consequence, cell turgor is dramatically increased (Booth and Louis, 1999), the cell swells and is faced with rupture. Most prokaryotes respond to such live-threatening conditions via the rapid release of small osmotically active compounds, like ions, amino acids, or compatible solutes. This fast efflux of cytoplasmic compounds is mediated by mechanosensitive channels (Berrier *et al*., 1992; Sukharev *et al*., 1997), which could be shown to be present in pro- as well as eukaryotic cells (Morris, 1990). In the Gram-negative bacterium *Escherichia coli*, Berrier *et al.* (1996) could identify various mechanosensitive channels which were, concerning their conductance, divided into three groups: MscM, MscS and MscL (**m**echano**s**ensitive **c**hannel of **m**ini, **s**mall, and **l**arge conductance). These are located in the cytoplasmic membrane and were shown to be consecutively activated with an increased membrane strain (Berrier *et al*., 1996), thus allowing the graded response to osmotic downshifts. In *C. glutamicum* two mechanosensitive channels could be identified at biochemical and molecular level, which show similar conductances as the *E. coli* MscL and MscS pores (Ruffert *et al*., 1999; Nottebrock *et al*., 2003). However, the analyses of an *mscS* and *mscL* deficient mutant pointed on the presence of at least one more efflux system, which seems to be as efficient as the MscS and MscL pores (Nottebrock *et al.*, 2003).

1.2.2 Osmoregulation in response to hyperosmotic environmental conditions

In case of hyperosmotic stress, the internal osmolarity of a bacterial cell is lowered compared to the outside. Therefore, water efflux occurs, which results in a loss of turgor; the cell dehydrates and is endangered by plasmolysis. As consequence of the loss of water, cell metabolism and -division is negatively affected (Wood, 1999). To prevent these deleterious effects, microorganisms developed different strategies, which allow adaptation to

hyperosmotic conditions (Galinski and Trüper, 1994; Csonka and Epstein, 1996; Miller and Wood, 1996). One possibility, the co-called salt-in strategy, is used by halophilic archaea and halotolerant bacteria (Galinski and Trüper, 1994). These organisms colonize saline environments and respond to external osmotic upshifts with the internal accumulation of salts as KCl and NaCl to high concentrations (in molar range). Bacteria known to accept only less saline habitats, like *E. coli, C. glutamicum* or *B. subtilis*, make use of the salt-out strategy. These species prevent high intracellular salt concentrations and accumulate organic substances instead, which do not negatively affect cellular metabolism processes, even in case of high (molar) internal concentrations (Galinski and Trüper, 1994; Wood, 1999). These compounds are referred to as compatible solutes and include sugars (trehalose and succrose), polyols (glycerol and glucosylglycerol), amino acids (proline, glutamate, and glutamine), amino acid derivatives (ectoine and taurine), and other zwitterionic substances (glycine betaine and proline betaine). Among bacteria, glycine betaine, ectoine, proline, and trehalose (Fig. 2) have been described to be the most commonly used compatible solutes (Bremer and Krämer, 2000). The intracellular accumulation of these compounds has, next to re-hydration of the cytoplasm, a stabilizing effect on the native conformation of proteins (Yancey, 1994). Compatible solutes were also shown to provide protection of microorganisms and plants against different environmental challenges, for example heat- (Fletcher and Csonka, 1995; Malin and Lapidot, 1996; Caldas *et al*., 1999; Canovas *et al.,* 2001; Diamant *et al.,* 2001) and cold stress (Ko *et al*., 1994; Deshnium *et al*., 1997; Rajashekar *et al.,* 1999; Bayles and Wilkinson 2000; Xing and Rajashekar, 2001).

Compatible solutes can be internally accumulated in two ways. If present in the environment, the uptake of these substances is favored due to lower energy cost of the cell, however, they can also be gathered independently of the their external availability via *de novo* synthesis.
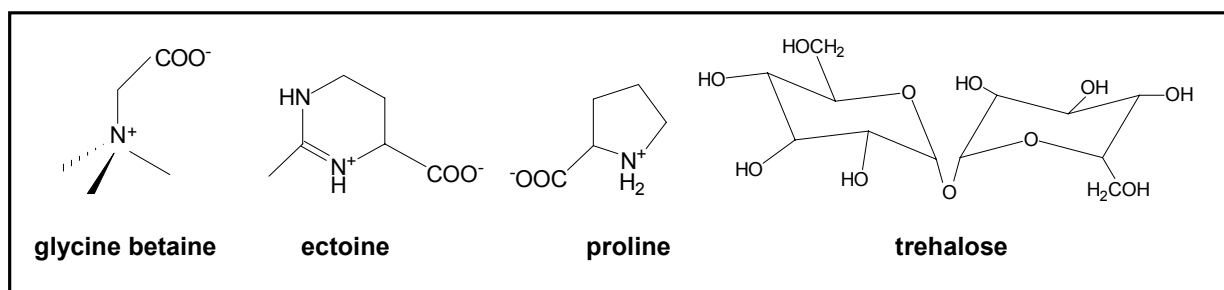
Fig. 2: Commonly used compatible solutes in bacteria.

In response to hyperosmotic environmental conditions, *C. glutamicum* accumulates glutamate, serving as counter-ion for potassium, as well as the compatible solutes proline, trehalose, and glutamine, which can be provided by *de novo* synthesis (Rönsch *et al.*, 2003, Wolf *et al.*, 2003). If sufficient amounts of osmoprotectants are available in the surrounding, the uptake of glycine betaine, ectoine, and proline into the cytoplasm is favored (Rönsch *et al.*, 2003). Uptake of compatible solutes in *C. glutamicum* is mediated by five carrier systems, of which four were shown to be osmotically regulated in their activity (Peter *et al.*, 1996; Peter *et al.*, 1998; Steger *et al.*, 2003). The secondary transport systems BetP, EctP, LcoP, and ProP (Fig. 3) catalyze the symport of the above-mentioned compounds with Na$^+$-ions or protons, each exhibiting different substrate specificities and -affinities (compare Fig. 3), thereby allowing an effective adaptation to osmotic changes of the environment. These carriers are regulated at the level of activity, i.e. the transport rate is adapted to the extend of hypertonicity (Peter *et al.*, 1996; Peter *et al.*, 1997; Steger *et al.*, 2003). Recently, a regulation at the level of expression was shown as well; transcription of the genes *proP*, *betP*, *ectP* and *lcoP* was found to be induced after an osmotic upshift (Möker, *et al.*, 2004).
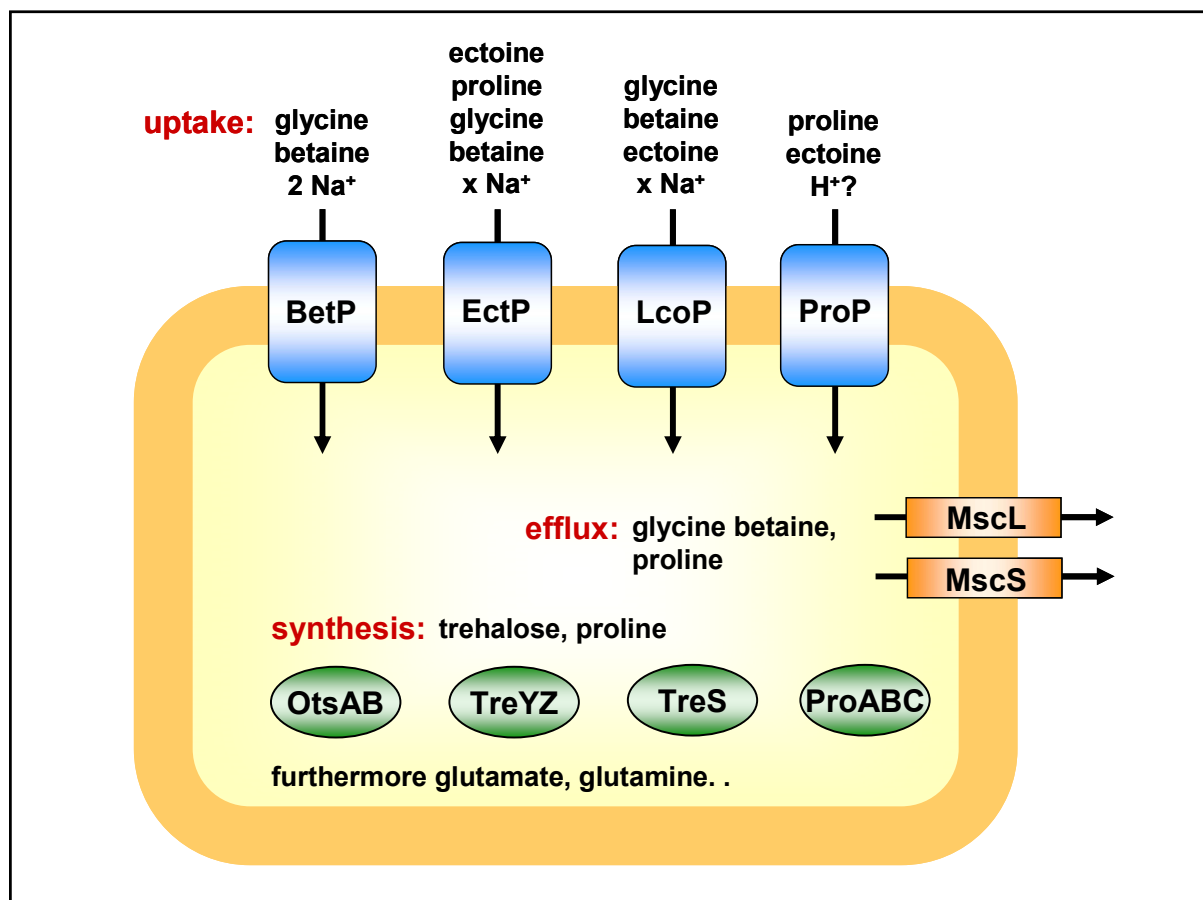
Fig. 3: Important osmoregulation systems of *C. glutamicum*.

De novo synthesis of proline in *C. glutamicum* starts with glutamate as substrate and is catalyzed by the enzymes γ-glutamate-kinase, 4-glutamyl-phosphate-reductase, and pyrroline carboxylate-reductase, which are encoded by the *proB*, *proA* and *proC* genes, respectively (Ankri *et al*., 1996). These genes were shown to be transcriptionally activated after an upshift of the medium osmolarity (Ley, 2001), whereas an activity regulation of proline biosynthesis proteins remains unclear.

C. glutamicum employs three different pathways for the biosynthesis of the disaccharide trehalose: the OtsAB-, the TreYZ-, and the TreS-pathway (Wolf *et al*., 2003). This sugar can be produced starting from the substrates glucose-6-phosphate and UDP-glucose (OtsAB-pathway), maltooligodextrine (TreYZ-pathway), as well as maltose (TreS-pathway,). Regarding the TreYZ-pathway, an osmotic regulation at the level of protein activity was observed, however, all three pathways were shown to be osmotically influenced at the level of gene expression (Wolf *et al*., 2003).

1.3   Chill stress

In addition to osmolarity, temperature is an important physical factor influencing cell physiology of microorganisms. Bacteria can be divided into different classes concerning the temperature ranges providing optimal cell growth and -division. Most bacteria, as e. g. *E. coli* and *C. glutamicum*, are referred to as *mesophilic*, meaning that maximum growth rates are reached at moderate temperatures between 20 and 42 °C. A decrease in temperature causes immediate reduction of molecular dynamics resulting in lowered diffusion rates and conformational alterations of molecular structures. Consequently, three major problems arise from exposing a cell to a sudden decrease in temperature. (I) Chill stress has dramatic effects on enzymatic reactions, thus influencing cell physiology in general. (II) Membrane fluidity decreases, which affects many vital membrane and membrane-associated functions, such as transport, cell division, or energy production. (III) Nucleic acid topology changes causing halts in processes such as transcription, translation, or replication. Bacteria make use of at least three different mechanisms to prevent cease of growth and finally cellular death. Some organisms, as e. g. *B. subtilis*, respond to a temperature downshift by the production of specific proteins, so-called cold shock proteins (Neuhaus *et al*., 1999; Derzelle *et al*., 2003). These are low molecular mass proteins, which can be involved in diverse cellular processes allowing the adaptation to low temperatures. The reduced membrane fluidity in case of low temperatures can be prevented by the synthesis and lipid incorporation of fatty acids with lowered melting points. These include branched-chain and unsaturated fatty acids (Aguilar *et al*., 2001; Klein *et al*., 1999; Mansilla *et al*., 2004; Weber *et al*., 2002; Weber *et al*., 2001). One further possibility to adapt to low temperature is the accumulation of

compatible solutes, which was reported for some *mesophilic* organisms, as e. g. *Listeria monocytogenes* (Ko *et al*., 1994).

In *C. glutamicum*, the uptake carriers for compatible solutes BetP, LcoP, and EctP, belonging to the betaine-carnitine-choline transporter (BCCT) family, were shown to be osmotically regulated in their activity. Recently, these were also analyzed for their responses to chill stress at the level of activity (Özcan *et al*., 2005). It could be shown, that LcoP was activated by chill to low extent, whereas BetP was significantly stimulated at low temperature, with maximum glycine betaine uptake activity at 10-15 °C (Özcan *et al*., 2005). In contrast, EctP was not stimulated by chill. RNA hybridization experiments furthermore revealed that all three genes, *betP*, *lcoP*, and *ectP*, were transcriptionally induced in *C. glutamicum* after exposure of cells to low temperature (15 °C, Özcan 2003).

1.4   Bacterial two-component systems

The cellular responses to environmental stimuli, such as nutrient starvation, or temperature and osmolarity-induced stress situations, are commonly regulated by a phosphorelay system, which was found in nearly all bacterial species (Nixon *et al*., 1986) as well as some eukaryotic organisms belonging to yeast, amoeba, fungi, or plants (Ota and Varshavsky, 1993; Maeda *et al*., 1994; Schuster *et al*., 1996; Alex *et* al*.,* 1996; Chang *et al*., 1993), whereas it is missing in metazoic animals. The standard organization of this phosphorelay system is shown in Figure 4 and comprises a membrane-bound dimeric sensor histidine kinase, generally containing one or two membrane-spanning domains, and a cognate, cytoplasmic response regulator. Because of these two essential compounds this regulation system is commonly known as two-component system. However, there are also examples of soluble sensor kinases, like CheA from *E. coli*, which is involved in chemotaxis, or multi-component systems, including those related to chemotaxis, which are composed of more than seven proteins (Egger *et al*., 1997). External stimuli, which are sensed by the histidine kinase, regulate the autokinase activity of this protein (Fig. 4). The sensor catalyses the ATP-dependent *trans*-autophosphorylation, in which one subunit of the dimer phosphorylates a specific, highly conserved histidine residue within the other subunit, resulting in a phosphoimidazole. Subsequently, the phosphoryl group is transferred to a specific, highly conserved aspartate residue within the regulatory domain of the response regulator (Fig. 4). This reaction is catalyzed by the response regulator and results in a conformational change of the protein, thereby causing the activation of its effector domain (Klumpp and Krieglstein, 2002). This domain mediates the specific cellular response, in most cases the regulation of gene expression, in which the response regulator acts as transcription factor (Hakenbeck and Stock, 1996). In addition, this protein class can also exhibit distinct functions, as for example the mediation of chemotaxis (Lupas and Stock*,* 1989). The stability of the

phosphorylated response regulator varies, depending on the system, between few seconds and several hours (Hess *et al*., 1988; Weis and Magasanik, 1988; Igo *et al*., 1989; Makino *et al*., 1989; Wright *et al*, 1993). The signal transduction is turned off by dephosphorylation of the activated response regulator. Dephosphorylation is catalyzed either by a separate bacterial phosphatase (e. g. CheZ in case of CheA/CheY of *E. coli*), a phosphatase activity of the sensor kinase (e. g. EnvZ or KdpD of *E. coli*), or the combined action of the histidine kinase, the response regulator, and an accessory protein (e. g. in case of NtrB/NtrC of *E. coli* (Comeau *et al*., 1985; Ninfa *et al*., 1995; Blat and Eisenbach, 1994).
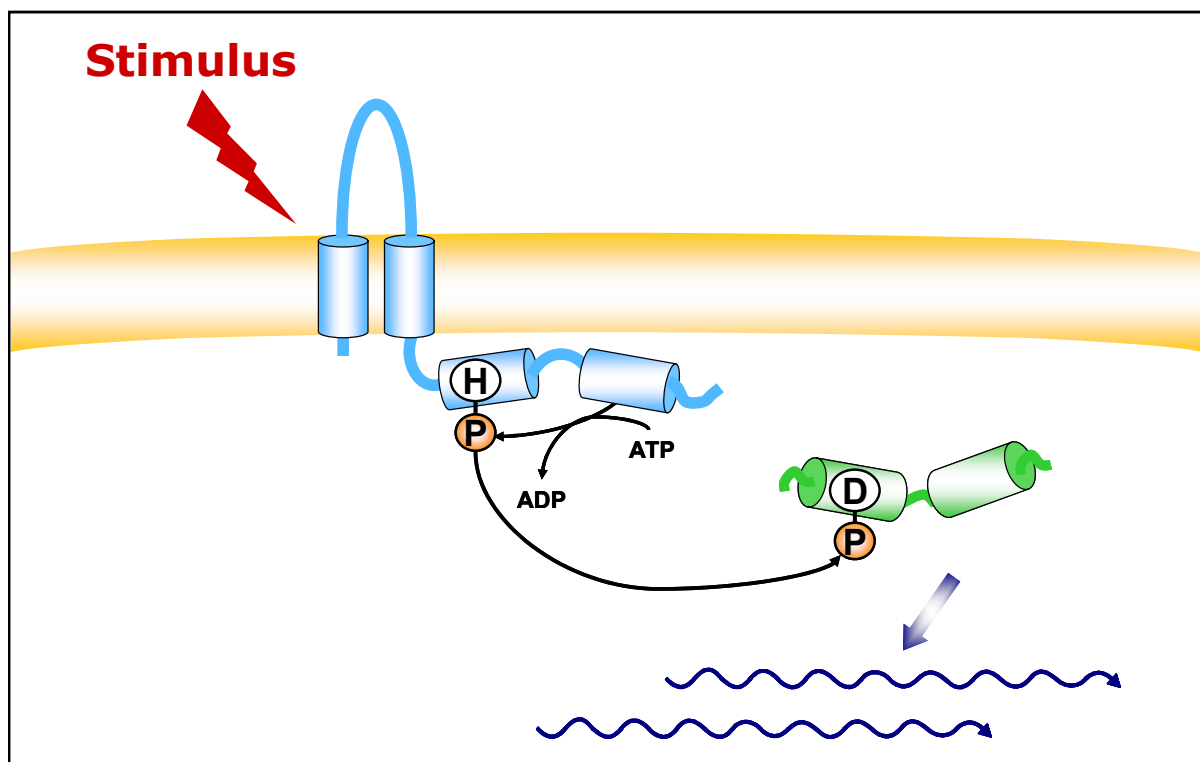
Fig. 4: Model of the two-component system-mediated signal transduction resulting in the expression regulation of genes in response to environmental stimuli.

1.5   The MtrB-MtrA two-component system of *Corynebacterium glutamicum*

In *C. glutamicum* 13 putative two-component systems have been identified: CgtSR1, 2, 4-11, CitAB, MtrBA, and PhoSR (Kocan *et al*., 2006). Among these systems, the physiological function of only two was proposed: the CitAB system belongs to a family of two-component systems controlling the uptake and metabolism of citrate. Regarding PhoSR, Kocan *et al*.

(2006) have recently shown an involvement in the adaptation of *C. glutamicum* to phosphate-limiting conditions.

In order to examine the involvement of two-component systems in the osmostress response of *C. glutamicum*, a set of twelve deletion mutants lacking those genes encoding one of the two-component systems each (Kocan *et al.*, 2006), was analyzed. Only one out of twelve examined two-component systems exhibited an involvement in the transcription regulation of osmostress-related genes in this bacterium (Möker, 2002). RNA hybridization experiments, which were carried out with an *mtrAB* deficient mutant, resulted in an altered expression pattern of four osmoregulated genes (Möker *et al.*, 2004). In *C. glutamicum* WT exposure to hyperosmotic stress results in the transcriptional induction of genes encoding the secondary uptake carriers for compatible solutes BetP, ProP, LcoP, and EctP, as well as the mechanosensitive channels MscL and MscS. As consequence of the *mtrAB* deletions, the mRNA levels of *betP*, *proP*, and *lcoP* were strongly decreased in the Δ*mtrAB* mutant both, before and after an upshift of medium osmolarity (Fig. 5). With regard to these genes, the MtrBA system seems to be essential for the activation of transcription. In contrast, transcription of the *mscL* gene was increased in the deletion strain before and up to 30 minutes after the hyperosmotic shock (Fig. 5). Thus, the expression of this gene is repressed via MtrBA.
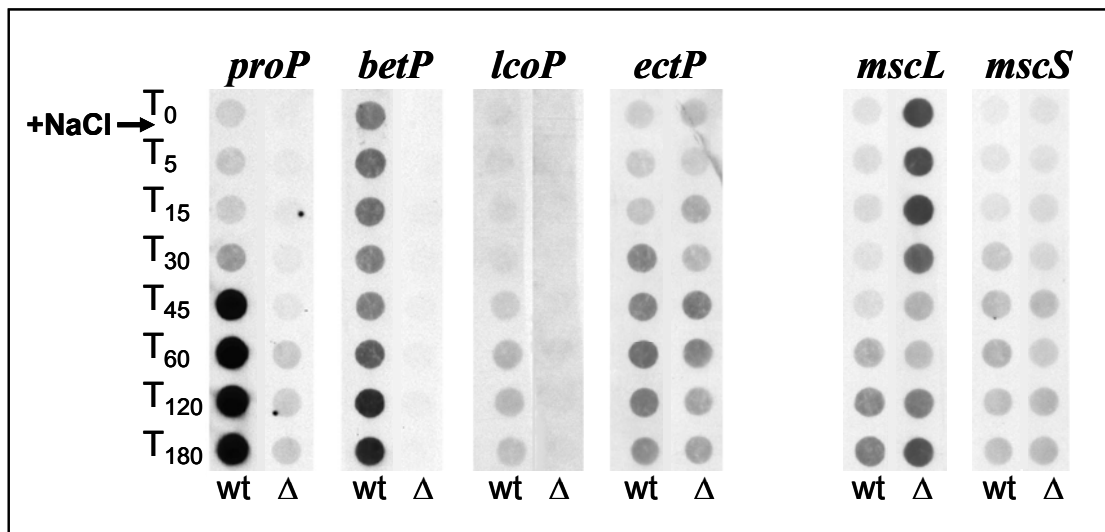
Fig. 5: Expression pattern of the uptake carrier- and mechanosensitive channel encoding genes in response to an increased medium osmolality. Shown are the transcript amounts of the uptake carrier genes *proP*, *betP*, *lcoP*, and *ectP*, as well as the mechanosensitive channel genes *mscL* and *mscS* in *C. glutamicum* WT (**wt**) and Δ*mtrAB* (Δ) before (T_0) and 5 to 180 minutes after a hyperosmotic shift from 0.3 to 2.2 osm (T_5 to T_{180}), Möker *et al.*, 2004.

The plasmid-encoded expression of the *mtrAB* genes using pEKEx2-mtrAB could complement the changes of the mRNA levels of *proP*, *betP*, *lcoP*, and *mscL*, therefore proving, that the described effects were indeed a consequence of the deletion, and not of polar effects (Möker *et al.*, 2004).

In contrast to the four above-mentioned genes, the mRNA levels of further genes known to be regulated after an osmotic upshift were unchanged (Möker *et al.*, 2004). They encode a secondary uptake carrier for compatible solutes, EctP, a mechanosensitive channel, MscS, and genes encoding enzymes of each pathway for the biosynthesis of the compatible solutes trehalose and proline, namely OtsA, ProB, TreS, and TreY.

Previous studies using RT-PCR revealed that *proP* and *betP* are expressed individually, but also together with the open reading frames (orfs) 3447 and 1449, respectively, which are localized upstream of the two genes (Möker, 2002). The putative product of orf 3447 reveals similarities to membrane protease subunits belonging to the stomatin/prohibitin family, whereas orf 3447 encodes a putative uroporphyrin-III C/tetrapyrrole methyltransferase with unknown function. In order to determine whether these genes are also regulated by the MtrBA two-component system, their expression, and additionally that of the orf located upstream of *mscL*, was examined in *C. glutamicum* WT and the *mtrAB* deletion mutant before and after an increase in medium osmolarity (Fig. 45, section 7.1). It turned out that, similar to *betP*, *proP*, and *mscL*, the transcription of these genes was osmotically induced in *C. glutamicum* WT. The open reading frames located upstream of *proP* and *betP*, orf 3447 and 1449, showed decreased expression levels in the Δ*mtrAB* mutant, indicating that their expression regulation is also mediated by the two-component system. In contrast, the orf upstream of *mscL* (1435) was not affected by the deletion of the *mtrAB* genes. Since the genes located upstream of *proP* and *betP* turned out to be regulated by MtrBA, it was necessary to investigate the transcriptional organization of the MtrBA target genes in more detail. Northern Hybridization experiments showed that *proP*, *betP* and *mscL* are mainly transcribed monocistronically (Fig. 46, section 7.2). In case of the two genes encoding uptake carriers weak signals corresponding to the sizes of polycistronic mRNA were also found.

In addition to osmoprotection, the uptake and synthesis of compatible solutes in bacteria has been shown to play a role in the response to thermal stresses, e. g. chill. It was recently shown, that the compatible solute uptake carriers BetP and LcoP are influenced by chill stress in their activity (compare section 1.3). Furthermore, the transcription of their encoding genes was regulated at the level of expression in response to low temperature. RNA hybridization experiments revealed that exposure of *C. glutamicum* cells to chill stress (15 °C) results in the transcriptional induction of the *lcoP* and *betP* genes. In contrast, in the *mtrAB* deletion mutant, these genes turned out to be transcribed to significantly lower levels,

before and after exposure to low temperature (Özcan, 2003). Consequently, MtrBA seems to mediate, in addition to expression regulation in response to osmotic stress, the chill stress-induced regulation of genes encoding uptake carriers for compatible solutes.

The findings of MtrBA-mediated regulation of gene expression described above were obtained with focus on responses to specific stress conditions. Furthermore, a global analysis of the consequences of the *mtrAB* deletions on the *C. glutamicum* genome was performed using DNA microarrays (M. Bott, Forschungszentrum Jülich). These indicated that the two-component system also regulates the expression of a set of genes involved in a different physiological function in *C. glutamicum*, the cell wall metabolism. In the Δ*mtrAB* mutant the mRNA levels of genes encoding the lipoproteins MepA and LpqB were significantly increased. The MepA protein shows similarities to a cell wall endopeptidase. A third gene with increased mRNA levels in the deletion mutant was named *ppmA*, for **p**utative **p**rotease **m**odulator (Möker *et al*., 2004). To verify the hypothesis that these genes are important for cell wall biosynthesis, *C. glutamicum* wild type (WT) and Δ*mtrAB* cells were analyzed using scanning electron microscopy. The mutant cells turned out to exhibit a significantly elongated cell morphology (compare Fig. 6). Heterologous expression of the plasmid-encoded *mepA* gene in *E. coli* (Fig. 6) resulted in elongated cells with a morphology more or less similar to that of *C. glutamicum* Δ*mtrAB* (Möker *et al*., 2004). These observations led to the suggestion that MepA has a cell wall endopeptidase activity targeting the peptidoglycan layer. These effects, the altered expression of *mepA* and the elongated cell morphology of the deletion mutant, were complemented by the plasmid-encoded expression of the *mtrAB* genes in the Δ*mtrAB* mutant using the vector pEKEx2-mtrAB (Möker *et al*., 2004)*.*

Taken together, the MtrB-MtrA system seems to be involved in three physiological functions in *C. glutamicum*, (I) osmoregulation, (II) chill stress response, and (III) cell wall metabolism. Regarding the sensor kinase MtrB of this system one has to conclude that either a single stimulus is detected, which can act as a measure for the three different purposes, or MtrB is able to detect a set of different stimuli. These signals would likely be connected to the different above-mentioned physiological functions. The MtrBA-mediated expression regulation of osmo- and chill stress-related genes was shown to occur in response to specific conditions connected with osmotic and chill-stress, therefore indicating that MtrB acts as a sensor for both, osmo- and chill-stress. In contrast, the conditions which lead to the repression or induction of the cell wall-related genes remain unknown. The phenomenon, that a sensor is able to detect both, stimuli related to osmo- and chill stress has already been reported for the compatible solute uptake carrier BetP (Peter *et al*., 1996; Peter *et al*., 1998, Özcan *et al*., 2003). A number of two-component systems involved either in chill stress

response, osmoprotection, or cell wall biosynthesis were also described recently (Aguilar *et al*., 2001; Jung *et al*., 2000; Mizuno *et al*., 1988; Raivio *et al*., 1999; Mascher *et al*., 2004), but few data are available on systems influencing all three of these processes.

A

B

C. glutamicum **wildtype**   *C. glutamicum* Δ*mtrAB*

C

D

E. coli **DH5**α **pEKEx2**   *E. coli* **DH5**α **pEKEx2-***mepA*
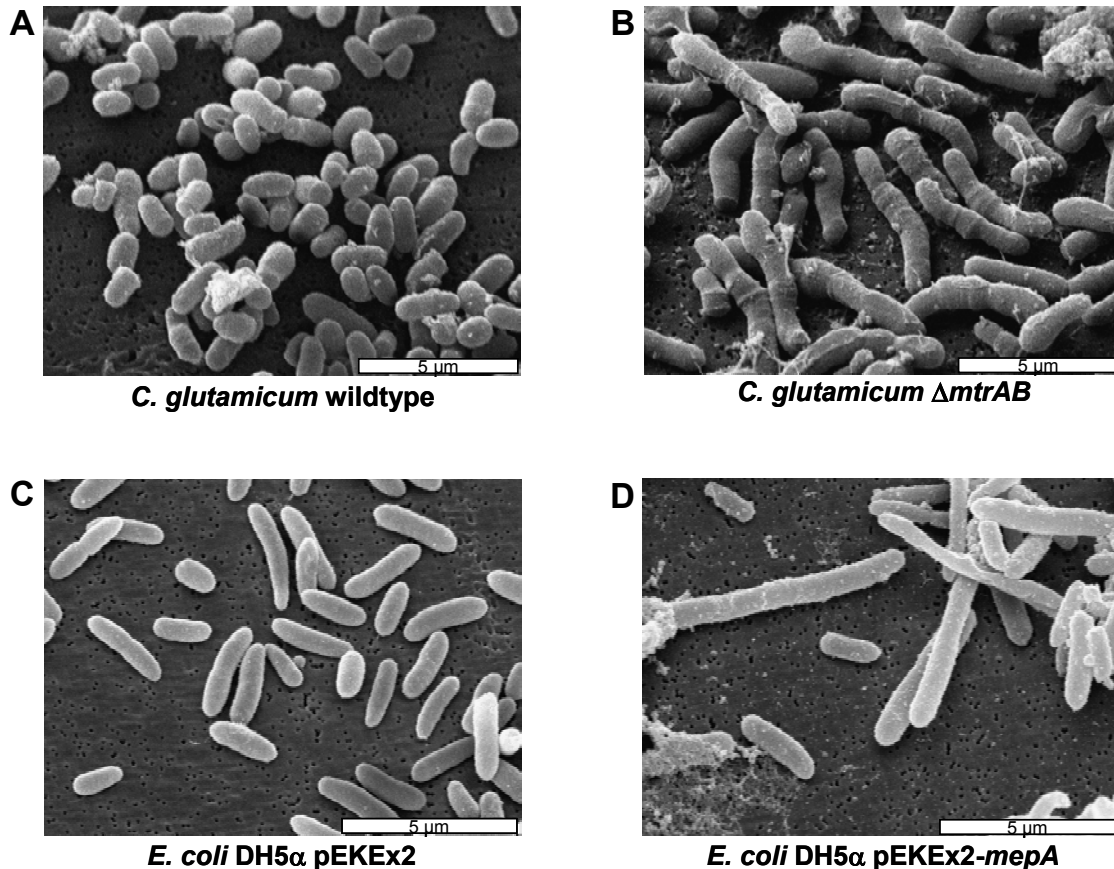
Fig. 6: Scanning electron micrographs showing *C. glutamicum* WT (A), and Δ*mtrAB* (B) as well as *E. coli* DH5α **containing pEKEx2 (C) or pEKEx2-mepA (D), Möker *et al*., 2004.**

1.6   Objectives of this thesis

The aim of this work was a detailed characterization of the sensing properties of the MtrB-MtrA two-component system of *C. glutamicum*. Recent investigations suggested that the histidine kinase MtrB acts as sensor for both, osmo- and chill stress-related stimuli. For a system acting as osmosensor a variety of stimuli are possible. These include changes in external osmolarity, ionic strength and concentration of ions or specific solutes, but also, resulting from the water fluxes across the cytoplasmic membrane, changes in turgor pressure, internal osmolarity, ionic strength, concentration of ions or specific solutes and membrane strain or -shrinkage. For a protein acting as a chill sensor the cellular

architectures offer three basic targets which respond almost immediately to a change in temperature, (I) phase condition of membrane-bound lipids, (II) conformation of proteins, or (III) conformation of nucleic acids (Weber and Marahiel, 2002).

Since a set of different parameters changes upon osmotic- and chill stress, a whole cell approach did not seem favorable for the detection of separate stimuli. Instead, for the investigation of the direct signals sensed by MtrB two *in vitro* membrane systems were chosen. In inverted membrane vesicles enriched with MtrB prepared from *E. coli* the membrane-spanning sensor kinase is integrated into the cytoplasmic membrane by the *E. coli* protein insertion machinery, which might provide a correct integration. However, in this system non-specific *E. coli* membrane proteins are also present. The proteoliposome system provides a more reduced complexity. The isolation of MtrB and the subsequent reconstitution into *E. coli* lipid liposomes would result in an *in vitro* membrane system carrying MtrB only. In recent years, proteoliposomes were shown to serve as suitable systems for the analyses of membrane-bound sensor histidine kinases.

Using the above-mentioned MtrB-enriched *in vitro* membrane systems it was first aimed to define the basic attributes of MtrB and MtrA, including the autokinase activity of membrane-bound MtrB, the phosphoryl group transfer to isolated MtrA, and the dephosphorylation of activated MtrA (MtrA-P). Once the *in vitro* activities of MtrB and MtrA were defined, the stimuli triggering the MtrB-MtrA signal transduction could be addressed by a systematic variation of possible stimuli related to osmotic and chill stress conditions.

2.   Materials and methods

2.1   Bacterial strains, plasmids, and oligonucleotides

2.1.1 Bacterial strains

The *E. coli* and *C. glutamicum* strains used in these studies are summarized in Table 1.

Tab. 1: *E. coli* and *C. glutamicum* strains that were used in this work.

Strain	Genotype	Reference
E.coli		
DH5αmcr	*endA1 supE44 thi-1 λ^- recA1 gyrA96 relA1 deoR Δ(lacZYA-argF) U196 ϕ80DlacZ ΔM15mcrA Δ(mmr hsdRMS mcrBC)*	Grant *et al*., 1990
BL21(DE3)	F$^-$ *ompT gal [dcm] [lon] hsd*S$_B$ (r$_B^-$m$_B^-$; an *E. coli* B strain) with DE3, a λ prophage carrying the T7 RNA polymerase gene	Novagen, Darmstadt
DK8	*bglR*, *thi-1*, *rel-1*, *HfrPO1*, (*uncB-uncC*), *ilv:Tn10* (lacks the whole F 0 F 1 genes)	Klionsky *et al*., 1984
C. glutamicum		
ATCC 13032	wild type	Abe *et al*., 1967
ATCC 13032 ΔmtrAB	Derivative of ATCC 13032 with an *in frame*-deletion of the *mtrAB* genes	Möker *et al*., 2004

2.1.2 Plasmids

In Table 2, the plasmids used in this work are listed. The construction of the vectors is described in detail in the appendix (7.3).

Tab. 2: Plasmids that were used in this study.

Plasmid	Description	Reference
pASK-IBA3	Ap^R, P$_{tet}$, expression vector	Skerra *et al*., 1994
pASK-IBA7	Ap^R, P$_{tet}$, expression vector	Skerra *et al*., 1994

Plasmid	Description	Reference
pASK-IBA3-mtrB-strep	pASK-IBA3 derivative containing *mtrB* in the PshAI cleavage site fused to the sequence encoding a C-terminal Strep-tag	This work
pASK-IBA7-strep-mtrB	pASK-IBA7 derivative containing *mtrB* in the PshAI cleavage site fused to the sequence encoding an N-terminal Strep-tag	This work
pASK-IBA3-mtrBΔ25	pASK-IBA3-*mtrB-strep* derivative encoding an MtrB-Strep derivative with a truncation of the N-terminal amino acids 1 to 25	This work
pASK-IBA3-mtrBΔ154	pASK-IBA3-*mtrB-strep* derivative encoding an MtrB-Strep derivative with a truncation of the N-terminal amino acids 1 to 154	This work
pASK-IBA3-mtrBΔ163	pASK-IBA3-*mtrB-strep* derivative encoding an MtrB-Strep derivative with a truncation of the N-terminal amino acids 1 to 163	This work
pASK-IBA3-mtrBΔ190	pASK-IBA3-*mtrB-strep* derivative encoding an MtrB-Strep derivative with a truncation of the N-terminal amino acids 1 to 190	This work
pASK-IBA3-mtrBΔL124	pASK-IBA3-*mtrB-strep* derivative encoding an MtrB-Strep derivative with a truncation of the N-terminal amino acids 31 to 164	This work
pASK-IBA3-mtrBΔL134	pASK-IBA3-*mtrB-strep* derivative encoding an MtrB-Strep derivative with a truncation of the N-terminal amino acids 36 to 159	This work
pASK-IBA7-strep-mtrA	pASK-IBA7 derivative containing *mtrA* in the PshAI cleavage site fused to the sequence encoding an N-terminal Strep-tag	This work
pEKEx2	Km^R, *lacI*^{q}, *ptac*, *E. coli* - *C. glutamicum* shuttle vector	Eikmanns *et al.*, 1991
pEKEx2-mtrAB	pEKEx2 derivative containing the *mtrAB* genes from *C. glutamicum* under control of the *tac* promoter	Möker *et al.*, 2004
pEKEx2-mepA	pEKEx2 derivative containing the *mepA* gene from *C. glutamicum* under control of the *tac* promoter	Möker *et al.*, 2004

Plasmid	Description	Reference
pET224b-mtrA	Km^R, P_{T7}, expression vector derivative containing *mtrA* fused to the sequence of a C-terminal $(His)_{10}$-tag	Brocker, unpublished data
pET28a	Km^R, P_{T7}, expression vector	Novagen, Inc. Madison, USA
pMW151	pET28a derivative containing *dcuS* fused to the sequence encoding an N-terminal $(His)_6$-tag.	Janausch *et al.*, 2002
pDrive	Ap^R, Km^R, *lacZα*, A-T insertion vector	Qiagen, Hilden
pDrive1435	pDrive derivative containing a 0.51 kb fragment of the orf 1435 (upstream of *mscL*)	This work
pDrive1449	pDrive derivative containing a 0.47 kb fragment of the orf 1449 (upstream of *proP*)	This work
pDrive3447	pDrive derivative containing a 0.48 kb fragment of the orf 3447 (upstream of *betP*)	This work
pGEM-3Z	Ap^R, P_{T7} and P_{SP6}	Promega, Mannheim
pGEM-4Z	Ap^R, P_{T7} and P_{SP6}	Promega, Mannheim
p16Sr	pGEM-3Z derivative containing a 0.5 kb fragment of the *16s rRNA* gene	Nolden, 2001
pbetP	pGEM-4Z derivative containing a 0.44 kb fragment of the *betP* gene	Möker *et al.*, 2004
pectP	pGEM-4Z derivative containing a 0.76 kb fragment of the *ectP* gene	Möker *et al.*, 2004
plcoP	pGEM-4Z derivative containing a 0.73 kb fragment of the *lcoP* gene	Möker *et al.*, 2004
pmscL	pGEM-4Z derivative containing a 0.4 kb fragment of the *mscL* gene	Möker *et al.*, 2004
pproP	pGEM-4Z derivative containing a 0.51 kb fragment of the *proP* gene	Möker *et al.*, 2004

Ap^R, resistence towards ampicillin. Km^R, resistence towards kanamycin

2.1.3 Oligonucleotides

The oligonucleotides used in this work are listed in Table 8 in the appendix (7.3).

2.2   Growth media and cultivation conditions

2.2.1 Growth media

The growth media used in these studies are listed in Table 3. For agar plates 15 g/L Bacto-Agar (Difco, Detroit, USA) were added. If appropriate, the antibiotics kanamycin or carbenicillin were added to the growth media with a final concentration of 50 µg/mL.

E. coli strains were generally cultivated in LB- (Luria Bertani-) medium (Tab. 3). *C. glutamicum* was either grown in BHI complex medium (Brain Heart Infusion, Difco, Detroit, USA), MMI- (Kase and Nakayama, 1972) or CgXII- (Keilhauer *et al*.,1993) minimal medium. The medium osmolality of MMI was, if indicated, increased from 0.3 to 2.2 osm/kg by the addition of 1.05 M NaCl.

Tab. 3: Culture media used in this study.

Medium	Ingredients (per liter)
LB	10 g trypton, 5 g yeast extract, 10 g NaCl
BHI	37 g/L Brain Heart Infusion
CgXII (0.9 osm/kg)	42 g MOPS, 20 g $(NH_4)_2SO_4$, 5 g urea, 1 g KH_2PO_4, 1 g K_2HPO_4, pH (NaOH) = 7.0, ad 914 mL H_2O_{dd}. After heat sterilization, 80 mL 50 % (w/v) sucrose or glucose, 1 mL 1 % (w/v) $CaCl_2$, 1 ml 1 M $MgSO_4$, 1 mL 0.02 % biotin, 600 µL protocatechuate (50mg/mL), and 1 mL trace element solution were added.
MMI (0.3 osm/kg)	5 g $(NH_4)_2SO_4$, 5 g urea, 2 g KH_2PO_4, 2 g K_2HPO_4, pH (NaOH) = 7.0, ad 916 mL H_2O_{dd}. After heat sterilization, 80 mL 50 % (w/v) sucrose or glucose, 1 mL 1 % (w/v) $CaCl_2$, 1 ml 1 M $MgSO_4$, 1 mL 0.02 % biotin, and 1 mL trace element solution were added.
Trace element solution	1 g $FeSO_4$ X $7H_2O$, 1 g $MnSO_4$ X H_2O, 0,1 g $ZnSO_4$ X $7H_2O$, 0.021 g $CuSO_4$ X $5H_2O$, 2 mg $NiCl_2$ X $6H_2O$ ad 100 mL H_2O_{dd}.

2.2.2 Cultivation conditions

E. coli and *C. glutamicum* cells were routinely cultivated in shaking flasks under aerobic conditions at 37 °C or 30 °C, respectively. The growth of the bacterial cultures could be determined by the optical density (OD_{600}). An OD_{600} of 1 corresponds to a bacterial suspension of approximately 10^9 cells per mL.

For the heterologous synthesis of proteins, *E. coli* BL21(DE3), -DH5α*mcr*, or -DK8 cells were cultivated over night in 5 mL LB medium at 30 °C. Subsequently, the cells were transferred into fresh LB medium with an optical density (OD_{600}) of 0.1 and cultivated at 30 °C. When the cultures reached an optical density of 0.5, gene expression was induced by the addition of 50 µM IPTG or 40 to 200 µg/L AHT and cells were harvested after 1 to 4 h growth.

To study the expression of specific genes under hyperosmotic stress conditions, the standard inoculation schema for *C. glutamicum* was modified. Routinely, the cells are first cultivated in 5 mL BHI medium at 30 °C for 8 h. This culture is washed in 0.9 % NaCl and used to inoculate 25 mL MMI to an optical density (OD_{600}) of 0.5 for adaptation to the minimal medium. After 16 h, the cells are transferred into a fresh MMI culture with an optical density of 2 and incubated at 30 °C until the exponential phase is reached. *C. glutamicum* Δ*mtrAB* turned out to exhibit an altered growth behaviour after long adaptation to MMI minimal medium (Möker, 2002). Consequently, the cultivation time in the minimal medium was reduced as follows: *C. glutamicum* wild type and Δ*mtrAB* cells were first cultivated in 5 mL BHI medium at 30 °C for 8 h. These cultures were used to inoculate 25 mL BHI medium to an optical density of 0.5 for growth at 30 °C. After 16 h, the cells were washed in 0.9 % NaCl, transferred into 25 mL of MMI to an optical density of 2, and cultivated at 30 °C. When the exponential growth phase (OD_{600} of 6 to 7) was reached, 2 mL of the cell suspension were harvested. The residual culture was exposed to hyperosmotic conditions (2.2 osm/kg) by transfer into minimal medium supplemented with 1.05 M NaCl or 2 M trehalose. Subsequently, 2 mL of the cell suspension were harvested 5, 15, 30, 45, 60 and 120 min after the hyperosmotic shock, frozen in liquid nitrogen and stored at -80 °C.

For the analyses of gene expression under chill stress conditions, 5 mL of a *C. glutamicum* culture were incubated over night at 30 °C. This culture was used to inoculate 25 mL BHI medium for 8 h cultivation at 30 °C. Subsequently, the cells were washed with 0.9 % NaCl and transferred into 25 mL CgXII minimal medium. After 16 h cultivation at 30 °C, cells were transferred into 100 mL of fresh CgXII medium with an optical density (OD_{600}) of 2, and further cultivated at 30 °C. When reached the exponential growth phase (OD_{600} of 6 to 7), 2 mL of the cell suspension were harvested. The residual culture was divided into 4 CgXII cultures (25 mL each), centrifuged at 30 °C, and subsequently diluted into 25 mL pre-tempered CgXII medium for cultivation at either 30 °C or 15 °C. The growth phase of

C. glutamicum cells at 15 °C is approximately reduced to ½ in comparison to cultivation at 30 °C. To achieve both, a comparison of gene expression at similar growth phases as well as similar time points of incubation, the samples were taken before and 2, 4, 6 and 20 h after exposure to 15 °C, while the cells grown at 30 °C were collected before and 1, 2, 3, 4, 5, 6 and 20 h after the division of the CgXII culture. After harvesting, cells were frozen in liquid nitrogen and stored at -80 °C.

2.3   Molecular biological approaches

2.3.1 Preparation of competent *E. coli* cells and transformation

To prepare competent *E. coli* cells, 20 mL LB medium were inoculated with *E. coli* cells and cultivated for 8 h at 37 °C. 1 mL of this culture was used to inoculate 250 mL SOB medium. Cells were cultivated for 16 h at 20 °C in a 2 L shaking flask. Subsequently, the culture was chilled on ice for 10 min. Cells were harvested by centrifugation (4000 X g, 4 °C, 8 min). The cell pellet was resuspended in 80 mL ice-cold TB buffer. After centrifugation (4000 X g, 4 °C, 10 min), cells were suspended in 40 mL TB buffer supplemented with 1.4 mL DMSO, and incubated for 10 min on ice. Aliquots of 100 µL were transferred into pre-cooled reaction tubes, immediately frozen in liquid nitrogen and stored at -80 °C.

For transformation, a 100 µL aliquot of competent *E. coli* cells was thawed on ice and plasmid DNA was added. The cells were incubated for 30 min on ice. After heat shock at 42 °C for 30 s, cells were mixed with 400 µL SOC medium and cultivated for 1 h at 37 °C. The cell suspension was plated on LB plates containing the appropriate antibiotic, and cultivated for 16 h at 37 °C.

<u>TB buffer:</u> 10 mM Pipes, 15 mM $CaCl_2$, 250 mM KCl, pH (KOH) = 6.7. After adjustment of pH, 55 mM $MnCl_2$ were added. The buffer was sterilized by filtration.

<u>SOB medium:</u> 20 g/L Tryptone, 5 g/L yeast extract, 0.5 g/L NaCl, 2.5 mM KCl. After heat sterilization, 5 mL 2 M $MgCl_2$ were added.

<u>SOC medium:</u> 10 g/L Tryptone, 5 g/L yeast extract, 5 g NaCl, 3.6 g/L glucose. After heat sterilization, 5 mL 2 M $MgCl_2$ were added.

2.3.2 Preparation of competent *C. glutamicum* cells and transformation

To prepare competent *C. glutamicum* cells, 20 mL BHI medium were inoculated with *C. glutamicum* cells and cultivated for 8 h at 30 °C. Subsequently, this culture was used to inoculate 200 mL LB medium supplemented with 4 g/L isonicotine acid hydrazide, 25 g/L glycine, and 0.1 % (v/v) Tween 80 to an OD_{600} of 0.35. The cells were cultivated at 20 °C in a 2 L shaking flask. After 16 h, the cultures were chilled on ice for 10 min, before harvested by centrifugation (4000 X g, 4 °C, 8 min). The cells were washed five times in ice-cold 10 % glycerol. After the final washing, the cell pellet was resuspended in 1 mL ice-cold 10 % glycerol. Aliquots of 50 µL were transferred into pre-cooled reaction tubes, immediately frozen in liquid nitrogen and stored at -80 °C.

Prior to transformation, a 50 µL aliquot of competent *C. glutamicum* cells was thawed on ice and transferred to a pre-cooled electroporation cuvette (Peqlab, Erlangen). Plasmid DNA was added and electroporation was performed with a Gene-Pulser (Biorad, München) at 2.5 kV, 600 Ω, and 25 µF. The cell suspension was transferred to a cultivation tube and 1 mL BHIS medium was added. The cells were cultivated for 90 min at 30 °C. Subsequently, the cell suspension was plated on a BHI plate containing the appropriate antibiotic.

LB medium with growth inhibitors: 10 g/L Tryptone, 5 g/L yeast extract, 5 g/L NaCl, 4 g/L isonicotine acid hydrazide, 25 g/L glycine, 0.1 % (v/v) Tween 80; sterilization by filtration

BHIS medium: 37 g/L Brain Heart Infusion, 91 g/L sorbitol; sterilization by filtration

2.3.3 DNA techniques

2.3.3.1 Isolation of plasmid DNA from *E. coli*

The isolation of plasmid DNA from *E. coli* cells was performed following the principle of alkaline lysis (Birnboim and Doly, 1979). For this purpose, *E. coli* cells were cultivated as described in 2.2.2. For the isolation of plasmid DNA from these cultures, the NucleoSpin® Plasmid DNA Purification kit (Macherey-Nagel, Düren) was used as recommended by the supplier.

2.3.3.2 Isolation of genomic DNA from *C. glutamicum*

The isolation of genomic DNA from *C. glutamicum* was performed as described by Eikmanns *et al.* (1994). *C. glutamicum* cells were cultivated overnight in 5 mL LB medium. Subsequently, cells were harvested by centrifugation (14.000 X g, 30 s, RT) and the cell pellet was resuspended in 1 mL TE buffer supplemented with 15 mg lysozyme (Sigma,

Deisenhofen). After shaking for 3 h at 37 °C, 200 µL 10 % SDS was added. The samples were kept for 2 min at 37 °C. Subsequently, 3 mL lysis buffer, as well as 125 µL proteinase K (Roche Diagnostics) were added. The suspension was incubated at 37 °C. After 16 h, 2 mL of a saturated NaCl solution was added and the suspension was gently mixed. After centrifugation (4000 X g, 30 min, RT), the supernatant was transferred to a 50 mL tube, and ice-cold ethanol was added to a final volume of 50 mL. The precipitated genomic DNA was washed three times with 70 % ethanol, dried, and resuspended in H_2O_{dd}.

2.3.3.3 Gel electrophoresis and extraction of DNA from agarose gels

Gel electrophoresis of DNA was performed using 0.8 to 2 % agarose gels in 1X TAE buffer as described by Sambrook *et al.* (1989). For this purpose, DNA samples were mixed with 5X Loading Dye (MBI Fermentas, St. Leon-Roth). After electrophoresis, DNA was stained with ethidium bromide. For detection of stained DNA, the Image Master VDS system (Amersham Biosciences, Freiburg) was used. DNA was isolated from agarose gels using the NucleoSpion® Extract kit (Macherey-Nagel, Düren) as recommended by the supplier.

1X TAE buffer: 40 mM Tris, 0.5 mM EDTA, pH (acetic acid) = 7.5

2.3.3.4 Polymerase chain reaction (PCR)

The *in vitro* amplification of specific DNA fragments was performed by the polymerase chain reaction (PCR, Mullis *et al.*, 1986) using the Taq PCR Master Mix (Qiagen, Hilden) as recommended by the supplier. For this purpose, two primers were used, flanking the DNA region, which should be amplified. Primers were diluted to a concentration of 10 pmol/µL. The annealing temperature was chosen with respect to the forward and reverse primer. For each guanine and cytosine 4 °C, for each adenine and thymine 2 °C are required to separate the hydrogen bonds. As template, total DNA, plasmid DNA, or a cell suspension, which was diluted in H_2O_{dd} and incubated for 10 min at 95 °C, could be used. The PCR reaction was performed using the thermocycler Mastercycler® personal or Mastercycler® gradient (Eppendorff, Hamburg). A 20 µL PCR reaction mixture was prepared as follows:

10 µL Master-Mix (Qiagen, Hilden)
1 µL primer forward [10 µM]
1 µL primer reverse [10 µM]
1 µL template
H_2O_{dd} ad 20 µL

The amplification reaction was initiated by denaturing the template for 4 min at 95 °C. The following steps were performed in 30 cycles: Denaturing the DNA for 30 seconds at 95 °C, hybridization of the primers for 30 seconds at the specific annealing temperature, and polymerisation for 1 min per kb at 72 °C. After final incubation for 10 min at 72 °C, the samples were kept at 4 °C or -20 °C. If appropriate, the PCR product was purified either with the NucleoSpin® Extract Kit (Macherey-Nagel, Düren) as recommended by the supplier, or by gel electrophoresis as described in section 2.3.3.3

2.3.3.5 Restriction, ligation, and sequencing of DNA

For restriction of DNA, restriction enzymes were used as recommended by the suppliers (NEB, Frankfurt/Main; MBI Fermentas, St. Leon-Roth). If dephosphorylation of 5' ends was necessary, 1 µL shrimp alkaline phosphatase (SAP) or 1 µL calf intestinal alkaline phosphatase (CIP; NEB, Frankfurt/Main) was added to the samples. For removal of 3′-end A overhangs, the 3′- to 5′-end exonuclease activity of the T_4 DNA polymerase (NEB, Frankfurt/Main) was used.

After restriction, dephosphorylation, or blunting, DNA was purified either with the NucleoSpin® Extract kit (Macherey-Nagel, Düren) following the supplier's protocol or by gel electrophoresis as described in section 2.3.3.3.

For the ligation of DNA fragments into restricted vectors, the Rapid DNA Ligation kit (MBI Fermentas, St. Leon-Roth) was used as recommended by the supplier. For direct ligation of PCR products into the pDrive vector by T/A-cloning, the QIAGEN PCR Cloning kit (Qiagen, Hilden) was used. After ligation, 5 µL of the reaction mix was used to transform competent *E. coli* cells as described in section 2.3.1.

DNA sequence analyses were carried out by the bioanalytics service unit at the *Center for Molecular Medicine Cologne* (ZMMK).

2.3.4   RNA techniques

2.3.4.1 Isolation of total RNA from *C. glutamicum*

For the isolation of total RNA from *C. glutamicum*, cells were cultivated as described in section 2.2.2. 2 mL of the cells grown under different stress conditions were collected by centrifugation (14000 X g, 30 s, 30 °C) and the resulting pellet was immediately frozen in liquid nitrogen and stored at -80 °C. For the preparation of RNA, the cell pellet was thawed at room temperature and subsequently diluted in 700 µL RA1 buffer (NucleoSpin RNA II Kit, Macherey-Nagel, Düren) supplemented with 0.1 % (v/v) β-mercaphoethanol. The resulting suspension was transferred into cryo tubes containing 300 mg glass beads (diameter 0.2-0.3 mm). Cell disruption was performed by 3 cycles of vigorous shaking in the FastPrep FP120

instrument (Q-BIOgene, Heidelberg) for 30 seconds at 6.5 m/s. The cell debris and glass beads were subsequently removed by centrifugation (14000 X g, 2 min, RT) and the supernatant was mixed with 500 µL 70 % ethanol. In the following, total RNA was isolated using the NucleoSpin® RNA II kit (Macherey-Nagel, Düren) as recommended by the supplier. The integrity of isolated total RNA was analyzed by gel electrophoresis. For this purpose, 3 µL of purified total RNA was mixed with 10 µL RNA loading buffer and incubated for 10 min at 70 °C. Subsequently, the samples were kept on ice for 5 min. As quality control, gel electrophoresis and detection of RNA was performed in accordance to the analysis of DNA described in section 2.3.3.3.

Prior to Dot blot or Northern RNA hybridization experiments, the concentration of total RNA samples was measured spectroscopically at a wavelength of 260 nm (ε = 25 cm^2/mg). The purity of isolated RNA was analyzed by determination of the quotient of A_{260} / A_{280}, which is 2.0 for pure RNA.

For subsequent RT-PCR analyses, total RNA was, after isolation, additionally treated with RQ1 RNase-free DNase (Promega, Mannheim) as recommended by the supplier.

RNA loading buffer: 250 µL formamide, 83 µL 37 % formaldehyde, 50 µL 10X MOPS buffer, 50 µL glycerol, 0.01 % bromphenol blue, 0.01 % xylene cyanole, 1 µL 10 g/L ethidium bromide, 120 µL RNase-free H_2O_{dd}

MOPS buffer: 200 mM MOPS, 50 mM sodium acetate, 10 mM EDTA, pH = 7.0

2.3.4.2 Synthesis of digoxigenin-labelled RNA probes

Digoxigenin-labelled RNA probes were produced by *in vitro* transcription. As template, a pDrive or pGEM plasmid containing an insert with the appropriate DNA sequence was used. These plasmids harbour one promoter at each side of the multiple cloning side, for the RNA polymerases SP6 or T7, respectively. Depending on the orientation of the insert, the plasmid was linearized by restriction at the 5´- or 3´-end of the insert and purified by gel electrophoresis and subsequent gel extraction (2.3.3.3). After elution in RNAse-free H_2O_{dd}, the concentration of the linearized and purified plasmid was estimated by gel electrophoresis (2.3.3.3). The *in vitro* transcription was started from the SP6 or T7 promoter. The labelling of the RNA probes was performed by the use of digoxigenin-11-dUTP instead of dUTP. The reaction mixture for the *in vitro* transcription was composed of:

1 µg template DNA (restricted and purified plasmid)

2 µL DIG RNA Labelling Mix (Roche, Mannheim)

2 µL 10X Transcription Buffer (Roche, Mannheim)

2 µL SP6 or T7 RNA polymerase (Roche, Mannheim)

13 µL RNase-free H_2O_{dd}

After the reaction mixture was incubated for 2 h at 37 °C, 1 µL DNase (Roche, Mannheim) was added and the solution was incubated for another 20 min at 37 °C. The resulting digoxigenin-labelled RNA probe was stored at -80 °C.

2.2.4.3 RNA hybridization experiments (Dot blots)

The expression pattern of specific genes was analyzed by RNA hybridization experiments. For the preparation of RNA Dot blots, 3 µg of total RNA was mixed with 100 µL 10X SSC and spotted onto a nylon membrane (Nylon Membranes positively charged, Roche Diagnostics, Mannheim), which was pre-equilibrated in 10X SSC, using the Minifold I Dot Blotter (Schleicher & Schuell, Dassel). Subsequently, the nylon membrane was dried and the total RNA was crosslinked by UV radiation (125 mJ/cm^2) using a Bio-Link instrument (LFT-Labortechnik, Wasserburg). The membrane was equilibrated for 1 h at 50 °C in 20 mL hybridization mix. Subsequently, 1 µL digoxigenin-labelled RNA probe was added and hybridization was performed at 68 °C. After 16 h, the membrane was washed twice in 20 mL washing buffer 1 for 15 min at RT, another two times in 20 mL washing buffer 2 for 15 min at 68 °C, and finally once in 20 mL washing buffer 3 for 5 min at RT. To prevent non-specific binding reactions, the membrane was incubated for 30 min in 20 mL 1X blocking buffer. 2 µL alkaline phosphatase conjugated anti-digoxigenin Fab fragments (Roche, Mannheim) were added and the membrane was incubated for another 30 min at RT. After three washing steps in washing buffer 3 for 30 min at RT, the membrane was equilibrated in detection buffer for 5 min. 15 µL CSPD reagent (Roche, Mannheim) dissolved in 1.5 mL detection buffer were used to moisten the membrane, which was subsequently covered with transparent plastic foil. After incubation for 15 min at 37 °C, light emission was detected using a Fuji Luminescent Image Analyser LAS1000 (Raytest, Straubenhardt). The intensities of hybridization signals were determined using the software AIDA 2.0 (Raytest, Straubenhardt).

20X SSC: 3 M NaCl, 0.3 M sodium citrate, pH (HCl) = 7.0

Hybridization mix: 50 mL formamide, 20 mL 10X blocking buffer, 25 mL 20X SSC, 1 mL 10 % sodium lauryl sarconisate, 0.2 mL 10 % SDS, ad 100 mL H_2O_{dd}

Washing buffer 1: 2X SSC, 0.1 % SDS

Washing buffer 2: 0.1X SSC, 0.1 % SDS

10X blocking buffer: 10 % blocking reagent (Roche, Mannheim) in maleic acid buffer. 10X blocking buffer was diluted 1:10 in maleic acid buffer to obtain 1X blocking buffer.

Maleic acid buffer: 0.1 M maleic acid, 0.15 M NaCl, pH (NaOH) = 7.5

Washing buffer 3: 0.3 % (v/v) Tween 20 in maleic acid buffer

Detection buffer: 0.1 M Tris, 0.1 M NaCl, pH (NaOH) = 9.0

2.3.4.4 Northern blot analyses

Using Northern blot analyses, mRNA molecules were separated by gel electrophoresis and detected by the use of RNA probes (2.3.4.2). For this purpose, 3 µg of total RNA was denatured by addition of 4 µL 40 % deionized glyoxal, 10 µL 100 % DMSO, and 2 µL 10X phosphate buffer for 1 h at 50 °C. Subsequently, the samples were chilled on ice and supplemented with 5 µL loading buffer. The separation of the denatured RNA samples was performed by means of gel electrophoresis using 3 to 5 V/cm. The pH value of the electrophoresis buffer was kept constant by turning of the gel and reversion of the polarity of the electrophoresis unit every 30 min. After electrophoresis, the resulting gel was equilibrated for 10 min in 10X SSC. Subsequently, the gel was placed on top of a 10X SSC-equilibrated nylon membrane (Nylon Membranes positively charged, Roche Diagnostics, Mannheim) inside of a vacuum blotting system (LKB VacuGene XL, Amersham Pharmacia, Freiburg). The RNA transfer was performed for 2 h at 50 mbar. After drying of the nylon membrane, the total RNA was crosslinked by UV radiation (125 mJ/cm^2) using a Bio-Link instrument (LFT-Labortechnik, Wasserburg). To visualize the ribosomal RNA and the molecular weight standard, the membrane was dyed with methylene blue, photographed and decolorized using H_2O_{dd}. For the subsequent hybridization with RNA probes, the total RNA had to be deglyoxylated in 20 mM Tris, pH (HCl) = 8 for 15 min at 65 °C. After two washing steps in H_2O_{dd}, the membrane was equilibrated for 1 h at 50 °C in 20 mL hybridization mixture. Subsequently, 1 µL digoxigenin-labelled RNA probe was added and hybridization was performed at 68 °C overnight. The subsequent washing and detection steps were performed according to 2.3.4.3.

<u>10X electrophoresis buffer:</u> Solution A: 0.2 M KH_2PO_4; solution B: 0.2 M K_2HPO_4. 255 mL of solution A were mixed with 245 mL of solution B and H_2O_{dd} ad 1 L. The resulting pH value was 6.8.

<u>Loading buffer:</u> 50 % (w/v) glycerol, 0.05 % bromophenol blue in 1X phosphate buffer

<u>Methylene blue dye:</u> 0.5 M Na acetate, 5 % acetic acid, 0.04 % methylene blue

<u>Deionization of glyoxal:</u>
One third of a 2 mL Eppendorf reaction cup was filled with AG 501 resin (Biorad, München). Glyoxal was added and, after 3 min of incubation, placed into a new reaction cup supplemented with resin. This procedure was repeated until the pH of glyoxal reached a value of 5. The deionized glyoxal was frozen in liqid nitrogen and stored at -20 °C.

2.3.4.5 RT-PCR

The identification of specific mRNA transcripts in total RNA samples was performed by means of RT-PCR. For this purpose, the OneStep-RT-PCR-Kit (Qiagen, Hilden) was used as recommended by the supplier. Total RNA treated with RQ1-DNase served as template. A 50 µL reaction mixture was prepared as follows:

10 µL 5X RT-PCR-Buffer
2 µL dNTP-Mix [10 mM each]
3 µL primer forward [10 µM]
3 µL primer reverse [10 µM]
2 µL RT-PCR-enzyme-Mix
6 µL template (3-4 µg total RNA)
RNase-free H_2O_{dd} ad 50 µL

The RT-PCR program was initiated by reverse transcriptase catalyzed cDNA synthesis for 30 min at 50 °C. Subsequently, a 15 min incubation step at 95 °C inactivated the reverse transcriptase and activated the Taq-polymerase. The cDNA amplification was then performed by standard PCR (2.3.3.4).

2.4   Biochemical approaches

2.4.1   Determination of protein concentrations

2.4.1.1 Bradford analyses

The protein content of soluble protein preparations or cell extract was measured as described by Bradford (1976). For this purpose, 1 to 10 µg of protein were diluted in 100 µL H_2O_{dd} and supplemented with 900 µL Bradford reagent. Known concentrations of bovine serum albumine (BSA, NEB, Frankfurt/Main) were used as standard. The optical density of the samples was measured at 578 nm and the concentration of the protein solution could be determined by the use of a BSA calibration curve.

Bradford reagent:

35 mg Coomassie Brillant Blue G250, 50 mL phosphoric acid, 25 mL ethanol, H_2O_{dd} ad 500 mL

2.4.1.2 Amido Black analyses

In order to determine the concentration of membrane proteins after affinity purification or reconstitution, the Amido black method (Schaffner and Weissmann, 1973) was used. For this purpose, 1 to 10 µg of protein were diluted in 225 µL H_2O_{dd}. Known concentrations of bovine serum albumine (BSA, NEB, Frankfurt/Main) were used as standard. 30 µL solution 1 and 50 µL solution 2 were added. The samples were mixed and subsequently incubated for 2 min at RT. A nitrocellulose filter (HA membrane filters, pore diameter 0.45 µm, Millipore, Schwalbach) was equilibrated in H_2O_{dd} and placed on the Millipore filter system. The samples were applied as distinct spots on the filter and washed with 200 µL solution 3. After rinsing the filter in another 2 mL solution 3, the samples were dyed for 10 min in Amido Black dye solution. The filter was washed in H_2O_{dd}, decolorized 3 times using solution 4, rinsed again with water, and dried at 60 °C. Each protein spot was then transferred into 1 mL of solution 5 and incubated for 10 min by constant shaking at RT. The optical density of the solutions was measured at 630 nm and the concentration of each sample could be determined by the use of a BSA calibration curve.

Solution 1: 1 M Tris, 2 % SDS, pH (HCl) = 7.4

Solution 2: 90 % TCA

Solution 3: 6 % TCA

Solution 4: 90 % (v/v) methanol, 2 % (v/v) acetic acid

Solution 5: 25 mM NaOH, 50 µM EDTA, 50 % (v/v) ethanol

Amido Black dye solution: 0.25 % (w/v) Amido Black, 45 % (v/v) methanol, 10 % (v/v) acetic acid

2.4.2 SDS-Polyacrylamide Gel Electrophoresis (PAGE)

For the electrophoretic analyses of proteins under denaturing conditions, cell extract, inverted membrane vesicles, isolated proteins, or proteoliposomes were diluted in loading dye and subjected to SDS-PAGE using 12 to 15 % SDS polyacrylamide gels (Laemmli *et al*., 1970).

A 15 % separation gel was composed of:
6 mL separation gel buffer
6 mL H_2O_{dd}
12 mL acrylamide : bisacrylamide (30 : 0.8)
160 µL ammonium persulfate (100 mg/mL)
16 µL TEMED

The stacking gel was composed of:
2.5 mL stacking gel buffer
5.86 mL H_2O_{dd}
1.64 mL acrylamide : bisacrylamide (30 : 0.8)
45 µL ammonium persulfate (100 mg/mL)
15 µL TEMED

Gel electrophoresis was performed in MINI Vertical Dual Plate Electrophoresis Units (Carl Roth GmbH, Karlsruhe) at 50 to 60 V for 45 min and subsequently at 125 to 160 V for 1 to 2 h.

Separation gel buffer: 1.5 M Tris, 0.4 % SDS, pH (HCl) = 8.8

Stacking gel buffer: 0.5 M Tris, 0.4 % SDS, pH (HCl) = 6.76

Loading buffer (1X): 4 % SDS, 12 % glycerol (w/v), 50 mM Tris, 2 % mercaptoethanol (v/v), 0.01 % serva blue G, pH (HCl) = 6.8.

10X Electrophoresis buffer: 250 mM Tris, 1.92 M glycine, 35 mM SDS, pH (HCl) = 8.2 to 8.3

2.4.3 Staining of SDS-gels

2.4.3.1 Coomassie Brilliant Blue staining

By means of SDS-PAGE (2.4.2) separated proteins were routinely made visible by staining in Coomassie Brilliant Blue (Sambrook *et al*., 1989). For this purpose, the SDS-gels were incubated in staining solution for 1 to 16 h, followed by decolorizing of the gels using 10 % acetic acid.

Staining solution: 0.2 % Coomassie Brilliant Blue G-250, 45 % (v/v) methanol, 10 % acetic acid

2.4.3.2 Silver staining

The silver staining of SDS-gels (2.4.2) was carried out as described by Blum *et al*. (1987). For this purpose, the gels were incubated for 1 h in fixing solution, washed 3 times for 20 min in 50 % (v/v) ethanol, pre-treated for 1 min in 0.2 g/L $Na_2S_2O_3$ and subsequently rinsed with H_2O_{dd}. The staining was performed for 20 min, and the gels were shortly developed in water. When reached the desired signal intensity, the staining reaction was stopped in stop solution.

Fixing solution: 50 % (v/v) methanol, 12 % acetic acid, 0.5 mL formaldehyde

Staining solution: 2 g/L $AgNO_3$, 0.75 mL/L formaldehyde

Stop solution: 50 % (v/v) methanol, 12 % (v/v) acetic acid

2.4.4 Immunoblot analyses

The detection of specific proteins was carried out by means of immuno blotting. After SDS-PAGE (2.4.2), the proteins were transferred from the SDS-gels to a PVDF membrane (Millipore Immobilon P, Roth, Karlsruhe) by semi dry blotting. For this purpose, the membrane was first moistened in methanol and then equilibrated in transfer buffer. Subsequently, the membrane was placed on top of six filters (Schleicher & Schüll, Dassel), which were equilibrated in the same buffer. The SDS-gel was applied on top of the membrane and covered with another six filters, which were equilibrated in transfer buffer.

The protein transfer reaction was carried out inside of a semi dry blotter (Pharmacia Biotech, GE Healthcare, München) for 45 min at 0.8 mA / cm^2. After incubation for 60 min in blocking buffer at RT, the membrane was incubated for another 60 min in blocking buffer supplemented with the first antibody (Strep-tag antibody, IBA GmbH, Göttingen, or Penta His antibody, Qiagen, Hilden), using a 1 : 5000 to 1 : 10000 dilution, respectively. After 3 washing steps for 20 min each, the second antibody (Anti-Mouse IgG alkaline phosphatase, Sigma-Aldrich, Deisenhofen), was diluted 1 : 20000 in blocking buffer, and the membrane was incubated for 60 min at RT. After 3 further washing steps (20 min each), the signal detection was achieved by the addition of the alkaline phosphatase substrate BCIP/NBT (final concentration 0.02 % and 0.03 %, Roth, Karlsruhe) in reaction buffer. Depending on the desired signal intensity, the membrane was incubated for 5 to 60 min in the dark, before the reaction was stopped by the addition of H$_2$O$_{dd}$.

Transfer buffer: 10 mM CAPS, 10 % (v/v) methanol, pH (NaOH) = 11

Blocking buffer: 50 mM Tris, 0.15 M NaCl, 3 % (w/v) BSA, pH (HCl) = 7.5

Washing buffer: 50 mM Tris, 0.15 M NaCl, 0.3 % (w/v) BSA, pH (HCl) = 7.5

Reaction buffer: 100 mM Tris, 100 mM NaCl, 5 mM MgCl$_2$, pH (HCl) = 9.5

2.4.5 Identification of MtrB-Strep

The heterologous synthesis of MtrB-Strep in *E. coli* resulted in a partly degradation of the protein. In order to test, if the major fraction of purified MtrB-Strep consists of intact protein, elution fractions after affinity purification were analyzed by means of Edman degradation analyses (Edman *et al*., 1950). The identification of the protein was carried out by the bioanalytics service unit at the *Center for Molecular Medicine Cologne* (ZMMK). For this purpose, the regarding band was excised from a Ponceau Red stained Western blot membrane (2.4.4). The protein was analyzed by the separation of single amino acids from the N-terminus of a protein using the ABI Procise 491-Sequencer.

2.4.6 Purification of MtrA-(His)$_{10}$ by Ni-NTA affinity chromatography

For the isolation and purification of MtrA-(His)$_{10}$, *E. coli* BL21(DE3) cells transformed with pET224b-mtrA (Brocker, unpublished data) were cultivated as described in section 2.2.2. This strain was used to isolate MtrA from *C. glutamicum* fused to a (His)$_{10}$-tag at its C-terminus by chromatography using 2 mL columns of Ni-NTA sepharose (Qiagen, Hilden). The heterologous expression of the *mtrA* gene was induced by the addition of 50 µM IPTG to

the cultures. The cells were harvested 4 h after induction, washed and stored at -20 °C. For further preparation, the cells were thawed on ice, diluted in lysis buffer and disrupted by three passages through a French® Pressure Cell Press (1100 psi, SLM Aminco, Colora, Lorch). The cell debris was removed by centrifugation (13000 X g, 30 min, 4 °C). Prior to the Ni-NTA chromatography, the column was equilibrated in lysis buffer. The supernatant was added with a flow rate adjusted to 0.1 mL/min. The column was washed by the addition of 20 mL wash buffer supplemented with 20 mM imidazole, before MtrA-(His)$_{10}$ was eluted with 10 mL of wash buffer supplemented with 100 mM imidazole. The eluate was collected in 1 mL fractions and dialyzed (MWCO = 8000 Da) against 5 L reaction buffer at 4 °C for 36 h, frozen in liquid nitrogen and stored at -80 °C.

Washing buffer: 50 mM Tris, pH (HCl) = 8.0

Lysis buffer: 50 mM Tris, 300 mM NaCl, 10 % glycerol, 10mM β-mercaptoethanol, 1 tablet/50 mL Complete (Roche Diagnostics, Mannheim), 5 µg/mL Dnase1, pH (HCl) = 8.0

Reaction buffer: 50 mM Tris, pH (HCl) = 8.0

2.4.7 Purification of Strep-MtrB, MtrB-Strep, and truncated derivatives of MtrB-Strep by Strep-tagII/StrepTactin affinity chromatography

For the isolation and purification of Strep-MtrB, MtrB-Strep, and the MtrB-Strep-derivatives MtrBΔ25, -Δ154-, -ΔL124-, and -ΔL134-Strep, *E. coli* BL21(DE3) or -DH5α*mcr* cells transformed with pASK-IBA7-*strep-mtrB* or pASK-IBA3-*mtrB-strep*, -*mtrB*Δ25-, -*mtrB*Δ154-, -*mtrB*ΔL124-, or -*mtrB*ΔL134-*strep* were cultivated as described in section 2.2.2. These strains were used to isolate MtrB from *C. glutamicum* fused to a Strep-tag at its C- or N-terminus, respectively, by Strep-tagII/StrepTactin affinity chromatography. The heterologous expression of the *mtrB* derivatives was induced by the addition of 40 µg/L anhydrotetracycline (AHT) to the cultures. The cells were harvested 3 h after induction, washed (100 mM Tris, pH [HCl] = 7.5) and stored at -20 °C. For further preparation, the cells were thawed on ice, diluted in lysis buffer and disrupted by three passages through a French® Pressure Cell Press (1100 psi, SLM Aminco, Colora, Lorch). The cell debris was removed by centrifugation (13000 X g, 60 min, 4 °C) and the membranes were isolated by ultracentrifugation (223000 X g, 60 min, 4 °C), washed with lysis buffer and collected by ultracentrifugation (223000 X g, 60 min, 4 °C). The membrane pellets were diluted in lysis buffer and adjusted to 50 mM Tris, 10 % glycerol, 10 mM β-mercaptoethanol and 1 mM EDTA, pH (HCl) = 8.0. While stirring at 4 °C, membrane proteins were extracted with *N*-

dodecyl α-D-maltoside (DDM), which was added stepwise until a final concentration of 2 % was reached. After stirring at 4 °C for 30 min, the solubilizate was centrifuged for 20 min at 67000 X g in a Beckman TLX ultracentrifuge (Beckman, Munich, Germany). The supernatant fraction containing solubilized Strep-MtrB or MtrB-Strep, respectively, was purified by Strep-tagII/StrepTactin affinity chromatography (IBA, Göttingen), using a 2-ml column of StrepTactin resin. The column was pre-equilibrated with purification buffer. The supernatant was diluted with four volumes of purification buffer (lacking DDM) before addition to the column to allow binding of proteins to StrepTactin. The flow rate was adjusted to 0.1 ml/min and the chromatography was performed at 4 °C. The column was washed with 40 mL washing buffer and 20 mL purification buffer, before MtrB was eluted with 10 mL purification buffer supplemented with 5 mM desthiobiotin. The eluate was collected in 1 mL fractions, frozen in liquid nitrogen and stored at -80 °C.

Lysis buffer: 100 mM Tris, 1 tablet/25 mL Complete (Roche Diagnostics, Mannheim), 5 µg/mL Dnase1, pH (HCl) = 7.5

Purification buffer: 50 mM Tris, 200 mM NaCl, 10 % glycerol, 10 mM β-mercaptoethanol, 0.1 % DDM, pH (HCl) = 8.0

Washing buffer: 50 mM Tris, 500 mM NaCl, 10 % glycerol, 10 mM β-mercaptoethanol, 0.1 % DDM, pH (HCl) = 8.0

2.4.8 Purification of MtrBΔ190 by Strep-tagII/StrepTactin affinity chromatography

The MtrB-Step derivative MtrBΔ190-Strep only consists of the soluble part of MtrB. The heterologous synthesis of this protein in *E. coli* DHα*mcr*, the collection of the cells, and subsequent cell rupture was performed as described in section 2.4.7. After separation from the cell debris (compare section 2.4.7), Triton-X-100 was added stepwise to a final concentration of 0.5 % in order to separate possibly membrane-associated MtrBΔ190 from the cytoplasmic membrane.

The Strep-tagII/StrepTactin-column was pre-equilibrated with purification buffer, before the crude extract was added to allow binding of MtrBΔ190 to StrepTactin. The flow rate was adjusted to 0.1 ml/min and the chromatography was performed at 4 °C. The column was washed with 100 mL washing buffer and 50 mL purification buffer, before MtrB was eluted with 10 mL purification buffer supplemented with 5 mM desthiobiotin. The eluate was collected in 1 mL fractions, frozen in liquid nitrogen and stored at -80 °C.

Purification buffer: 100 mM Tris, 1 mM EDTA, 10 % glycerol, pH (HCl) = 8.0

Washing buffer: 100 mM Tris, 500 mM NaCl, 1 mM EDTA, 10 % glycerol, pH (HCl) = 8.0

2.4.9 Purification of (His)$_6$-DcuS by Ni-NTA affinity chromatography

For the overexpression and isolation of (His)$_6$-DcuS, a pET28a vector containing the *dcuS* gene fused to the sequence encoding a His$_6$-tag at the N-terminus of the DcuS protein, called pMW151 (Janausch *et al*., 2002, kindly provided by Unden, G., University of Mainz), was transformed into *E. coli* BL21(DE3). The cells were cultivated as described in section 2.2.2. The homologous expression of *dcuS* was induced using 1mM IPTG, and the cells were harvested after 3 h of cultivation. The cell disruption and membrane preparation were carried out as described for MtrB in section 2.4.7. The membrane fractions were adjusted to 50 mM Tris, 10 % glycerol, 2 mM β-mercaptoethanol, 1 mM EDTA and 2 % DDM, pH (HCl) = 8.0. The solubilization of the membrane proteins was performed as with MtrB (2.4.7) and the resulting fraction was loaded on Protino® Ni prepacked columns (Macherey-Nagel, Düren). After several washing steps (2.4.7) the bound protein was eluted in 10 mL elution buffer, collected in 1 mL fractions, frozen in liquid nitrogen and stored at -80 °C.

Elution buffer: 50 mM Tris, 200 mM NaCl, 10 % glycerol, 10 mM β-mercaptoethanol, 0.1 % DDM, 250 mM imidazole, pH (HCl) = 8.0

2.4.10 Preparation of inverted membrane vesicles (IMV) enriched with Strep-MtrB or MtrB-Strep

For the investigation of the kinase activity of Strep-tagged MtrB, the ATP-dependent autophosphorylation was measured. Since the membrane bound bacterial ATP synthase is known to interfere with ATP-dependent reactions (Jung, personal communication), the ATP synthase deficient strain *E. coli* DK8 (Klionsky *et al*., 1984) was chosen for the analysis of MtrB in membrane vesicles. For the heterologous expression of *mtrB* fused to the sequence encoding a C- or N-terminal Strep-tag, respectively, the cells were cultivated as described in section 2.2.2 and gene expression was induced by the addition of 40 μg/L AHT. After 2 h of growth, cells were harvested by centrifugation, washed and stored at -20 °C. For further preparation, the cells were thawed on ice and diluted in lysis buffer. Membrane vesicles were prepared by three passages through a French® Pressure Cell Press (1100 psi, SLM Aminco, Colora, Lorch) and centrifuged at 13000 X g for 30 min to remove unbroken cells. Membranes were isolated by ultracentrifugation (223000 X g, 60 min, 4 °C), washed with

lysis buffer and collected by ultracentrifugation (223000 X g, 60 min, 4 °C). The IMV were adjusted to 20 mg/mL in reaction buffer, frozen in liquid nitrogen and stored at -80 °C.

Lysis buffer: 100 mM Tris, 1 tablet/25 mL Complete (Roche Diagnostics, Mannheim), 5 µg/mL DNase1, pH (HCl) = 7.5

Reaction buffer: 50 mM Tris, 10 % glycerol, pH (HCl) = 8.0

2.4.11 Reconstitution of Strep-MtrB, MtrB-Strep, truncated derivatives of MtrB-Strep, or (His)$_6$-DcuS into *E. coli* lipid liposomes

Liposome preparation

For the preparation of liposomes, *E. coli* phospholipids (polar lipid extract, 20 mg/mL in chloroform, Avanti polar lipids, Alabaster, AL), or synthetic phosphoatidylglycerols (POPG, 1-Palmitoyl-2-Oleoyl-*sn*-Glycero-3-[Phospho-*rac*-(1-glycerol)], 16:0-18:1, Avanti polar lipids, Alabaster, AL) were first dried in a rotary evaporator, and then lyophilized for 16 h. Subsequently, the lyophilized lipids were dissolved in 100 mM potassium P$_i$, 2 mM β-mercaptoethanol, pH = 7.5, to a final concentration of 20 mg of phospholipids/mL, frozen in liquid nitrogen and stored at -80 °C. To avoid oxidation, the lipids were kept under a nitrogen atmosphere during preparation. Prior to use, liposomes were formed by extrusion (Liposofast, Avestin, Ottawa, Canada) 14 to 20 times through polycarbonate filters (pore diameter 400 nm).

Reconstitution of Strep-MtrB, MtrB-Strep, truncated derivatives of MtrB-Strep, or (His)$_6$-DcuS into *E. coli* liposomes

The purified sensor kinases were reconstituted as described by Rigaud *et al*., (1995). *E. coli* lipids prepared from *E. coli* polar lipid extract (Avanti polar lipids, Alabaster, AL) were diluted in extrusion buffer to a concentration of 5 mg/mL and extruded (Liposofast; Avestin, Ottawa, Canada) 14 to 20 times through polycarbonate filters (pore diameter 400 nm). The liposomes were solubilized by stepwise addition of 20 % (v/v, in extrusion buffer) Triton-X-100. The insertion of detergent was followed by measurement of the turbidity at 540 nm. Upon saturation with detergent, the liposomes were incubated for 20 min at RT and subsequently mixed with Strep-MtrB, MtrB-Strep, MtrBΔ25-, -Δ154-, -ΔL124-, and -ΔL134-Strep, or (His)$_6$-DcuS in elution buffer at a lipid-to-protein ratio of 20 : 1 (w/w). The mixture was incubated for 35 min at RT under gentle stirring. To remove detergent, Bio-Beads, pre-washed with H$_2$O$_{dd}$, were added at a Bio-Bead (wet weight, filter-dried) : Triton X-100 ratio of 5 and a Bio-Bead :

DDM ratio of 10 (w/w). The mixture was kept under gentle stirring at room temperature for 1 h, and the same amount of fresh Bio-Beads was added. After 1 h of gentle stirring, the double amount of fresh Bio-Beads was added, and the mixture was stirred at 4 °C. After 16 h, the single amount of Bio-Beads was added and the mixture was gently stirred for 1 h at 4 °C. Subsequently, the supernatant was centrifuged at 337000 X g in a Beckman TLX ultracentrifuge (Beckman, Munich, Germany), extruded 14 to 20 times through polycarbonate filters (pore diameter 400 nm) in reaction buffer and washed with the same buffer. The proteoliposomes were adjusted to 0.8 to 1 µg/µL in reaction buffer, frozen in liquid nitrogen, and stored at –80 °C.

Extrusion buffer: 100 mM potassium P_i buffer, pH = 7.5

Reaction buffer: 50 mM Tris, 10 % glycerol, pH (HCl) = 8.0

2.4.12 Variation of the lipid composition

To vary the membrane composition in the liposome system, proteoliposomes made from *E. coli* phospholipids (2.4.10) were fused with liposomes composed of synthetic phospholipids. The fraction of synthetic lipids was adjusted to 33 % of the total lipid content of the preparation. For this purpose proteoliposomes were prepared as described in section 2.4.10 with a lipid-to-protein ratio of 13 : 1 (w/w). These proteoliposomes were mixed with POPG (1-Palmitoyl-2-Oleoyl-*sn*-Glycero-3-[Phospho-*rac*-(1-glycerol)], 16:0-18:1, Avanti polar lipids, Alabaster, AL) liposomes (2.4.10) in the indicated ratio and extruded (14 to 20 times) before they were frozen in liquid nitrogen and stored at -80 °C.

2.4.13 Determination of the orientation of reconstituted MtrB-Strep by site-specific proteolysis

The accessibility of the C-terminal domain of MtrB-Strep was measured both, using intact and solubilized proteoliposomes. For this purpose, proteoliposomes enriched with MtrB-Strep were diluted in citrate buffer (pH = 6), in order to meet the conditions required for peptidase activity, and extruded 14 to 20 times in the same buffer. Subsequently, 2.25 µg of reconstituted MtrB were diluted in citrate buffer to a final volume of 20 µL. The reaction was performed in the presence or absence of 0.2 µg/µL carboxypeptidase Y and 1 % Triton-X-100. Proteolysis was carried out at 25 °C. At given time intervals the reaction was stopped by addition of SDS loading buffer (section 2.4.2). The proteins were subjected to SDS-PAGE (12 %, compare section 2.4.2) and gels were either stained with Coomassie Blue or immunoblot analysis was performed using a Strep-tag antibody (compare section 2.4.4).

2.4.14 Phosphorylation assays

Autophosphorylation of Strep-MtrB, MtrB-Strep, truncated derivatives of MtrB-Strep, or (His)$_6$-DcuS in proteoliposomes or inverted membrane vesicles (IMV)

To test autophosphorylation activity of membrane bound Strep-MtrB, MtrB-Strep, or (His)$_6$-DcuS, 1.6 to 2 µg reconstituted sensor kinase, or 75 µg total protein in IMV, were diluted into 50 mM Tris, 1 mM DTT, 5 to 10 mM MgCl$_2$, pH (HCl) = 8.0 to a final volume of 10 µL. If indicated, autophosphorylation activity was determined in the presence of various solutes. For this purpose, proteoliposomes were prepared in two ways:

I) The proteoliposomes were slowly thawed at RT, diluted in 950 µL reaction buffer, and extruded 14 to 20 times through polycarbonate filters (pore diameter 400 nm). Subsequently, the proteoliposomes were collected by ultracentrifugation (337000 X g in a Beckman TLX ultracentrifuge, Beckman, Munich, Germany) and adjusted to the desired concentration with reaction buffer.

II) To achieve an equal concentration of macromolecules in the lumen and exterior, the samples were frozen rapidly in liquid nitrogen and slowly thawed at 22 °C for three cycles. After the final thawing the proteoliposomes were kept for 1 h at 22 °C.

The autophosphorylation reaction was initiated by the addition of 0.22 µM [γ^{33}P]ATP (110 TBq mmol^{-1}) and the samples were incubated at 30 °C. At the indicated time points, the reaction was stopped by the addition of 9 µL 2.4X SDS loading buffer, and the samples were directly subjected to SDS-PAGE. The gels were dried and exposed to storage Phosphor Imaging Plates (BAS-IP MP 2025, Fujifilm, Düsseldorf). Phosphorylation of proteins was detected by the use of a phosphorimager (Fujifilm BAS-1800, Fujifilm, Düsseldorf). For quantification of the phosphorylation signals, PcBAS version 2.09c was used.

Phosphotransfer from membrane-bound Strep-MtrB or MtrB-Strep to MtrA-(His)$_{10}$

To analyze the MtrB-MtrA phosphotransfer activity *in vitro*, 2 µg of reconstituted Strep-MtrB or MtrB-Strep were diluted into 50 mM Tris, 2 mM DTT, 10 mM MgCl$_2$, 20 mM KCl, pH (HCl) = 8.0 to a final volume of 10 µL. If indicated, phosphotransfer activity was determined in the presence of various solutes. The samples were frozen rapidly in liquid nitrogen and slowly thawed at 22 °C for three cycles. After the final thawing the proteoliposomes were kept for 1 h at 22 °C. MtrB autophosphorylation was initiated by the addition of 0.22 µM [γ^{33}P]ATP (110 TBq mmol^{-1}). After incubation at 30 °C for 10 min, purified MtrA-(His)$_{10}$ was added with a 4 : 1 MtrA (132 pmol) : MtrB (33 pmol) ratio for further incubation at 30 °C. At the indicated time points, the reaction was stopped by the addition of 9 µL 2.4X SDS loading buffer, and the samples were directly subjected to SDS-PAGE.

Dephosphorylation of MtrA by membrane-bound MtrB-Strep

To measure phosphatase activity of membrane-bound MtrB, 16 µg of reconstituted MtrB-Strep were diluted into the buffer described in 2.4.12.2 supplemented with 0.5 M KCl to a final volume of 100 µL. MtrB autophosphorylation (2.4.12.1) was performed for 10 min at 30 °C. Subsequently, 34 µg of MtrA were added and the phosphotransfer reaction (2.4.12.2) was performed for 20 min at the same temperature. For purification of phosphorylated MtrA, the MtrB containing proteoliposomes were removed by ultracentrifugation (2.4.12.1). Subsequently, $[\gamma^{33}P]$ATP was removed from the supernatant by gel filtration (NAP-5^{TM} columns, Amersham Biosciences, Freiburg). Purified phosphorylated MtrA (34 µg) was eluted in 1 mL 50 mM Tris, 2 mM DTT, 0.5 M KCl, pH (HCl) = 8.0. For the MtrB catalyzed dephosphorylation of MtrA, 200 µL of the eluate (6.8 µg MtrA) were supplemented with 20 mM $MgCl_2$ and, if indicated, 1.6 mM ADP, before IMV (1.075 mg total protein) enriched with MtrB-Strep were added. The dephosphorylation reaction was performed for 1 to 60 min at 30 °C.

Reaction buffer: 50 mM Tris, pH (HCl) = 8.0

2.4.15 Fluorescence assays

Determination of high osmolarity induced shrinkage of *E. coli* polar lipid extract liposomes

The measurement of high osmolarity induced shrinkage of *E. coli* lipid liposomes was performed as described by Racher *et al*. (2001). For this purpose, *E. coli* lipid (2.4.10) was slowly thawed at RT and collected by ultracentrifugation (2.4.12). 10 mM Calcein (Invitrogen/Molecular Probes, Karlsruhe) was diluted in 20 mM sodium P_i, 50 mM KCl, pH = 7.4. The pH value of the calcein solution was adjusted to 7.2 by stepwise addition of 1 M KOH. The *E. coli* lipid was dissolved in the calcein solution to a concentration of 250 mg/mL, and extruded 14 to 20 times through polycarbonate filters (pore diameter 400 nm) to entrap 10 mM calcein in the liposomal lumen. External calcein was removed by three gel filtration steps using G75 sepharose (Amersham Biosciences, Freiburg) columns. Calcein-loaded liposomes were eluted in 1 mL 20 mM sodium P_i buffer, 100 mM KCl, pH = 7.4. Fluorescence measurements were made with an Aminco Bowman Series 2 Spectrometer (SLM Aminco, Büttelborn) at an excitation wavelength of 495 nm and an emission wavelength of 520 nm (slit width of 8 nm). Osmotic upshifts were imposed by diluting 5 to 15 µL calcein-loaded liposomes (5 mg/mL lipid) into 500 µL reaction buffer with or without added osmolyte in a 1 mL cuvette. Samples were kept at RT.

Determination of MgCl$_2$-induced permeabilization of *E. coli* polar lipid extract liposomes

For the determination of the effect of MgCl$_2$ on *E. coli* polar lipid extract liposomes, liposomes were loaded with the fluorescein derivatives 5,6-carboxyfluorescein or calcein, repectively, as described above for calcein. The fluorescein derivatives were previously diluted in 50 mM Tris-, 5 mM HEPES-, or 20 mM Sodium Pi-buffer, and the pH value was adjusted to 7.4 using KOH. After removal of external calcein or 5,6-carboxyfluorescein by gel filtration, the liposomes were diluted in 1 mL buffer of the respective buffer. Subsequently, various concentrations of MgCl$_2$ were added, ranging from 0.02 to 10 mM. The samples were incubated for 1 to 30 minutes in the dark and fluorescence was monitored as described above.

2.4.14 Determination of the osmolality

For the determination of the osmolality of buffers and media, a freezing point osmometer (Osmomat 030, Gonotc, Berlin) was used as recommended by the supplier. 9.463 g NaCl / kg H$_2$O$_{dd}$ (300 mosm) served as standard.

3.   Results

The MtrB-MtrA two-component system of *Corynebacterium glutamicum* was shown to play an important role in the osmostress response of this bacterium, mediating the transcription regulation of osmostress-related genes in response to hyperosmotic stress conditions. In addition, this system turned out to be involved in the chill stress response of *C. glutamicum*. MtrBA was shown to mediate the expression regulation of genes of the chill stress regulation in response to exposure to low temperature (Möker *et al*., 2004; Özcan, 2003). Consequently, the sensor histidine kinase of this system, MtrB, may act as sensor for osmo- as well as chill stress. The work described in the following focused on the detailed characterization of the sensory properties of the MtrB-MtrA two-component system.

3.1   Development of *in vitro* phosphorylation assays for the MtrB-MtrA two-component system

The MtrBA two-component system is composed of the sensor histidine kinase MtrB and the response regulator MtrA. Starting from a putative GTG codon, the *mtrB* gene encodes a 499 amino acid protein containing two predicted transmembrane helices, extending from residues 5 to 24 and 171 to 191, which enclose a periplasmic domain of 144 amino acids, and a cytoplasmic C-terminal tail of 310 amino acids (Fig. 7). The C-terminal soluble part of MtrB comprises a HAMP-linker domain (residues 192 to 244) and a kinase core with the dimerization domain (residues 253 to 319) as well as the catalytic or ATP/ADP-binding phosphotransfer domain (residues 365 to 476, Fig. 7). Sequence alignments revealed that the kinase core of MtrB comprises all conserved histidine kinase homology boxes (Grebe and Stock, 1999) including the H-box, which contains the highly conserved histidine residue (position 262), as well as the X-, N-, D-, and G-box (Fig. 7). Consequently, MtrB belongs to the HPK1a family of histidine kinases (Grebe and Stock, 1999). The *mtrA* gene presumably encodes a soluble 226 amino acid protein consisting of an N-terminal receiver domain (residues 6 to 117) and a C-terminal helix-turn-helix motif containing DNA-binding domain (residues 145 to 222), belonging to the OmpR family of response regulators.
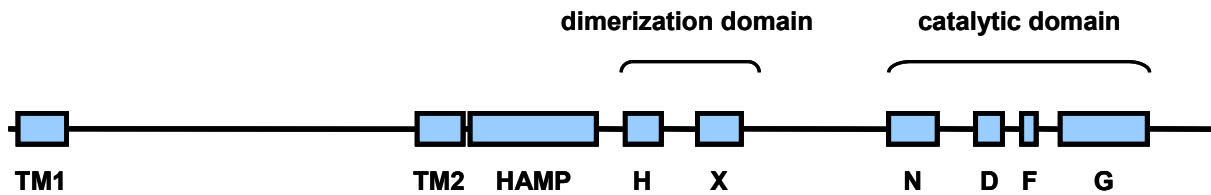
Fig. 7: Sequence-based predicted MtrB domains. Shown are the putative transmembrane (**TM**) domains, the **HAMP**-linker domain, the dimerization-, as well as the catalytic domain, comprising the **H**-, **X**- **N**-, **D**-, **F**-, and **G**-homology boxes published by Grebe and Stock (1999).

For a detailed analysis of the two-component system, it was necessary to establish a functional *in vitro* phosphorylation assay for MtrB and MtrA activity. This required the heterologous synthesis of MtrA in *E. coli* and the subsequent purification of the response regulator. For the analysis of the membrane-spanning sensor histidine kinase, it was further necessary to provide an *in vitro* membrane system. For this purpose MtrB enriched inverted *E. coli* membrane vesicles (IMV) and proteoliposomes made from *E. coli* lipid were chosen. The prerequisites for development of the *in vitro* membrane systems were the heterologous synthesis of MtrB in *E. coli* and the subsequent isolation of the sensor protein.

3.1.1 Heterologous synthesis and affinity purification of MtrA-(His)$_{10}$

For the isolation and purification of MtrA, the plasmid pET224b-mtrA (kindly provided by M. Brocker, Forschungszentrum Jülich) was chosen. In this expression vector, the *mtrA* gene is fused to the sequence encoding a (His)$_{10}$-tag at its 3´end, resulting in a C-terminal fusion of the encoded protein. After transformation of this plasmid into *E. coli* BL21(DE3), the cells were cultivated as described in section 2.2.2. Gene expression was induced by the addition of IPTG. Various induction parameters (including cultivation temperature, IPTG concentration, and induction time) were examined with regard to optimal conditions for heterologous synthesis of the response regulator. The highest amount of cytoplasmic MtrA-(His)$_{10}$ was achieved when the cells were cultivated at 25 °C, and the induction of gene expression was initiated using 50 µM IPTG (data not shown). In Figure 8, the protein content of lysed cells collected before (lane 1) and 4 hours after induction (lane 2) is shown after separation by means of SDS-PAGE. These induction conditions resulted in a high concentration of a 25 kDa protein. This value matches with the expected molecular mass of MtrA. For the purification of MtrA, cells were harvested 4 hours after induction, washed and disrupted by three passages through a French® Pressure Cell Press (1100 psi, SLM Aminco, Colora, Lorch). Isolation of the protein was performed as described in section 2.4.6 via Ni-NTA chromatography. Using the given conditions it was possible to efficiently purify MtrA-(His)$_{10}$ (Fig. 8). This was verified by means of immunoblot analysis using a Penta-His

antibody (data not shown). Starting from a 333 mL culture a total yield of approximately 6 mg could be achieved.
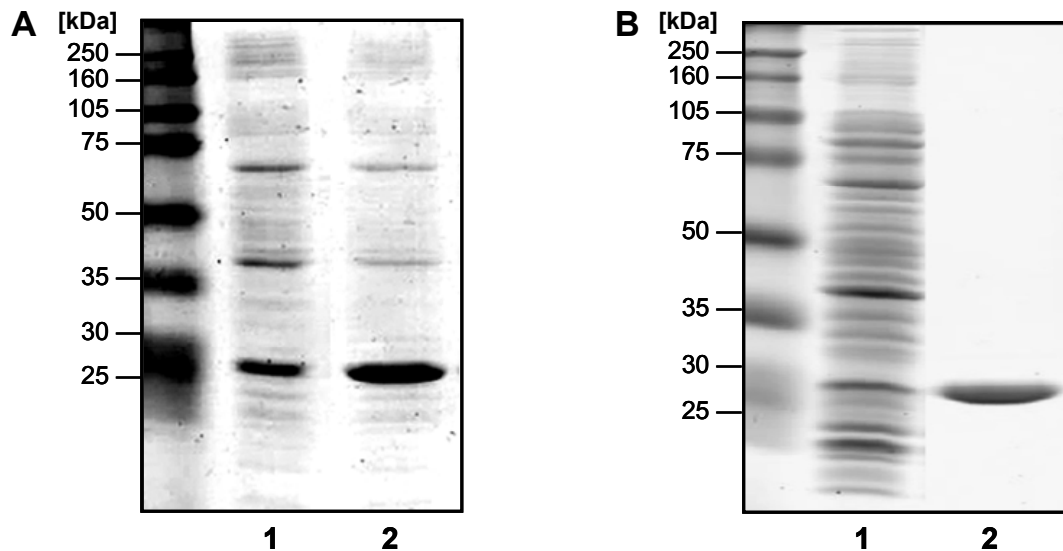
Fig. 8: SDS-PAGE after heterologous synthesis (A) and affinity chromatography (B) of MtrA-(His)$_{10}$. A MtrA-(His)$_{10}$ synthesis in *E. coli* BL21(DE3)/pET224b-mtrA cells before (**1**) and 4 hours (**2**) after induction using 50 µM IPTG. **B** Affinity purification of MtrA-(His)$_{10}$ via Ni-NTA columns. Shown is the crude extract (**1**) and one elution fraction (**2**). Left lanes: Full-range Rainbow™ molecular mass (kDa) marker (GE Healthcare, München).

3.1.2 Heterologous synthesis of MtrB in *E. coli*

Both, the preparation of inverted membrane vesicles, as well as the isolation of the sensor kinase, required the heterologous synthesis of MtrB in *E. coli*. For this purpose, the *mtrB* gene was cloned in frame into pASK-IBA expression vectors in two ways, resulting in a 3´- as well as a 5´-end fusion to the sequence encoding a Strep-tag. The detailed construction of the two expression vectors is described in the appendix (section 7.3). After transformation of the resulting plasmids into *E. coli* BL21(DE3), or -DH5α*mcr*, respectively, the cells were cultivated as described in section 2.2.2. The *mtrB* expression was induced by addition of anhydrotetracycline (AHT) to the cultures and samples were collected before (T$_0$), and 1 to 4 h (T$_1$ to T$_4$) after induction. In the following, the MtrB derivative containing the C-terminal Strep-tag will be referred to as MtrB-Strep, whereas the term Strep-MtrB indicates the MtrB derivative carrying an N-terminal Strep-tag. After separation of the total protein content via SDS-PAGE, Strep-MtrB and MtrB-Strep were detected by means of immunoblot analysis using a Strep-tag antibody (IBA-GmbH, Göttingen). As demonstrated in Figure 9 for *E. coli* DH5α*mcr* synthesizing MtrB-Strep, the heterologous synthesis of both MtrB derivatives was

successful. In both cases, the 56 kDa protein signal corresponding to the predicted molecular mass of MtrB could be made visible. However, the analysis resulted in further distinct protein signals with molecular masses lower than expected for the MtrB protein. Immunoblot analysis using raw extract of similarly treated *E. coli* cells containing the empty pASK-IBA3 or -7 vectors, respectively, lacked all protein signals which were obtained with MtrB comprising cells (data not shown). Consequently, the additional protein signals corresponded to degradation fragments of the sensor kinase, and not to non-specific protein signals due to cross-reaction of the Strep-tag antibody. Cells were lysed with SDS directly after harvesting, which resulted in the fast inactivation of *E. coli* proteases. Thus, MtrB degradation could be shown to occur during heterologous synthesis, and not during subsequent preparation steps. The heterologous synthesis of membrane proteins can in general be problematic. Obviously the synthesis of Strep-MtrB and MtrB-Strep in *E. coli* both resulted in partial degradation of the membrane proteins. Protein stability could neither be improved by the use of alternative *E. coli* strains, e. g. *E. coli* BL21(DE3) or -DK8, nor by various induction or cultivation conditions (data not shown). The amount of heterologously expressed MtrB turned out to be highest in *E. coli* BL21(DE3). Consequently, this strain was used for the isolation of the sensor kinase.
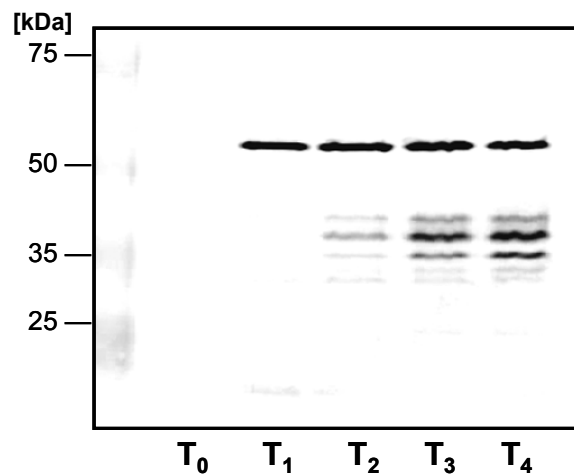
Fig. 9: Heterologous synthesis of MtrB-Strep in *E. coli* DH5α*mcr*. Shown is the crude extract before (**T₀**) and 1 to 4 hours (**T₁** to **T₄**) after induction using 200 µg/L AHT. Detection was performed by means of immunoblot analyses using a Strep-tag antibody. Left lane: Full-range Rainbow™ molecular mass (kDa) marker (GE Healthcare, München).

Various induction parameters (including cultivation temperature, IPTG concentration, and induction time) were altered during heterologous expression experiments to optimize membrane integration of the sensor kinase. The highest amount of membrane-bound MtrB

was achieved when cells were cultivated at 30 °C, and the induction of *mtrB* expression was initiated using 40 µg/L AHT (data not shown).

3.1.3 Production of MtrB-enriched *E. coli* inverted membrane vesicles

Bacterial histidine kinases generally catalyze the ATP-dependent autophosphorylation reaction of a conserved histidine residue resulting in a phosphoimidazole. The histidine kinase activity of MtrB was measured as the autophosphorylation in presence of $[\gamma^{33}P]$ATP using inverted membrane vesicles enriched with Strep-MtrB or MtrB-Strep, respectively.

Since the membrane-bound bacterial ATP synthase is known to interfere with ATP-dependent reactions (K. Jung, personal communication), the ATP synthase deficient strain *E. coli* DK8 (Klionsky *et al.*, 1984) was chosen. For the heterologous synthesis of MtrB, *E. coli* DK8/pASK-IBA7-strep-mtrB or -IBA3-mtrB-strep cells were cultivated as described in section 2.2.2, and gene expression was induced by addition of 40 µg/L AHT. Cells were harvested after 2 h of cultivation and the membrane fractions were isolated as described in section 2.4.10, and subsequently adjusted to 20 mg total protein/mL. This preparation of the *E. coli* membranes using a French® Pressure Cell Press has been shown to result in membrane vesicles carrying transmembrane proteins in an inside-out orientation (Siebers and Altendorf, 1988). Western blot analysis revealed that, as already shown for *E. coli* DH5α*mcr* cells, in DK8 both MtrB derivatives were found in the membrane fraction and underwent partial degradation during heterologous synthesis (data not shown). These preparations were used for the *in vitro* MtrB phosphorylation assay. DK8 cells transformed with the empty pASK-IBA7 and -IBA3 vectors, which were treated identically, lacked the respective protein signals after immunoblot analyses (data not shown) and served as negative control.

3.1.4 Autophosphorylation activity of MtrB in inverted membrane vesicles

The test assay for investigation of the autophosphorylation activity of MtrB basically followed the method described by Nakashima *et. al.* (1993). The ATP-dependent MtrB autokinase activity was analyzed by incubation of membrane vesicles in presence of $[\gamma^{33}P]$ATP for 10 min at 30 °C. The reaction was stopped by the addition of SDS loading buffer. Samples were directly subjected to SDS-PAGE, the gels were dried and subsequently exposed to Phosphor Imaging plates to determine the radioactive signals using a phosphorimager (see section 2.4.14). As control, membrane vesicles prepared from *E. coli* cells transformed with the empty pASK-IBA vectors were treated identically. The resulting phosphorylation image (Fig. 10) shows, that distinct protein phosphorylation signals are present using IMV enriched with MtrB-Strep, which are lacking in the negative control. Comparison to immunoblot analyses

proves that MtrB, and furthermore some of the degradation fragments, exhibited autophosphorylation activity in inverted membrane vesicles (Fig. 10). Thus, MtrB was functionally integrated into the *E. coli* cytoplasmic membrane, and the inverted membrane vesicle system provides a test assay for the *in vitro* MtrB autophosphorylation activity. However, in addition to the MtrB-corresponding phosphorylation signals, a number of prominent phosphorylation signals corresponding to *E. coli* membrane proteins were present in the phosphorylation image (Fig. 10). For this reason it was necessary to further reduce the complexity of the *in vitro* membrane system.
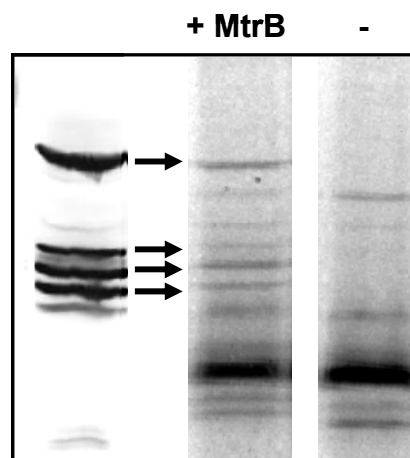
Fig. 10: Detection of *in vitro* autophosphorylation activity of MtrB-Strep in *E. coli* DK8 membrane vesicles. 75 µg of total protein in membrane vesicles were diluted in phosphorylation buffer (50 mM Tris, 2 mM DTT, 5 mM MgCl$_2$, 100 mM KCl, pH (HCl) = 8.0) to a final volume of 10 µL. Autophosphorylation of MtrB was initiated by the addition of 0.25 µM [γ^{33}P]ATP (110 TBq mmol^{-1}). Shown are phosphorylation signals in comparison to immunoblot analyses of MtrB in inverted membrane vesicles (left lane). The arrows indicate putative MtrB signals present in MtrB containing MV (**+MtrB**) and lacking in the negative control (**-**).

3.1.5 Preparation of proteoliposomes enriched with MtrB

In contrast to inverted membrane vesicles, in the proteoliposome system only membrane-bound MtrB is present. This means that all reactions which are monitored occur as a consequence of the presence of MtrB and not of additional non-specific proteins. The prerequisite for the preparation of proteoliposomes enriched with MtrB was the purification of the sensor protein.

3.1.5.1 Affinity purification of Strep-MtrB and MtrB-Strep

For the isolation and purification of the histidine kinase, *E. coli* BL21(DE3) cells transformed with pASK-IBA7-strep-mtrB or pASK-IBA3-mtrB-strep were cultivated as described in section

2.2.2. The *mtrB* expression was induced using 40 µg/L AHT and cells were harvested 2 to 3 hours after induction. After isolation of the cytoplasmic membranes, MtrB was extracted by stepwise addition of *N*-dodecyl α-D-maltoside (DDM) until a final concentration of 2 % was reached. The solubilizate was centrifuged and the supernatant fraction containing solubilized Strep-MtrB or MtrB-Strep, respectively, was used for Strep-tagII/StrepTactin affinity chromatography (compare section 2.4.7). It could be verified by SDS-PAGE and immunoblot analysis, that both MtrB derivatives were predominantly found in the membrane fraction. Furthermore, the solubilization using 2 % DDM as well as the StrepTactin binding of Strep-MtrB and MtrB-Strep turned out to be efficient (data not shown) under the given conditions.

The total yields after affinity purification differed between Strep-MtrB and MtrB-Strep. From 4.8 L of *E .coli* BL21(DE3) cultures each, 0.22 mg Strep-MtrB and 1.1 mg MtrB-Strep were obtained. SDS-PAGE of the resulting elution fractions (Fig. 11, lane 2) indicated, that those MtrB degradation fragments which still contain the intact C- or N-terminal Strep-tag, respectively, were co-purified. Comparison of the Coomassie-stained SDS-gels with immunoblot analyses (Fig. 11, lane 2 and 3) proves that the additional protein signals in the elution fragments indeed correspond to MtrB degradation fragments, and not to non-specific *E. coli* proteins.
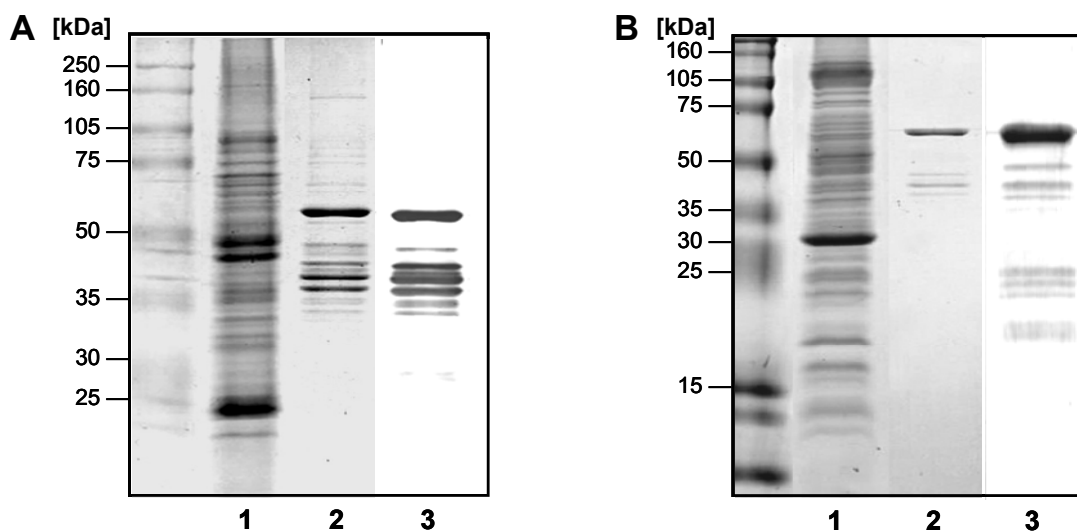
Fig. 11: Affinity purification of MtrB-Strep (A) and Strep-MtrB (B) via StreptagII/Streptactin columns. Shown are the crude extract (**1**) and an elution fraction after SDS-PAGE (**2**) and subsequent immunoblot analyses (**3**) using a Strep-tag antibody. Left lanes: Full-range Rainbow[TM] molecular mass (kDa) marker (GE Healthcare, München).

The major part of the elution fractions consisted of the 55-60 kDa protein shown in Figure 11, thus corresponding to the expected molecular mass of intact MtrB (56 kDa). As additional control, this protein band was examined by amino acid sequencing (Edmann degradation, see section 2.4.5). These studies revealed that 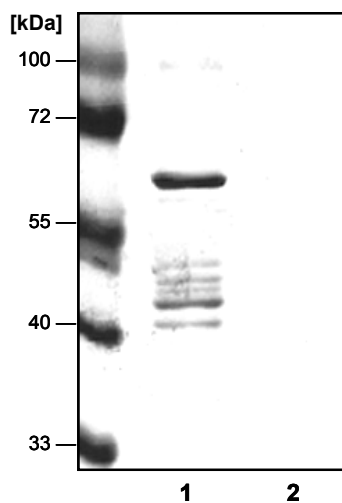the main part of isolated MtrB-Strep indeed consists of full-length MtrB-Strep. Consequently, these fractions could be used for the preparation of MtrB-enriched proteoliposomes.

3.1.5.2 Reconstitution of Strep-MtrB and MtrB-Strep into *E. coli* lipid liposomes

The reconstitution of MtrB-Strep and Strep-MtrB basically followed the method of Rigaud *et al*. (1995). *E. coli* polar lipid extract lipids (Avanti polar lipids, Alabaster, AL) were diluted in 100 mM potassium P_i (pH = 7.5) to a final concentration of 5 mg/mL and extruded 14 to 20 times through polycarbonate filters (pore diameter 400 nm) in order to form liposomes. The resulting liposomes were solubilized by stepwise addition of Triton-X-100, and subsequently mixed with Strep-MtrB or MtrB-Strep, respectively, in a lipid : protein ratio of 20 : 1 (w/w). After removal of the detergent (section 2.4.11), proteoliposomes were collected by ultracentrifugation and washed by extrusion and further ultracentrifugation steps. Subsequent to reconstitution, both MtrB derivatives were found in the liposome fraction as shown in Figure 12 for MtrB-Strep. The lack of MtrB in the supernatant fraction after the first ultracentrifugation step (Fig. 12) indicates that the reconstitution was efficient. Using this method, proteoliposomes enriched with MtrB in an average final concentration of 1 µg/µL were achieved.

Fig. 12: Reconstitution of MtrB-Strep into *E. coli* liposomes. Shown are the proteoliposome fraction (**1**) and the supernatant after the first ultra-centrifugation of the proteoliposomes (**2**). Left lane: PageRuler[TM] protein ladder (kDa, MBI Fermentas, St. Leon-Roth).

3.1.6 Autophosphorylation activity of MtrB in proteoliposomes

In order to determine autophosphorylation activity of MtrB-Strep after purification and subsequent reconstitution into *E. coli* liposomes, the membrane-bound sensor kinase was incubated in presence of $[\gamma^{33}P]ATP$. To achieve a defined diameter of the membrane system, proteoliposomes were, prior to use, extruded 14 to 20 times through polycarbonate filters (pore diameter 400 nm) and subsequently washed by centrifugation. The autokinase activity

of MtrB enriched in proteoliposomes was determined in relation to the reaction time. Samples were taken at different time points and the time course of autophosphorylation was followed over 45 min at 30 °C.

Using the proteoliposome system it could be shown that MtrB exhibits autophosphorylation activity *in vitro* (Fig. 13). As already observed with inverted membrane vesicles, not only intact MtrB-Strep, but also some of the degradation fragments, still exhibited autokinase activity (Fig. 13). For quantification of MtrB autophosphorylation using PcBAS (version 2.09c) only those signals corresponding to intact MtrB were considered. The phosphorylation signal intensities strongly increased with the incubation time monitored in this assay. Figure 13 furthermore shows that, over the first 30 minutes, the relation between MtrB autophosphorylation and the reaction time was almost linear. The $t_{0.5}$ value obtained for MtrB autophosphorylation was approximately 15 minutes. Here, the time dependence of phosphorylation of MtrB-Strep is shown, however, the reconstituted Strep-MtrB derivative also showed autokinase activity under the chosen conditions (data not shown).
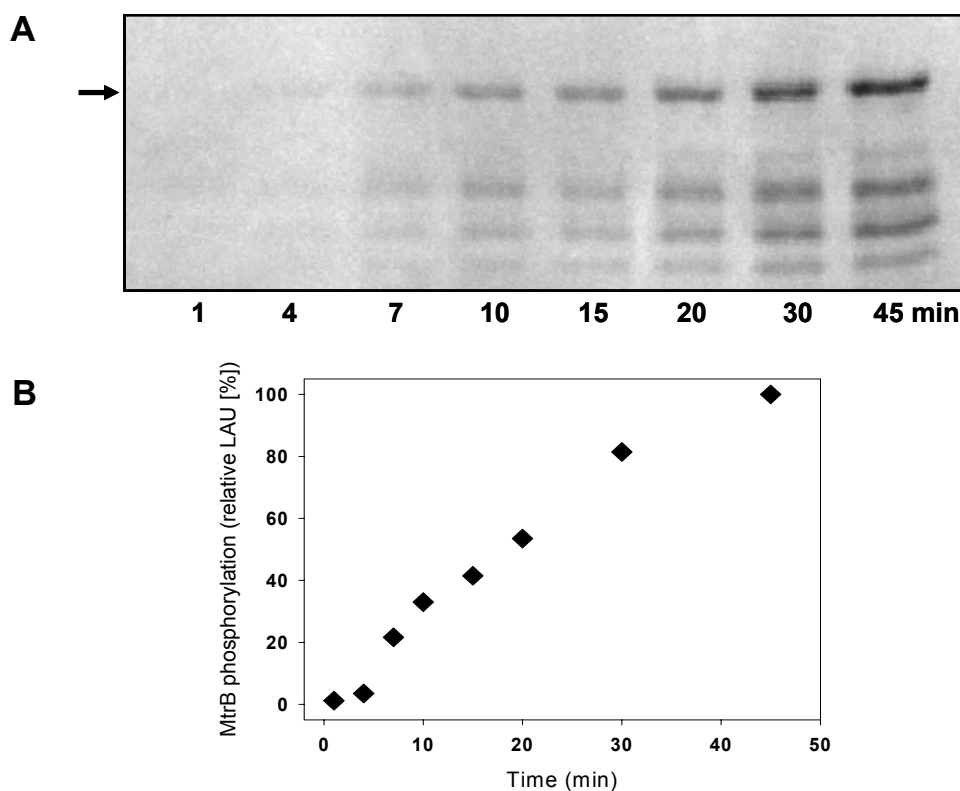
Fig. 13: Autophosphorylation activity of reconstituted MtrB-Strep in relation to the reaction time. 2 µg of reconstituted MtrB were diluted in phosphorylation buffer (50 mM Tris, 10 % glycerol, 1 mM DTT, 20 µM $MgCl_2$, 0.5 M KCl, pH (HCl) = 8) to a final volume of 10 µL. Autophosphorylation of MtrB was initiated by the addition of 0.22 µM $[\gamma^{33}P]ATP$ (110 TBq $mmol^{-1}$) and followed over 45 minutes. Samples were taken at the indicated time points and analyzed as phosphorimages (**A**). The arrow indicates signals corresponding to intact MtrB-Strep. **B** Quantification of the phosphorylation signals (light arbitrary units, LAU) corresponding to intact MtrB. The maximum signal intensity after autophosphorylation for 45 minutes was set 100 %.

Taken together, Strep-MtrB and MtrB-Strep exhibit autophosphorylation activity in both *in vitro* systems, inverted membrane vesicles as well as proteoliposomes. Most subsequent experiments were performed using MtrB-Strep. The examination of Strep-MtrB served as control, proving that the observed MtrB activity measurements were not influenced by the presence of the Strep-tag. Since, in case of inverted membrane vesicles, additional non-specific *E. coli* membrane protein signals are detected in the phosphorylation images, most subsequent studies were performed using proteoliposomes. Analyses of MtrB enriched membrane vesicles were performed serving as control using an additional *in vitro* phosphorylation system.

All *in vitro* phosphorylation experiments described in the following were, if not indicated, performed in phosphorylation buffer (50 mM Tris, 1 mM DTT, 20 µM to 10 mM $MgCl_2$, 10 % glycerol, pH (HCl) = 8.0) in presence of 0.22 µM [γ^{33}P]ATP at 30 °C for 10-20 minutes. The detailed reaction conditions for each experiment are summarized in the legends of the respective phosphorylation images.

Proteoliposomes are thought to be impermeant to ionic or polar substances as for example ATP. It has to be noted that for the phosphorylation assay using proteoliposomes as described in the following, two different experimental set-ups were used, resulting in different conditions. (I) Proteoliposomes were treated by three cycles of freezing and thawing, which is thought to result in a more or less equal concentration in lumen and exterior of all added substances (like $MgCl_2$, DTT, KCl, and others). (II) Proteoliposomes with a defined diameter were formed by extrusion through polycarbonate filters (pore diameter 400 nm). In this case, various compounds (like $MgCl_2$, DTT, KCl, and others) were subsequently added and are therefore thought to be present only in the exterior of the liposomes. The treatment of proteoliposomes prior to MtrB activity assays is indicated in the legends of the resulting images.

3.2   *In vitro* characterization of MtrB and MtrA activity

Inverted membrane vesicles and proteoliposomes were constructed in order to develop *in vitro* phosphorylation assays to monitor the enzymatic activity of MtrA and MtrB under various conditions. Before investigating the stimulus, or stimuli, respectively, which lead to the activation of MtrB and therefore initiate the signal transduction cascade, it was necessary to characterize the MtrBA phosphorylation assay in detail. In order to demonstrate, that the complete two-component system signal transduction cascade can be reconstructed *in vitro*, the autophosphorylation of membrane-bound MtrB, the phosphorelay to soluble MtrA, and the dephosphorylation of MtrA-P were examined.

3.2.1 Kinetics of the ATP-dependent MtrB autokinase activity

The histidine kinase activity of MtrB in proteoliposomes was measured as the autophosphorylation activity in presence of $[\gamma^{33}P]ATP$. In order to determine the kinetics of the ATP-dependent sensor kinase activity, autophosphorylation of 2 μg of reconstituted MtrB-Strep each was followed for 20 minutes at 30 °C in presence of 0.168 μM $[\gamma^{33}P]ATP$ and additional varying concentrations of non-labeled ATP, ranging from 1 to 10000 μM. Dilution of $[\gamma^{33}P]ATP$ by the addition of increasing amounts of non-labeled ATP reduced the radioactive signals in the resulting phosphorylation image (Fig. 14A). In order to achieve the phosphorylation rate as a function of ATP concentration, the phosphorylation intensity (LAU) corresponding to intact MtrB was multiplied with the ATP concentration in the samples and plotted *versus* the ATP concentration. The resulting graph (Fig. 14B) shows a Michaelis-Menten kinetic of the ATP-dependent histidine kinase activity. Plotting the inverse rate of phosphorylation (1 / (LAU * ATP [μM]) *versus* the inverse ATP concentration (1 / ATP [μM^{-1}]) results in a linear relation (R^2 = 1.0, Fig. 14C). From the Lineweaver-Burk plot a K_m value for ATP of 0.3 M can be estimated.
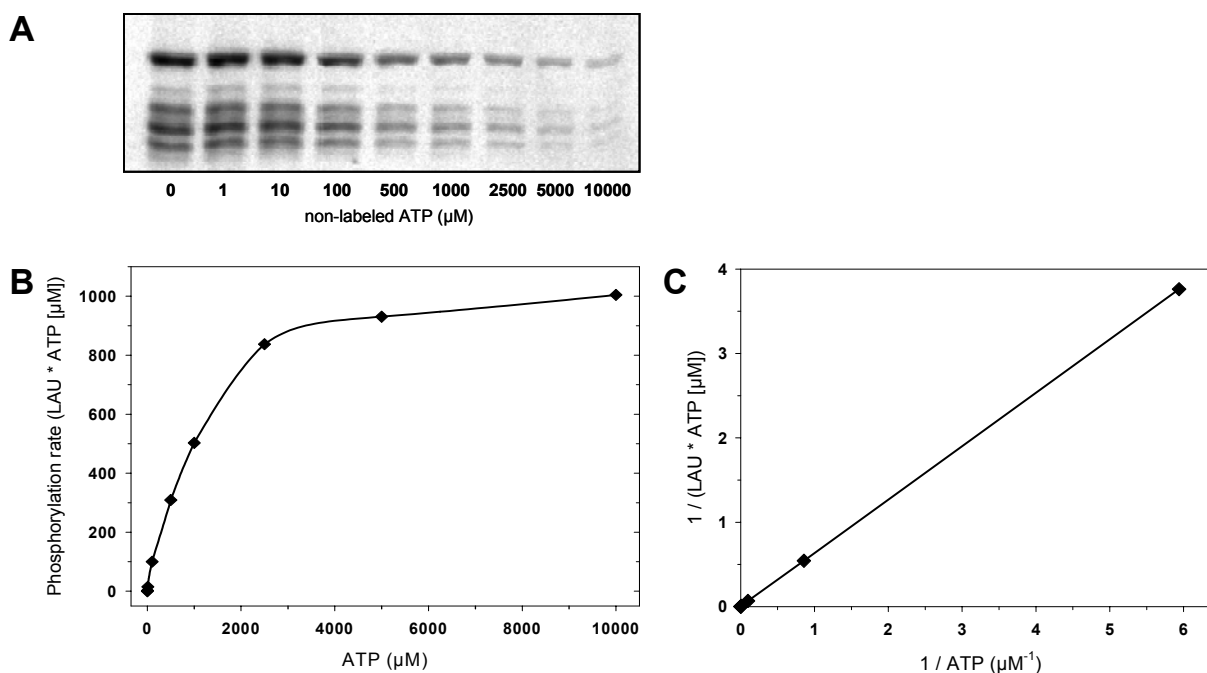
Fig. 14: Autophosphorylation of reconstituted MtrB-Strep in relation to the ATP concentration. Following extrusion of the proteoliposomes, MtrB autokinase activity was determined in phosphorylation buffer (50 mM Tris, 1 mM DTT, 10 mM MgCl$_2$, 0.1 M KCl, pH (HCl) = 8) in presence of 0.168 μM $[\gamma^{33}P]ATP$ (110 TBq mmol^{-1}) and various concentrations of non-labeled ATP. **A** Autophosphorylation of MtrB in presence of the indicated ATP concentration was analyzed as phosphorimage. **B** Phosphorylation rate of MtrB as function of ATP concentration. After quantification of the signals corresponding to intact MtrB, signal intensities (LAU) were multiplied with the ATP concentrations (μM) and plotted against the ATP concentrations (μM). **C** Lineweaver Burk plot. The inverse rate of phosphorylation (1 / (LAU * ATP [μM])) was plotted *versus* the inverse ATP concentration (1 / ATP [μM^{-1}]).

3.2.2 MtrB-MtrA phosphoryl group transfer

In bacteria, the response regulator protein catalyses the transfer of the phosphoryl group from the conserved histidine residue of the sensor kinase to the conserved aspartate residue of the response regulator.

The phosphoryl group transfer from membrane-bound MtrB to soluble MtrA was studied using proteoliposomes. For this purpose, MtrB autophosphorylation was performed for 10 minutes, before purified MtrA was added resulting in an MtrA : MtrB ratio of 4 : 1. The phosphotransfer reaction was followed over 20 minutes. It could be shown that, after addition of MtrA, the radiolabeled phosphoryl group was rapidly transferred from MtrB to the response regulator (Fig. 15). Interestingly, MtrB degradation fragments were also involved in the phosphorelay reaction (Fig. 15A). In this case, those signals corresponding to intact MtrB as well as to the degradation fragments were used for quantification.
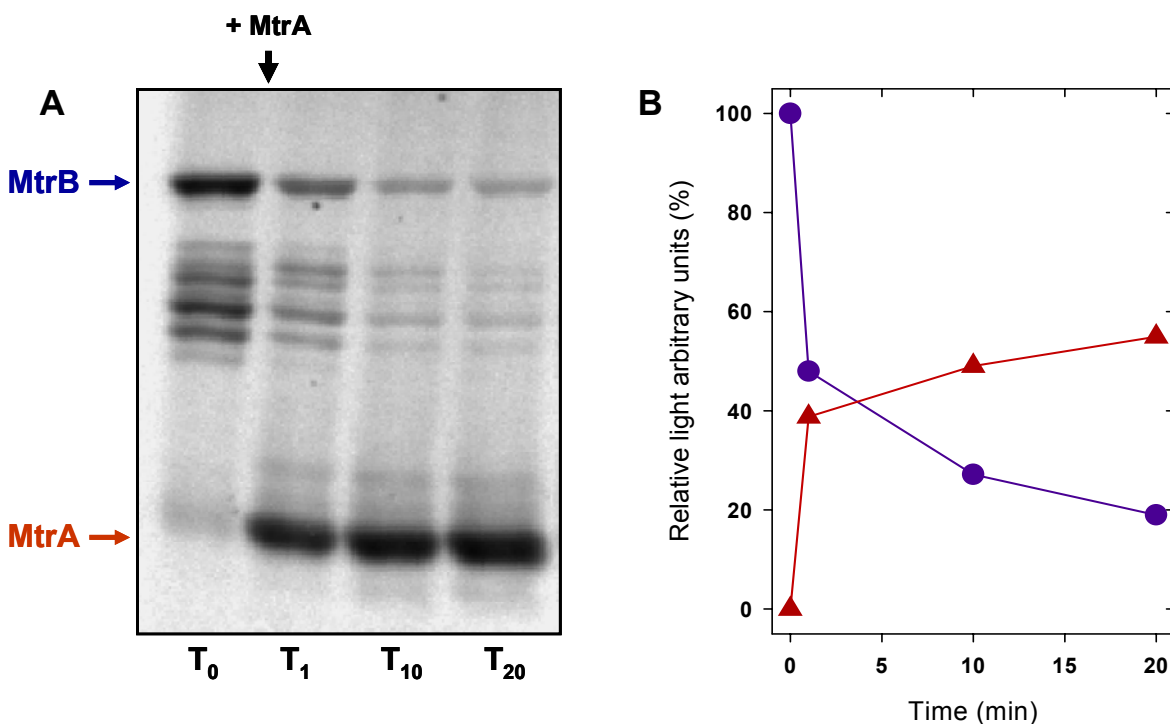
Fig. 15: Phosphotransfer from reconstituted MtrB to isolated MtrA. 2 µg of reconstituted MtrB-Strep were diluted in phosphorylation buffer (50 mM Tris, 10 % glycerol, 2 mM DTT, 10 mM $MgCl_2$, 0.1 M KCl, pH (HCl) = 8.0) to a final volume of 10 µL and prepared by three cycles of freezing and thawing. MtrB-Strep autophosphorylation was performed for 20 minutes at 30 °C in presence of 0.22 µM $[\gamma^{33}P]$ATP (110 TBq $mmol^{-1}$), before isolated MtrA-$(His)_{10}$ was added with an MtrA : MtrB ratio of 4 : 1. Samples were taken immediately before (T_0) and 1 to 20 minutes after the addition of MtrA (T_1 to T_{20}). **A** Phosphorimage of the phosphotransfer reaction. For quantification of MtrB phosphorylation, signals corresponding to intact MtrB as well as to all degradation fragments visible were considered. The MtrB phosphorylation signal intensity at the time point T_0 was set 100 %, and MtrB (**circles**) as well as MtrA (**triangles**) corresponding phosphorylation signals were plotted in relation to the reaction time (**B**).

As shown in Fig 15B, when the radioactivity found in MtrB at time point T_0 was set 100 %, one minute after MtrA addition approximately half of the radioactivity originally found in MtrB was transferred to MtrA (~50 % of original radioactivity in MtrB, ~40 % in MtrA). Thus, only approximately 10 % of the radiolabeled phosphoryl group got lost. The radioactivity found in MtrA further increased over the incubation time, indicating that MtrA-P was stable.

Thus, using MtrB-Strep reconstituted in *E. coli* liposomes, the MtrB-MtrA phosphorelay could be monitored *in vitro*. Similar experiments carried out using the Strep-MtrB derivative exhibited results according to those depicted in Figure 15 proving that the Strep-tag did not influence the phosphotransfer reaction (data not shown). Using MtrB enriched in inverted membrane vesicles as phospho-donor, the predicted MtrA corresponding signals were covered by strong radioactivity signals deriving from *E. coli* membrane proteins (data not shown). However, the transfer of the phosphoryl group from the histidine kinase to the response regulator could be followed by dephosphorlation of MtrB, which occured only in presence of MtrA (data not shown).

3.2.3 Dephosphorylation of MtrA-P

In order to shut down the output of two component system-mediated signal transduction, in most cases the regulation of gene expression, it is necessary that the activated response regulator becomes dephosphorylated. In literature, several possibilities are described how the dephosphorylation step is catalyzed. The phosphorylated response regulator can for example be dephosphorylated by a phosphatase activity of the sensor histidine kinase as was shown for KdpD from *E. coli* (Jung *et al.*, 1997). However, this reaction can also be catalyzed by distinct phosphatases (e. g. CheZ from *E. coli*, Blat and Eisenbach, 1994). Database searches revealed that the kinase core of MtrB, comprising the catalytic domains, shows close similarities to that of KdpD (E-value = $7e^{-31}$). Consequently, a possible phosphatase activity of the sensor kinase MtrB was investigated.

For this purpose, MtrB autophosphorylation activity was performed for 10 minutes using proteoliposomes, before the isolated response regulator was added, and the phosphotransfer reaction was carried out for another 20 minutes. Phosphorylated MtrA (MtrA-P) was separated from MtrB containing proteoliposomes and residual ATP or ADP, respectively, by ultracentrifugation and subsequent gel filtration of the supernatant (compare section 2.4.14). The dephosphorylation of MtrA-P was investigated by the addition of inverted *E. coli* DK8 membrane vesicles (1.1 mg of total protein) enriched with MtrB in presence or absence of ADP (1.6 mM). As control, membrane vesicles prepared from *E. coli* DK8 cells carrying the empty pASK-IBA3 vector were treated identically. Samples were taken at different time points and the time course of dephosphorylation was followed over 60 minutes. Figure 16A shows, that MtrA-P was comparatively stable over 60 minutes in the absence of

MtrB; after 60 minutes incubation MtrA still exhibited 60-70 % of the original phosphorylation signal intensity. Generally, the lifetime of aspartate phosphorylation in response regulator proteins can vary between seconds and hours (compare section 1.4). Many response regulators have autophosphatase activity that limits the lifetime of protein phosphorylation (Hess *et al.*, 1988). Such an intrinsic phosphatase activity is likely to cause the slow dephosphorylation of MtrA-P shown in Figure 16A. When MtrB incorporated in inverted membrane vesicles was added in the absence of ADP (Fig. 16B), no additional dephosphorylation of MtrA-P could be detected. Only if ADP (1.6 mM) was present, further MtrB-mediated dephosphorylation of MtrA-P occurred (Fig. 16C). The control using inverted membrane vesicles lacking the sensor kinase in presence ADP (Fig. 16D) resulted in the same pattern as obtained in the absence of the vesicles (Fig. 16A). Taken together, it could be shown, that MtrA-P was dephosphorylated specifically by membrane-bound MtrB in presence of ADP. Consequently, MtrB exhibited, in addition to the autokinase activity described above, a phosphatase activity. Furthermore, this phosphatase activity of MtrB was shown to depend on the presence of ADP. This ADP-dependence was also described for other sensor histidine kinases, e. g. EnvZ of the *E. coli* EnvZ/OmpR system (Igo *et al.*, 1989).
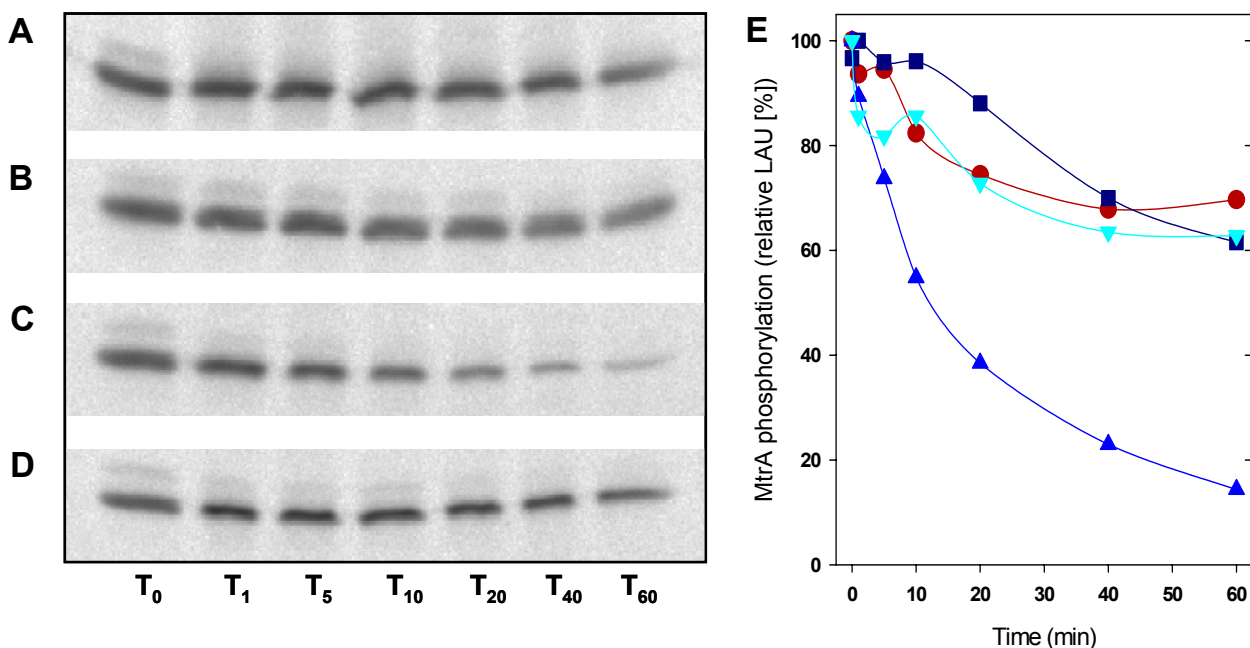
Fig. 16: MtrB-mediated dephosphorylation of MtrA-P. A - **D** Phosphorimages of MtrA-P after membrane-bound MtrB and [γ^{33}P]ATP and ADP, respectively, were removed by ultracentrifugation and subsequent gel filtration. MtrA-P was incubated in presence of 1.6 mM ADP (**A**), MtrB containing IMV in absence of ADP (**B**), MtrB enriched IMV in presence of 1.6 mM ADP (**C**), or MtrB-lacking IMV in presence of 1.6 mM ADP (**D**). Samples were taken immediately before (**T$_0$**) and 1 to 60 minutes after addition of IMV (**T$_1$** to **T$_{60}$**). MtrA phosphorylation signals were quantified and the intensities at time point T$_0$ were set 100 % (**E**).The time-dependent phosphorylation patterns of MtrA depicted in A (**circles**), B (**squares**), C (**triangles up**) and D (**triangles down**) are plotted in relation to the reaction time.

3.2.4 Orientation of MtrB-Strep in *E. coli* lipid liposomes

MtrB containing proteoliposomes were constructed to provide a system for the analysis of different stimuli. An important information for the investigation of osmostress-related stimuli is the orientation of MtrB in this system. The reconstitution of membrane proteins into liposomes can in principle result in a random or a unidirectional inside-out or right-side-out orientation. There are numerous examples for reconstituted two-component system histidine kinases, which have been shown to be membrane-integrated in an inside-out orientation, as e.g. KdpD of *E. coli* (Jung *et al*., 1997) and PhoQ of *Salmonella typhimurium* (Sanowar and Le Moual, 2005). In case of DcuS from *E. coli* (Janausch *et al*., 2002) good indications for an inside-out orientation were also obtained. A right-side-out orientation of a reconstituted sensor kinase has not been reported yet.

3.2.4.1 Influence of Mg^{2+} on the autophosphorylation activity of MtrB

Proteoliposomes are thought to be impermeable for polar or ionic substances such as K^+, Rb^+ or ATP. It has been shown that the addition of divalent cations, like Mg^{2+} or Ca^{2+} using concentrations of 5 mM and lower, results in the permeabilization of membrane vesicles or proteoliposomes made from *E. coli* total lipid extract (Liu *et al*., 1997). If Mg^{2+} turned out to have a permeabilizing effect on the MtrB containing proteoliposomes used in this study, which were made from *E. coli* polar lipid extract, this effect could be used to analyze the orientation of the reconstituted protein. To address this question, MtrB-Strep reconstituted in liposomes was analyzed under various $MgCl_2$ concentrations. For this purpose, defined proteoliposomes were formed by extrusion, before $MgCl_2$ was externally added to final concentrations varying between 0.02 and 30 mM. The addition of increasing $MgCl_2$ concentrations below 10 mM resulted in significantly increasing MtrB phosphorylation signals (Fig. 17). Since radiolabeled ATP was used in a very low concentration (0.22 µM), 20 µM $MgCl_2$ was sufficient to form the Mg-ATP complex required for autokinase activity. In contrast, when the $MgCl_2$ dependence of MtrB autophosphorylation activity was examined using inverted membrane vesicles, which are expected to carry MtrB in an inside-out orientation, the resulting MtrB phosphorylation signals did not vary between high (5 mM) and low (20 µM) $MgCl_2$ concentrations (data not shown). These data indicate that $MgCl_2$ has indeed a permeabilizing effect on the proteoliposomes used in this study, since $MgCl_2$ was thought to be required to make the catalytic domain of MtrB in proteoliposomes accessible to ATP. Since the phosphorylation domain is located in the cytoplasmic part of the kinase, these findings would indicate a right-side-out orientation of MtrB after reconstitution. Such an orientation would be in contrast to all reported sensor histidine kinases after reconstitution. Consequently, it was necessary to analyze in detail, whether $MgCl_2$ indeed has a permeabilizing effect on liposomes under conditions used in this study.
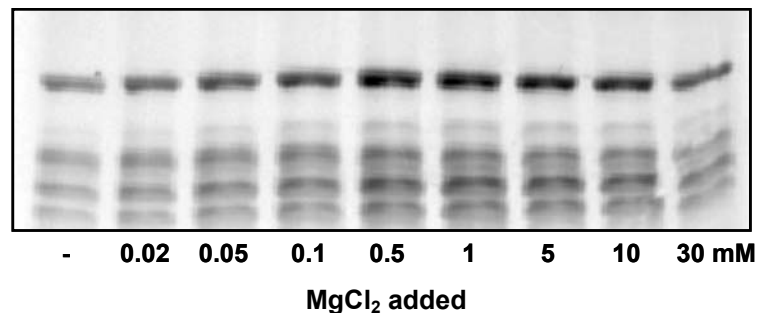
Fig. 17: Influence of various MgCl₂ concentrations on the autokinase activity of reconstituted MtrB. Following extrusion of the proteoliposomes, MtrB autokinase activity was determined in phosphorylation buffer (50 mM Tris, 1 mM DTT, 0.1 M KCl, pH (HCl) = 8) in presence or absence of 0.02 to 30 mM MgCl₂ for 20 minutes using 0.22 µM [γ^{33}P]ATP (110 TBq mmol^{-1}).

3.2.4.2 Investigation of the effect of Mg^{2+} on *E. coli* polar lipid extract liposomes

To determine, whether the utilized membrane systems are indeed permeabilized in the presence of Mg^{2+}, liposomes made from *E. coli* polar lipid extract were analyzed according to the method described by Liu *et al.* (1997), using the fluorescein derivatives 5, 6-carboxyfluorescein or calcein as indicators of liposome permeability. These substances can be entrapped in the liposomal lumen at high concentrations, which causes quenching of their fluorescence. If liposomes are permeabilized, the fluorescence would be reactivated, when the concentrations of the fluorescein derivatives decrease as a consequence of their release. High concentrations (50 to 100 mM) of 5, 6-carboxyfluorescein or calcein were entrapped in the liposomal lumen by extrusion. External fluorescein derivative was removed by gelfiltration and liposomes were diluted in 50 mM Tris, pH (HCl) = 8.0. Despite the fact that these liposomes showed high basal fluorescence, a 2 to 8 fold increase was observed, when the lipid was perforated by the addition of 1 % Triton-X-100 (Fig. 18). In contrast, when MgCl₂ was added to intact liposomes in final concentrations of 0.025 to 10 mM, the fluorescence intensity did not change (Fig. 18). These analyses were performed using various buffers. Under all tested conditions, a release of 5, 6-carboxyfluorescein or calcein was observed by increased fluorescence in presence of Triton-X-100, which could not be detected in presence of MgCl₂ (Fig. 18). These studies showed that MgCl₂ in concentrations of 10 mM and lower does not permeabilize *E. coli* polar lipid liposomes under the condition used in his work. Consequently, the increased MtrB phosphorylation signals in presence of MgCl₂ shown in Figure 17 did not occur as a consequence of permeabilization of the membrane system, and can therefore not be used as indication for the orientation of the reconstituted sensor kinase. It was necessary to determine the orientation of MtrB-Strep after reconstitution using an independent method.
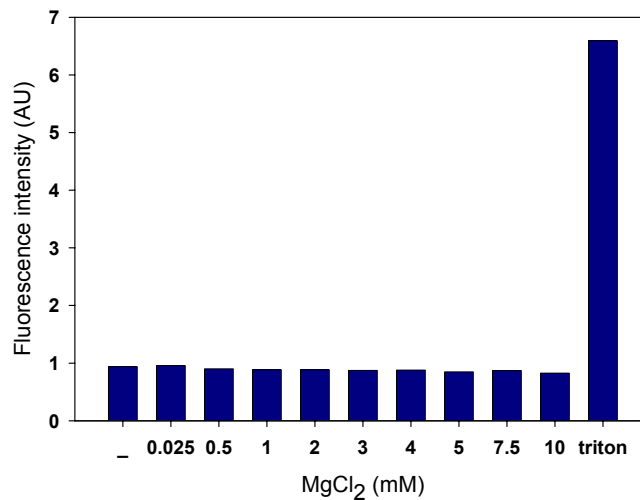
Fig. 18: Influence of MgCl$_2$ on the permeability of *E. coli* lipid liposomes. Shown is the fluorescence (arbitrary units, AU) of calcein-loaded liposomes in 20 mM Na P$_i$ buffer in absence (**-**) or presence of MgCl$_2$ varying from **0.025** to **10** mM. As control, liposomes were ruptured using 1 % triton-X-100 (**triton**).

3.2.4.3 Investigation of the orientation of reconstituted MtrB-Strep by site-specific proteolysis

Schiller *et. al.* (2004) showed for the reconstituted betaine carrier BetP C252T a unidirectional right-side-out orientation by site-specific proteolysis addressing the N-terminus. According to this method, the orientation of reconstituted MtrB-Strep in the described preparations was examined by analyzing the accessibility of the C-terminal cytoplasmic domain to proteolysis. For this purpose, proteoliposomes enriched with MtrB-Strep were exposed in both, the solubilized and the intact state, to an enzyme, which releases amino acids specifically from the carboxylic end of peptides. After forming proteoliposomes with a defined diameter by extrusion in citrate buffer (pH = 6.0) in order to meet the conditions required for peptidase activity, 2 µg of reconstituted MtrB-Strep were diluted in the same buffer in presence or absence of 1 % Triton-X-100. Carboxypeptidase Y was added to a final concentration of 0.2 µg/µL, and the time course of proteolysis was followed for 24 h at 25 °C. The reaction was stopped by addition of SDS loading dye and samples were analyzed by SDS-PAGE and subsequent immunoblot analysis using an antibody raised against the C-terminal Strep-tag. In both cases, using intact and ruptured liposomes, the C-terminal domain of MtrB-Strep was accessible to digestion by carboxypeptidase Y (Fig. 19). Treatment with carboxypeptidase Y resulted in a partial degradation of MtrB-Strep in all samples, even after incubation for 24 h, indicating that the protease was considerably retarded by specific amino acids upstream of the Strep-tag (Fig. 19A). However, comparison to immunoblot analysis proved that the C-terminal Strep-tag was already removed after 30 minutes of proteolysis

(Fig. 19B). The accessibilities of the C-terminal domain of MtrB-Strep to digestion using intact and solubilized proteoliposomes strongly indicates a unidirectional inside-out orientation of the protein, as was shown for other bacterial sensor kinases.
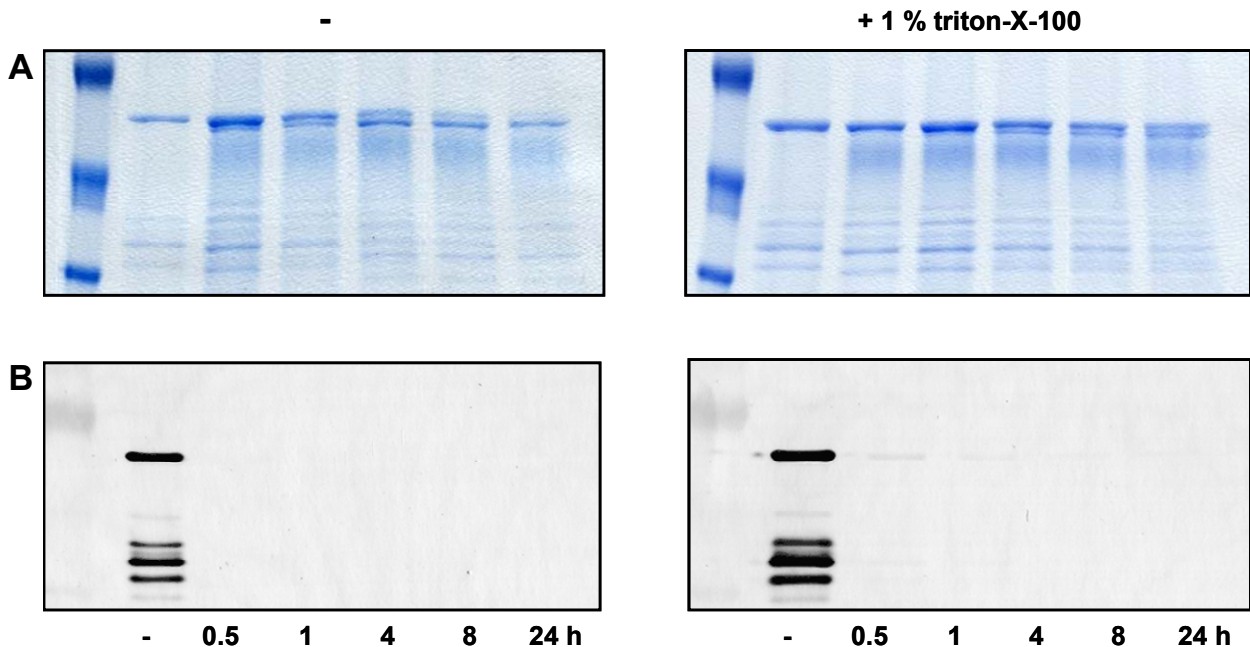
Fig. 19: Orientation of MtrB-Strep after reconstitution into *E. coli* liposomes. Intact (left panel) or solubilized proteoliposomes (right panel) were incubated with 0.2 µg/µL carboxypeptidase Y at RT. Proteolysis was followed over 24 h. As control, proteoliposomes were incubated for 24 h in the absence of the protease (**-**). Shown are the proteolysis patterns after SDS-PAGE (**A**) or immunoblot analyses using an antibody raised against the C-terminal Strep-tag (**B**).

Analysis of different proteoliposome charges supported this orientation (data not shown). These findings are in good agreement with the observed phosphoryl group transfer to MtrA by reconstituted MtrB. Obviously the soluble kinase core domain of the sensor kinase was accessible to the response regulator. The reason for the increased MtrB phosphorylation signal intensity in presence of $MgCl_2$ concentrations between 0.5 and 5 mM (Fig. 17) remains unclear; however this was obviously not caused by an increased permeability of the membrane system. For future *in vitro* studies, $MgCl_2$ was used in final concentrations of 5-10 mM.

3.2.5 Autokinase activity of MtrB in its solubilized state

All investigations of the *in vitro* activity of MtrB described so far were carried out after integration of the protein into a membrane bilayer, either in cells or liposomes. The question arose, whether the sensor kinase shows a comparable activity profile in its solubilized state.

To address this question, purified MtrB was dialyzed against phosphorylation buffer (50 mM Tris, 10 % glycerol, pH (HCl) = 8.0) supplied with 0.1 % DDM. The investigation of the activity of solubilized MtrB protein was performed as described above (compare section 3.2.1) in the additional presence of 0.1 % DDM. The resulting phosphorimage shows that the intact form of MtrB-Strep was not labeled when used in its solubilized state (Figure 20, lane 2). Instead, a signal with the apparent molecular mass of approximately 47 kDa is visible. Comparison to the phosphorylation pattern of MtrB after reconstitution into liposomes (Figure 20, lane 1) indicates that this signal corresponds to one of the degradation fragments with a molecular weight between 40 and 55 kDa.
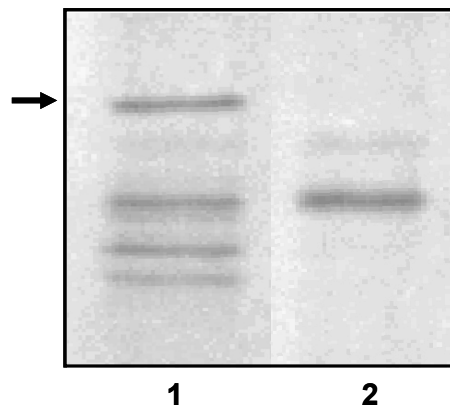
Fig. 20: *In vitro* **activity of solubilized MtrB.** Solubilized MtrB-Strep (**2**) was incubated in phosphorylation buffer (50 mM Tris, 0.1 M KCl, 5 mM $MgCl_2$, 10 % glycerol, pH (HCl) = 8.0) supplemented with 0.1 % DDM and 0.22 µM [γ^{33}P]ATP (110 TBq $mmol^{-1}$) for 10 minutes at 30 °C. As control, MtrB-Strep incorporated in liposomes was treated similarly in the absence of the detergent (**1**). The arrow indicates the signal corresponding to intact MtrB-Strep.

As a control, identically treated solubilized MtrB-Strep was analyzed by SDS-PAGE and immunoblot analysis, proving that the non-reconstituted protein does not exhibit altered electrophoresis properties compared to the reconstituted sensor (data not shown). It could thus be shown that MtrB-Strep is inactive in its solubilized state, indicating that membrane integration is the prerequisite for *in vitro* activity of the histidine kinase.

3.3   Investigation of the stimuli sensed by MtrB with focus on osmostress-related signals

The MtrBA two-component system has been shown to be involved in various physiological functions of *C. glutamicum*, namely osmostress-response, chill stress-response, and cell wall metabolism. For the determination of the stimuli which directly activate MtrB phosphorylation and thus initiate the signal transduction cascade, the described *in vitro* phosphorylation assays were developed (section 3.1 and 3.2). *In vivo* analyses already showed that MtrBA mediates the expression regulation of specific genes in response to high NaCl concentrations of the medium, thus indicating that MtrB acts as sensor for osmotic stress.

3.3.1   Expression regulation of *proP*, *betP*, and *mscL* after a hyperosmotic shock with trehalose

RNA hybridization experiments using total RNA isolated from *C. glutamicum* WT and Δ*mtrAB* strongly suggested that the MtrBA-mediated signal transduction cascade is induced by an increased external osmolarity caused by NaCl (Möker *et al*., 2004). Prior to examination of the influence of osmostress-related stimuli on MtrBA *in vitro*, it was necessary to determine, if the *in vivo* effects were specifically caused by NaCl, or whether they were a general consequence of the increased medium osmolarity.

In order to examine the effects of a non-ionic osmolyte on the expression of osmostress-related genes, trehalose was chosen, which is not taken up by *C. glutamicum* cells (Tropis *et al*., 2005). *C. glutamicum* WT and Δ*mtrAB* cells were exposed to a hyperosmotic shift from 0.3 to 1.7 osm/kg as described in section 2.2.2, and total RNA was isolated from cells harvested at different time points. Subsequently, RNA hybridization experiments were performed as recently described (Möker *et al*., 2004). The resulting transcription pattern of *proP*, *betP* and *mscL* after an osmotic upshift using trehalose (Fig. 21) was similar to the patterns obtained after NaCl-induced stress. These results supported the notion that the signal sensed by MtrB in order to regulate the expression of *proP*, *betP*, *lcoP*, and *mscL* is caused by general osmotic changes in the environment and not by more specific effects, as e. g. an altered external ionic strength. The observation that MtrBA mediates the transcriptional activation of osmostress-related genes in response to an increased external osmolarity strongly suggests that MtrB serves as sensor for osmotic stress. Consequently, a variety of possible stimuli, which are related to osmotic stress conditions, can serve as the activating stimulus for MtrB (compare section 1.6). These include changes in external as well as internal conditions of the bacterial cell, e. g. osmolarity, ionic strength, and concentrations of ions or specific solutes. Furthermore, an altered turgor pressure, as well as membrane strain or shrinkage are possible stimuli for a sensor measuring osmotic stress. Besides an

altered turgor pressure, which can not be monitored *in vitro*, the influence of these physico-chemical stimuli on the activities of MtrA and MtrB were determined using the *in vitro* phosphorylation assays described in section 3.1 and 3.2.
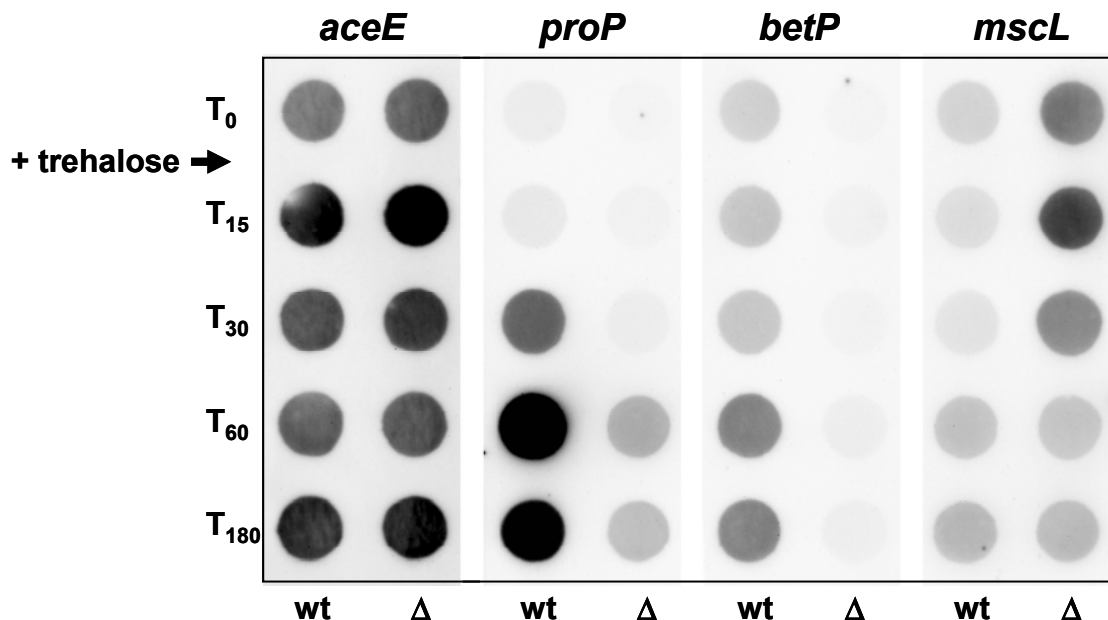
Fig. 21: Influence of an osmotic upshift imposed by trehalose on the expression profiles of *proP*, *betP*, and *mscL*. Total RNA was isolated from *C. glutamicum* WT (**wt**) and Δ*mtrAB* (Δ) cells before (**T₀**) and 15 to 180 minutes (**T₁₅** to **T₁₈₀**) after an upshift of the medium osmolarity from 0.3 to 1.7 osm/kg using trehalose. To confirm that similar amounts of total RNA were blotted, the mRNA of the *aceE* gene was detected identically.

3.3.2 Influence of various salts on the *in vitro* autokinase activity of MtrB

In order to investigate if the MtrB protein is activated *in vitro* by changes of the osmolarity in general or by the presence of specific solutes, autokinase activity under the influence of various salts was determined. For this purpose, autophosphorylation activity of MtrB-Strep enriched in proteoliposomes was monitored in presence or absence of 300 mM KCl, RbCl, NaCl, and LiCl for 20 minutes at 30 °C. Figure 22 shows that the activity of MtrB-Strep was significantly stimulated by the presence of K^+ and Rb^+. Highest activity was detected when KCl was added. RbCl also resulted in a strong stimulation, whereas NaCl lead to a weak stimulation of autokinase activity, and the presence of LiCl had no influence. MtrB autophosphorylation in presence of NH_4Cl resulted in somewhat increased radioactivity signals compared to those obtained with KCl (data not shown). Some of the degradation fragments were stimulated in a similar manner as the intact protein, indicating that the sensory function was unchanged in these fragments (Fig. 22A).
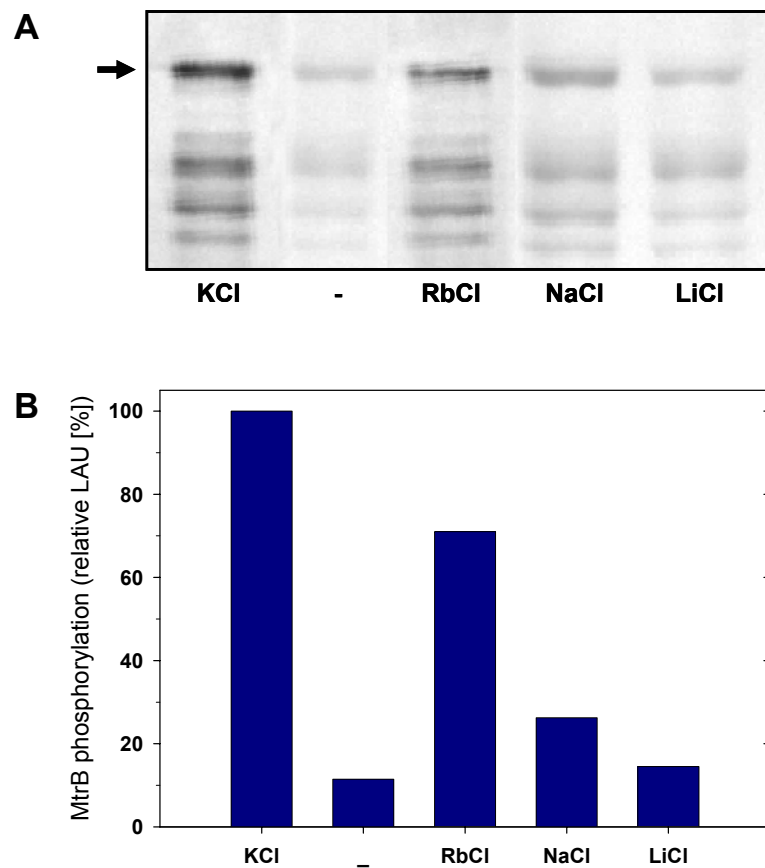
Fig. 22: Influence of various salts on the autokinase activity of reconstituted MtrB. Following extrusion, proteoliposomes enriched with MtrB-Strep were incubated in phosphorylation buffer (50 mM Tris, 1 mM DTT, 5 mM $MgCl_2$, 20 mM KCl, pH (HCl) = 8) in the absence (-) or presence of 300 mM **KCl**, **RbCl**, **NaCl**, and **LiCl**. The samples were analyzed as phosphorimages (**A**) or by quantification of the signals corresponding to intact MtrB-Strep (**B**), indicated by the arrow in 22**A**. The signal intensity in presence of KCl was set 100 %.

MtrB stimulation could be reproduced using MtrB-Strep and Strep-MtrB, respectively, enriched in proteoliposomes as well as in inverted membrane vesicles with the following sequence of efficiency:

$$NH_4Cl \geq KCl > RbCl >> NaCl >> LiCl$$

Activation of MtrB turned out to depend on the concentration of the added osmolytes. With low concentrations (25 mM) of these compounds significantly weaker phosphorylation signals were obtained, which still exhibited the pattern of MtrB stimulation shown in Figure 22 (data not shown).

Interestingly, the stimulation profiles of *C. glutamicum* MtrB in artificial membrane systems turned out to be similar to those of EnvZ of *E. coli*. As shown by Jung *et al.* (2001), the EnvZ sensor kinase of the EnvZ/OmpR two-component system was, after reconstitution,

stimulated in presence of K^+, Rb^+ and Na^+, with highest activity when KCl was added. The EnvZ/OmpR-mediated regulation of gene expression observed *in vivo* turned out to depend on the medium osmolarity (Pratt and Silhavy, 1995), as was also shown for MtrB. For that reason, the question arose, if the observed activity profiles are specific for sensors involved in osmoregulation. As a control whether the observed effects were MtrB specific, DcuS, a sensor histidine kinase of *E. coli*, which was shown not to be involved in osmoprotection (G. Unden, personal communication) was analyzed. The two-component system DcuSR controls the expression of genes of the C_4-dicarboxylate metabolism in response to extracellular C_4-dicarboxylates. The membrane-bound sensor DcuS was, after purification and reconstitution into *E. coli* liposomes, stimulated by C_4-dicarboxylates, particularly fumarate (Janausch *et al*., 2002).

3.3.3 Development of a control system to discriminate between specific and non-specific MtrB stimuli by use of the fumarate sensor DcuS

In order to construct a control system for MtrB-stimulating agents, the *E. coli* fumarate sensor DcuS was overexpressed, isolated, and reconstituted in *E. coli* liposomes similar to MtrB. For the overexpression and isolation of DcuS, a pET28a vector containing the *dcuS* gene fused to the sequence encoding a $(His)_6$-tag at the N-terminus of the respective protein, called pMW151 (Janausch *et al*., 2002, kindly provided by Unden, G., University of Mainz), was transformed into *E. coli* BL21(DE3). The cells were cultivated as described in section 2.2.2., *dcuS* expression was induced using 1mM IPTG, and further preparation steps were carried out as described for MtrB (section 3.1.5). Affinity chromatography was performed using Protino® Ni prepacked columns (Macherey-Nagel, Düren). As shown in Figure 23, the purification of DcuS was successful; a total yield of 0.5 mg $(His)_6$-DcuS per 1.6 L of cell culture could be obtained. The reconstitution of purified $(His)_6$-DcuS, performed as described for MtrB-Strep (section 3.1.5), resulted in proteoliposomes (Fig. 23) with an average DcuS concentration of 1 µg/µL.
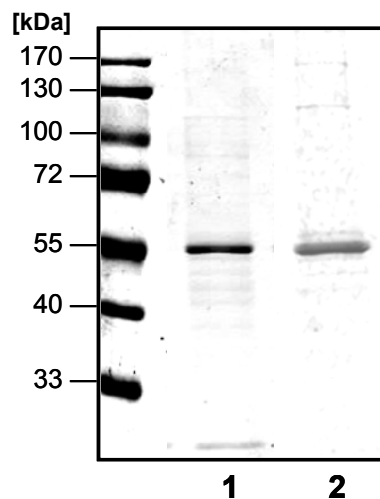
Fig. 23: Purification and reconstitution of the *E. coli* fumarate sensor DcuS. The samples were analyzed by means of SDS-PAGE. **1** Elution fraction after isolation of (His)$_6$-DcuS via affinity chromatography using Protino® Ni prepacked columns. **2** Proteoliposome fraction after reconstitution of (His)$_6$-DcuS into *E. coli* liposomes and subsequent washing steps. Left lane: PageRuler^{TM} protein ladder (kDa, MBI Fermentas, St. Leon-Roth).

In order to determine if the osmolytes, which were shown to stimulate MtrB autokinase activity *in vitro*, influence the autophosphorylation activity of the fumarate sensor, reconstituted (His)$_6$-DcuS was treated identical to MtrB (section 3.3.2). Phosphorylation activity was examined for 10 minutes at 37 °C. Surprisingly, DcuS also exhibited an increased autokinase activity in presence of KCl, NaCl, RbCl, and NH$_4$Cl, as shown in Figure 24 for KCl and NaCl.
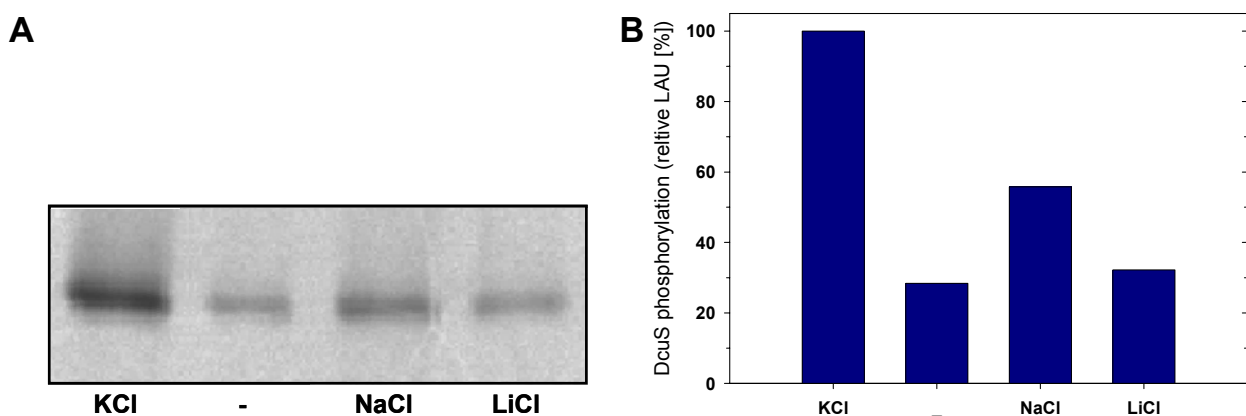
Fig. 24: Influence of various salts on the autophosphorylation activity of reconstituted DcuS. Proteoliposomes enriched with (His)$_6$-DcuS were incubated in absence (**-**) or presence of 300 mM **KCl**, **NaCl**, and **LiCl**. The samples were analyzed as phosphorimages (**A**) or by quantification of the DcuS phosphorylation signals (**B**). The signal intensity (LAU) in presence of KCl was set 100 %.

As in case of MtrB, the highest activity levels were determined with KCl, whereas NaCl resulted in a weaker stimulation. LiCl had no effect on the fumarate sensor. In presence of RbCl and NH_4Cl, DcuS phosphorylation intensity was similar to that obtained by KCl (data not shown), resulting in the following DcuS activation pattern of the osmolytes:

$$NH_4Cl \sim KCl \sim RbCl \gg NaCl \gg LiCl$$

The effects of salts on autophosphorylation were investigated in more detail by analyzing the activity of MtrB and DcuS in presence of various KCl concentrations. KCl turned out to efficiently stimulate both histidine kinases. However, the kinetics (Fig. 25) of the two enzymes did exhibit differences, whereby MtrB seems to be to some extent more sensitive (Fig. 25). In addition, DcuS exhibited a higher basal activity level (10-20 % of maximum) compared to MtrB (0-5 % of maximum).
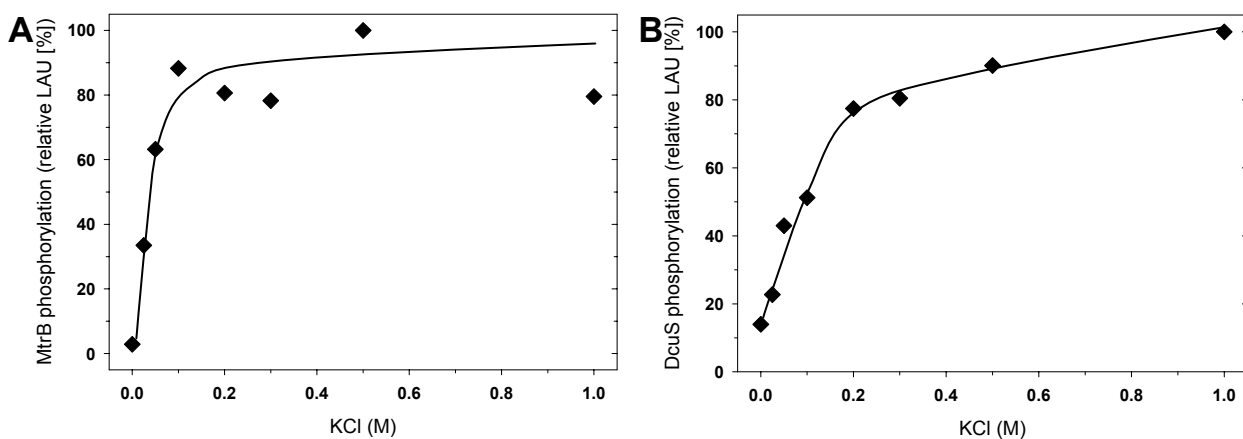
Fig. 25: Influence of various KCl concentrations on the autokinase activities of reconstituted MtrB and DcuS in proteoliposomes. Autophosphorylation signals corresponding to intact MtrB-Strep (**A**) and $(His)_6$-DcuS (**B**) in the respective phosphorimages (data not shown) were quantified. The intensities (LAU) corresponding to the strongest phosphorylation signal of intact MtrB or DcuS, respectively, were set 100 %.

An activation of DcuS autophosphorylation by monovalent salts was surprising, since this sensor was shown to be specifically stimulated by fumarate (Janausch *et al.* 2000). It was therefore necessary to prove, that DcuS showed the fumarate-dependent stimulation described by Janausch *et al.* (2002) under the conditions used in this study. Interestingly, a fumarate-dependent stimulation of DcuS activity could only be obtained in presence of KCl (Fig. 26). This observation, taken together with the K^+-dependent stimulation of MtrB, DcuS, and EnvZ of *E. coli* (Jung *et al.*, 2001), led to the hypothesis that monovalent ions, especially K^+, are necessary for correct *in vitro* functioning of two-component system sensor histidine kinases in general. Consequently, subsequent studies of *in vitro* stimulation of MtrB were

performed in presence of 20 mM KCl. Furthermore, DcuS obviously serves as a suitable control to discriminate between specific and non-specific stimulation of the sensor histidine kinase MtrB.
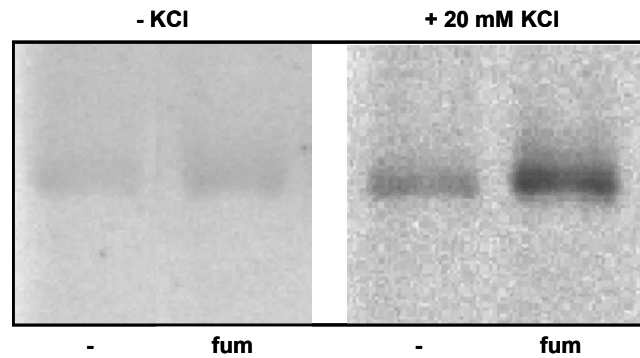
Fig. 26: Dependence of the DcuS sensing capacity on the presence of KCl. The influence of fumarate on (His)$_6$-DcuS *in vitro* activity was determined in absence (**-**) or presence of 20 mM fumarate (**fum**). DcuS autophosphorylation was monitored in buffer without (left panel) or with 20 mM KCl (right panel).

3.3.4 Detailed analyses of the osmostress-related *in vitro* stimulation of the MtrB-MtrA two-component system

For a detailed analysis of the influence of a broad variety of osmostress-related stimuli on the *in vitro* MtrB activity, proteoliposomes enriched with the sensor kinase were differently treated (compare section 3.1.6). The experiments described in the following were carried out with proteoliposomes prepared by extrusion. Consequently, the subsequently added compounds were, if not membrane-permeant, only present in the exterior of the membrane system. Autokinase activity was tested in phosphorylation buffer (50 mM Tris, 1 mM DTT, 5 mM MgCl$_2$) at 30 °C. In contrast to former studies, the buffer was routinely supplemented with 20 mM KCl. Since the addition of 10 % glycerol to the samples resulted in an increased buffer osmolarity, the following studies were performed in the absence of this compound. For quantification of the resulting phosphorylation signals only those signals corresponding to intact MtrB were considered. Proteoliposomes enriched with (His)$_6$-DcuS used under identical conditions at 37 °C served as a control, in order to verify that the results observed for MtrB stimulation are specific for the *C. glutamicum* sensor histidine kinase.

3.3.4.1 Influence of various amino acids and compatible solutes on the *in vitro* autokinase activity of MtrB

The autokinase activity of reconstituted MtrB-Strep was examined in presence of the compatible solutes glycine betaine, proline, and glutamate, which are known to be accumulated by *C. glutamicum* in response to hyperosmotic conditions (see section 1.2.2). In addition, the effects of the amino acids alanine and lysine, which are not involved in the osmostress response of this bacterium, were investigated. Glycine betaine, proline, alanine and lysine were added in a final concentration of 600 mM and compared to 300 mM each of Na-glutamate and KCl, resulting in approximately identical osmolalities of 600 mosm/kg, which was confirmed by freezing point osmolality measurements (data not shown). Strikingly, the presence of all examined compounds resulted in a strong stimulation of *in vitro* MtrB autokinase activity. As shown in Figure 27, MtrB autophosphorylation signals were significantly increased when glutamate, proline, alanine, glycine betaine, and lysine were added.
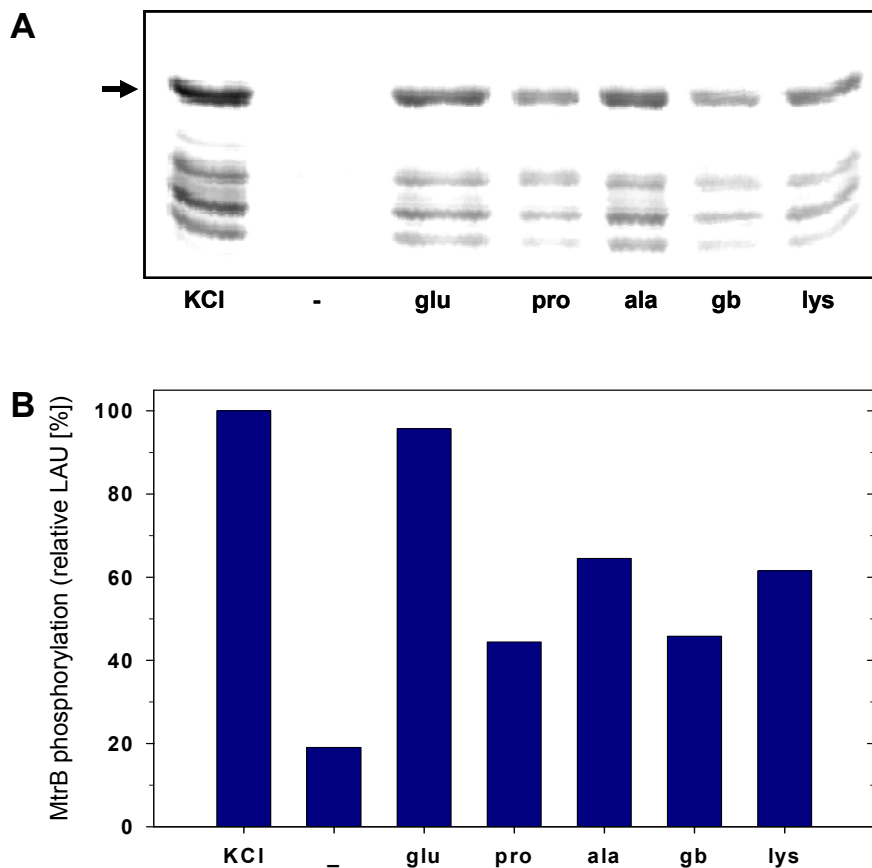
Fig. 27: Influence of various amino acids and compatible solutes on the autokinase activity of reconstituted MtrB. Following extrusion, proteoliposomes enriched with MtrB-Strep were incubated in absence (**-**) or presence of 300 mM **KCl** and Na-glutamate (**glu**), or 600 mM proline (**pro**), alanine (**ala**), glycine betaine (**gb**), and lysine (**lys**). The samples were analyzed as phosphorimages (**A**) or by quantification of the signals (LAU) corresponding to intact MtrB-Strep (**B**) indicated by the arrow. The signal intensity in presence of KCl was set 100 %.

The presence of Na-glutamate resulted in phosphorylation signals virtually similar to those obtained with KCl. Since NaCl in the same concentration only resulted in a faint stimulation of MtrB (section 3.3.2), this effect is mainly caused by the presence of glutamate, and not of Na^+. Proline, alanine, glycine betaine, and lysine had also strong MtrB activating effects, but to somewhat lower extent compared to glutamate.

Identically treated reconstituted $(His)_6$-DcuS did not result in a stimulation of the fumarate sensor (see Fig. 47, section 7.4.1). A weak signal increase in presence of Na-glutamate was observed with an intensity similar to that obtained with NaCl in the same concentration (Fig. 24). This faint stimulation is likely to be caused by the presence of Na^+ and not of glutamate in the samples.

Consequently, these studies showed that MtrB autophosphorylation is stimulated by both, compatible solutes and osmostress-independent amino acids. Additional investigations carried out in presence of varying concentrations of the osmolytes proved, that the stimulation occurs in a concentration-dependent manner (data not shown). The findings that the same osmolytes failed to stimulate DcuS phosphorylation (see section 7.4.1) strongly indicate, that the effects are specific for MtrB.

3.3.4.2 Influence of various sugars on the *in vitro* autokinase activity of MtrB

The *in vitro* autophosphorylation activity of MtrB was additionally analyzed in presence of various sugars. The influence of glucose, trehalose, sucrose, fructose, maltose, and maltotriose on reconstituted MtrB was examined using a final concentration of 600 mM each. As shown in Figure 28, MtrB-Strep autophosphorylation turned out to be strongly stimulated in presence of all monitored mono-, di-, and trisaccharides. In comparison, MtrB phosphorylation in presence of 300 mM KCl, resulting in an approximately identical osmolarity of 600 mosm, is shown. For the analysis depicted in Figure 28B, 600 mM KCl were used; thus buffer osmolarity was increased by a factor of approximately 2. Consequently, only the phosphorylation signals in Figure 28A served for quantification. It could be shown, that fructose, maltose, and maltotriose stimulated MtrB activity to an extent similar to that observed with glucose or trehalose. As in case of the compatible solutes and amino acids, the observed effects of the osmolytes stimulating MtrB autokinase activity occurred in a concentration-dependent manner (data not shown).

Examination of $(His)_6$-DcuS autophosphorylation activity in presence of the same sugars showed that autophosphorylation of the fumarate sensor was only faintly increased in presence of trehalose, sucrose, fructose, and maltose, whereas its activity was unchanged when incubated in presence of glucose or maltotriose (see Fig. 48, section 7.4.2).

Consequently, the described studies strongly indicate, that the MtrB sensor histidine kinase is significantly stimulated by a broad variety of osmolytes, including compatible solutes, amino acids, and sugars, and that this stimulation is specific for MtrB.
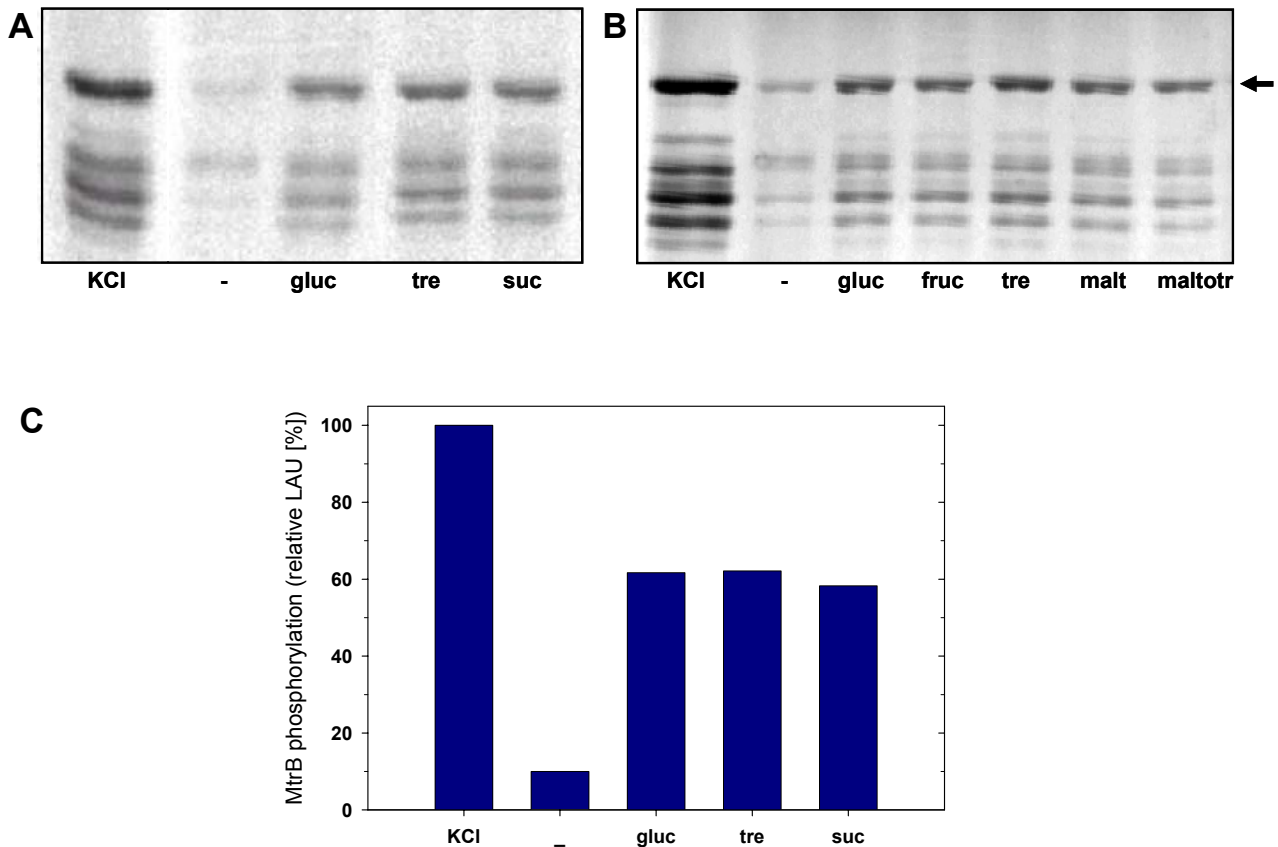
Fig. 28: Influence of various sugars on the autokinase activity of reconstituted MtrB. A, **B** Following extrusion, MtrB-Strep was analyzed of in the absence (**-**) or presence of 300 (**A**) or 600 (**B**) mM **KCl**, or 600 mM glucose (**gluc**), trehalose (**tre**), succrose (**suc**), fructose (**fruc**), maltose (**malt**), and maltotriose (**maltotr**). The reactions were performed in buffer supplemented with 20 mM KCl and analyzed as phosphorimages (**A**, **B**) or by quantification of the phosphorylation signals shown in 28A corresponding to intact MtrB-Strep (**C**). The signal intensity in presence of 300 mM KCl was set 100 %.

As already shown (Fig. 26), a fumarate-dependent stimulation of DcuS activity could only be obtained in presence of KCl (20 mM). In order to determine, whether the observed MtrB stimulating effects are still detectable in the absence of K$^+$, the stimulation of MtrB-Strep autophosphorylation by different osmolytes was compared in absence and presence of 20 mM of this salt. In contrast to the complete failure of the fumarate-induced stimulation of DcuS, the pattern of MtrB stimulation remained similar, but significantly weaker in the absence of KCl. (Fig. 29).

A

B
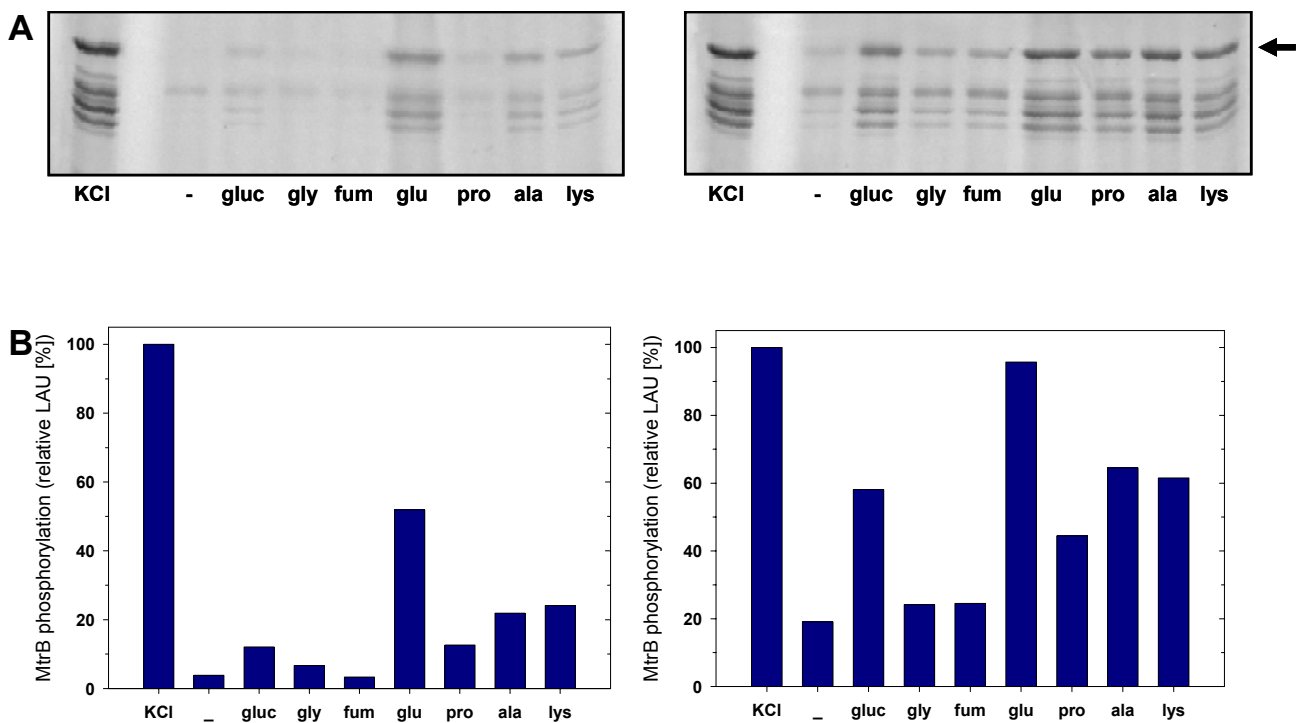
Fig. 29: Influence of various solutes on the autokinase activity of reconstituted MtrB in presence or absence of 20 mM KCl. Following extrusion, MtrB-Strep was analyzed in the absence (**-**) or presence of 300 mM **KCl**, Na-glutamate (**glu**), and lysine-Cl (**lys**), 600 mM glucose (**gluc**), glycerol (**gly**), proline (**pro**), and alanine (**ala**), or 20 mM fumarate (**fum**), respectively. The reactions were performed without (left panel) or with additional 20 mM KCl (right panel). Samples were analyzed as phosphorimages (**A**) or after quantification of the phosphorylation signals corresponding to intact MtrB-Strep (**B**) indicated by the arrow. The signal intensities in presence of 300 mM KCl were set 100 %.

3.3.4.3 Influence of various osmolytes on the *in vitro* MtrB-MtrA phosphoryl group transfer

The *in vitro* investigations concerning the primary stimuli of the MtrBA two-component system described so far were performed with focus on the autophosphorylation activity of MtrB. In addition, it was important to consider the subsequent signal transduction reaction. To address the question, whether the phosphotransfer reaction would also be affected by the presence of various osmolytes, the influence of these substances on the MtrB-MtrA phosphorelay reaction was determined. For this purpose, the *in vitro* phosphotransfer reaction was performed as described in section 3.2.2 in presence of 20 mM KCl and, in addition, various MtrB stimulating agents with a final osmolarity of approximately 600 mosm. After 15 minutes of MtrB-Strep autophosphorylation at these conditions, MtrA-(His)$_{10}$ was added in an MtrB : MtrA ratio of 1 : 4, and the phosphotransfer reaction was carried out for another 20 minutes. Under all conditions, phosphorylated MtrB was detected at a basal level (Fig. 30). In contrast, the resulting MtrA phosphorylation pattern (Fig. 30) demonstrates that

the response regulator exhibits increased phosphorylation levels in presence of Na-glutamate, glucose, trehalose, lysine, alanine, and proline. In contrast to the MtrB stimulation pattern (section 3.3.2), the presence of NaCl resulted in a strong MtrA phosphorylation signal. Despite NaCl, the pattern of phosphorylation of the response regulator was identical to that of the sensor histidine kinase. This indicates that no intermediate regulator protein is involved in the MtrB-MtrA phosphorelay.
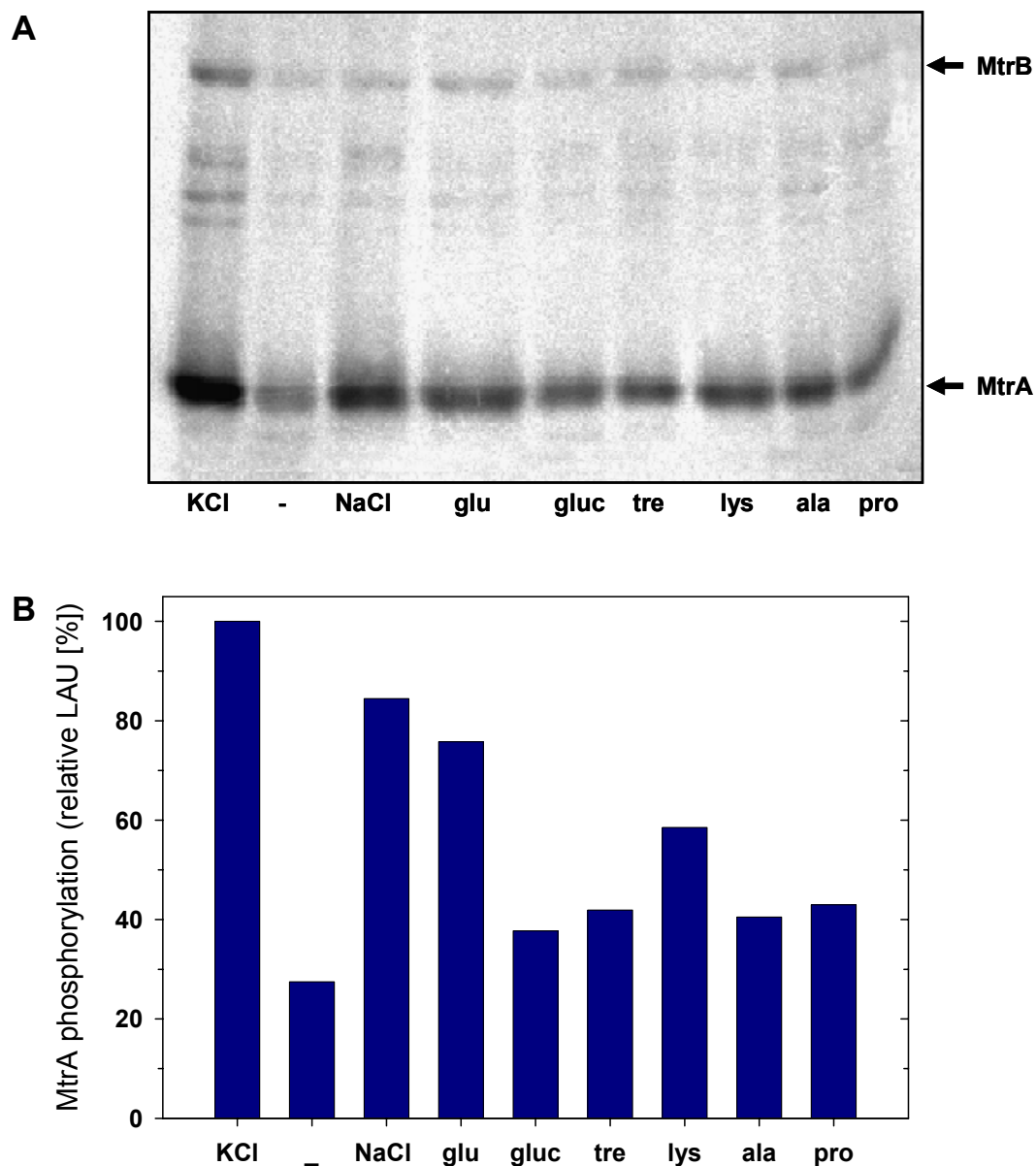
Fig. 30: Influence of various osmolytes on the MtrB-MtrA phosphotransfer reaction. The phosphorelay reactions were performed in the absence (**-**) or presence of 300 mM **KCl**, **NaCl**, Na-glutamate (**glu**), and lysine-Cl (**lys**), or 600 mM, glucose (**gluc**), trehalose (**tre**), alanine (**ala**), and proline (**pro**), respectively. The samples were analyzed as phosphorimages (**A**) or by quantification of the phosphorylation signals corresponding to MtrA-(His)$_{10}$ (**B**) indicated by the bottom arrow. The MtrA phosphorylation signal intensity in presence of 300 mM KCl was set 100 %.

Taken together, the similar reactions of reconstituted MtrB, EnvZ, and DcuS to monovalent ions, especially K^+, pointed on a requirement of these compounds for the correct *in vitro* functioning of these two-component system histidine kinases. MtrB could be shown to be strongly stimulated *in vitro* by a broad variety of osmolytes, including compatible solutes, amino acids, and sugars. Examinations of DcuS in presence of the same osmolytes showed that most MtrB stimulants failed to stimulate the fumarate sensor and thus strongly indicate that the observed effects are specific for MtrB.

Since it is very unlikely, that MtrB exhibits a binding site for such a broad variety of molecules, these findings strongly indicate that MtrB is, at least *in vitro*, stimulated by an increased osmolarity *per se*. One possibility of MtrB stimulation by an increased osmolarity would be given by membrane effects, as e. g. shrinkage, which occurs when osmotically active compounds are added to the membrane system. A further possible mechanism of MtrB stimulation is an altered hydration state of the protein surface in presence of osmotically active compounds. The investigation of the mechanism of MtrB stimulation by the presence of osmolytes was addressed by use of polyethylene glycols (PEGs) of various molecular sizes.

3.3.4.4 Influence of polyethylene glycols (PEGs) with various molecular sizes on the *in vitro* autokinase activity of MtrB

Synthetic polyethylene glycols (PEGs) with various molecular sizes were examined in order to explore a relationship between MtrB stimulation and membrane permeability of the agent. PEGs with low molecular size (ranging from monoethylene glycol to hexaethylene glycol, PEG 6) are thought to be membrane-permeant. Proteoliposomes enriched with MtrB-Strep were treated by extrusion, and autophosphorylation of 2 µg MtrB was determined for 20 minutes at 30 °C in presence of 20 mM KCl. The influence of external PEGs using various molecular sizes was monitored in final concentrations of 150 to 300 mM (approximately 150 to 300 mosm).

When 150 mM PEGs were applied in presence of 20 µM $MgCl_2$, autophosphorylation of MtrB was stimulated in relation to the molecular size of the PEGs used. It could be shown that the intensities of MtrB phosphorylation signals strongly increased with the molecular sizes of the supplied PEGs (Fig. 31). In presence of diethylene glycol (PEG 2), no stimulation of MtrB activity was observed. Starting from tetraethylene glycol (PEG 4), MtrB autophosphorylation signal intensities increased with the PEG sizes resulting in the pattern PEG 4 < PEG 6 ~ PEG 8 < PEG 12 < PEG 28. In a control experiment it could be shown, that PEGs had no effect on DcuS *in vitro* activity using identical conditions (compare Fig. 50, section 7.4.4), proving that these effects are specific for MtrB.

If PEGs were used with a higher concentration (300 mM), the signals observed with large PEGs (PEG 12 and 28) turned out to be weaker compared to those observed with smaller PEGs (PEG 6 and 8, Fig. 32A). Addition of high concentrations of these large molecules visibly increased sample viscosity, which likely inhibits all diffusion-driven processes, thus probably disturbing the stimulation of MtrB autophosphorylation. Furthermore, as shown for glycerol as well as PEG 2, the membrane-permeable reagent urea used in the same concentration (300 mM), completely failed to stimulate MtrB autophosphorylation (data not shown).
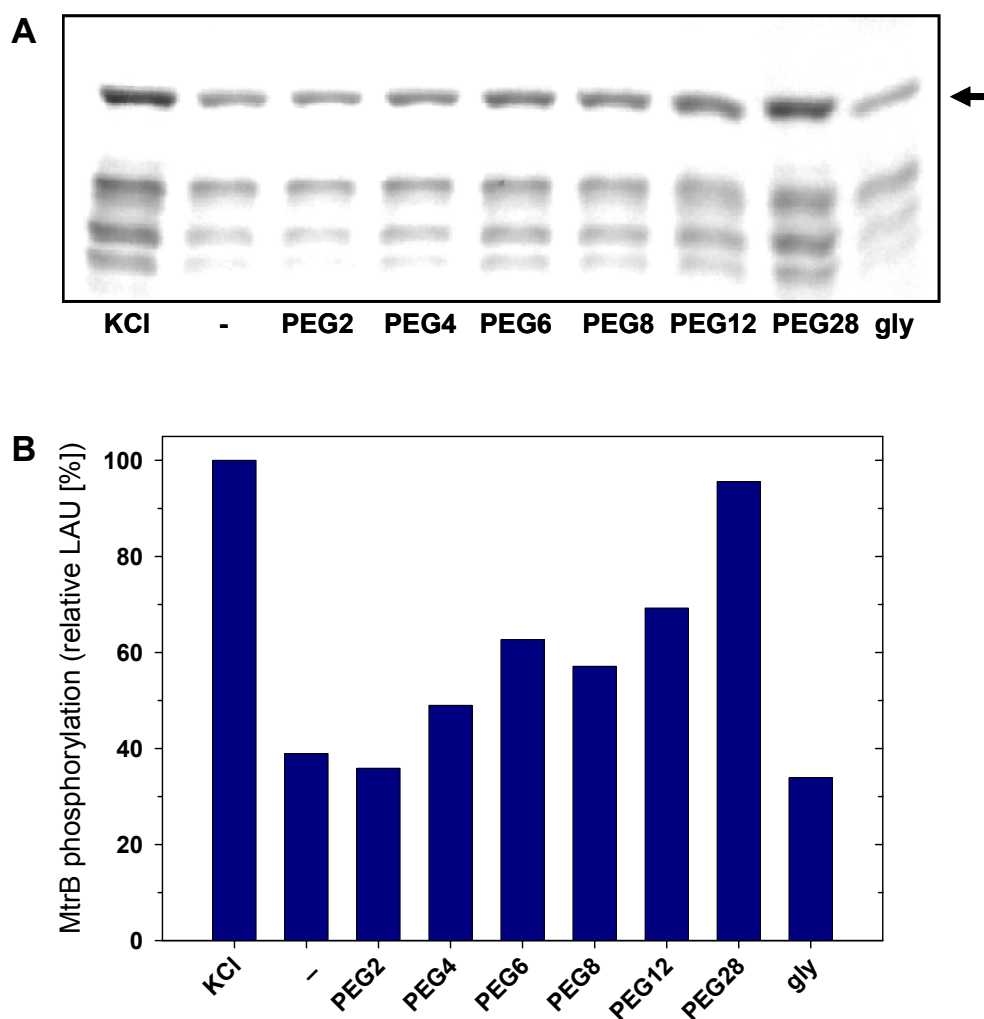
Fig. 31: Influence of polyethylene glycols (PEGs) with various molecular sizes on the autokinase activity of reconstituted MtrB. Following extrusion, proteoliposomes enriched with MtrB-Strep were incubated in absence (**-**) or presence of 75 mM **KCl**, or 150 mM **PEG2**, -**4**, -**6**, -**8**, -**12**, -**28**, and glycerol (**gly**), respectively, resulting in approximately identical osmolarities. The samples were analyzed as phosphorimages (**A**) or by quantification of the signals corresponding to intact MtrB-Strep (**B**) indicated by the arrow. The signal intensity in presence of KCl was set 100 %.

Interestingly, the observed PEG-mediated stimulation of MtrB was not obtained, when the reaction was performed in the presence of 5 mM $MgCl_2$ (Fig. 32A), which was routinely used for former analyses. In contrast, when reconstituted MtrB was incubated in presence of glucose, glutamate, or KCl, the signals in presence of high (5 mM) $MgCl_2$ concentrations were always stronger compared to those obtained with low (20 µM) concentrations (Fig. 32B). Whether this observation is a consequence of non-specific interactions between $MgCl_2$ and polyethylene glycols or of altered $MgCl_2$-dependent membrane permeabilities of the PEGs remains unclear.
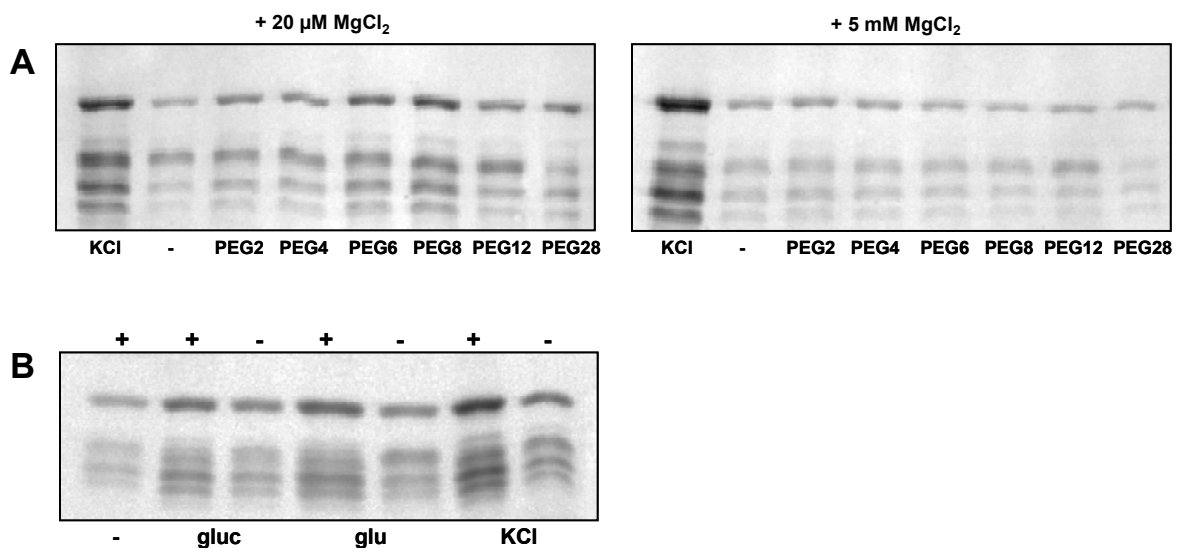
Fig. 32: Influence of polyethylene glycols (PEGs) with various molecular masses on the autophosphorylation activity of reconstituted MtrB in presence of low (20 µM, -) or high $MgCl_2$ concentrations (5 mM, +). A Following extrusion, proteoliposomes enriched with MtrB-Strep were incubated in absence (**-**) or presence of 150 mM **KCl**, or 300 mM **PEG2**, **-4**, **-6**, **-8**, **-12**, or **-28**, respectively. Autophosphorylation was performed in buffer supplemented with 20 µM (left) or 5 mM (right) $MgCl_2$. **B** Influence of 600 mM glucose (**gluc**), or 300 mM Na-glutamate (**glu**) and **KCl**, respectively, on MtrB autokinase activity in presence of 20 µM (**-**) or 5 mM MgCl2 (**+**).

Taken together, the results obtained with PEGs of varying molecular sizes indeed indicate a relation between membrane permeability and MtrB stimulating effects of the examined osmolytes. However, as described in section 3.2.4.2, using different lipids and/or conditions, the effect of Mg^{2+} on liposomes varied with the membrane system. It was therefore important, to experimentally determine the permeability of the osmolytes examined concerning MtrB stimulation using *E. coli* polar lipid extract liposomes.

3.3.4.5 Investigation of the high osmolarity-induced shrinkage of *E. coli* polar lipid extract liposomes

As mentioned, MtrB autokinase activity was significantly stimulated in presence of various membrane-impermeable osmolytes and remained unchanged, when incubated with the membrane-permeant substances PEG 2, glycerol, or urea. The relation between membrane permeability and the MtrB activating effect of the examined compounds was further analyzed. For this purpose, shrinkage of liposomes made from *E. coli* polar lipid extract induced by the substances of interest was determined. Liposomes were loaded with 10 mM calcein, purified by gel filtration, and diluted into buffer supplemented with various MtrB stimulants to a final approximate osmolarity of 150 or 300 mosm. Fluorescence was measured after sample incubation for 1 min in the dark. Liposome shrinkage would result in an increased internal calcein concentration causing increased self-quenching of the fluorescein derivative. Consequently, high osmolarity induced shrinkage could be determined as a decreased fluorescence. The analyzed osmolytes KCl, NaCl, LiCl, Na-glutamate, trehalose, maltose, proline, and glucose gave virtually identical results (Fig. 33). High osmolarity induced shrinkage could be detected in all cases, as fluorescence decreased from 2.6 arbitrary units (AU) in absence of osmolytes to values between 0.5 and 0.7 AU in presence of 300 mosm of the substances. In contrast, liposome shrinkage could not be detected in presence of glycerol, PEG 2, PEG 4, and PEG 6. Large polyethylene glycols (PEG 12 and PEG 28) turned out to be membrane-impermeant, as the fluorescence signal significantly decreased. The partial shrinkage observed with PEG 8 is probably caused by an intermediate membrane permeation. When PEG 28 was used with a final concentration of 300 mM, the fluorescence was increased compared to PEG 12, whereas 150 mM of PEG 28 resulted in determination of stronger liposome shrinkage (Fig. 33). Since samples supplemented with PEG 28 in high concentrations (300 mM) showed an extremely increased viscosity; these signals are probably caused by fluorescence scattering. In Figure 33, liposome shrinkage monitored using approximately 300 mosm of the osmolytes are shown. The illustrated effects could be reproduced when substances were used with final osmolarities of approximately 150 mosm.

The described experiments proved that MtrB was, after incorporation in *E. coli* liposomes or inverted membrane vesicles, significantly stimulated in presence of various osmolytes including compatible solutes, amino acids, sugars, and high molecular weight PEGs starting from PEG 4. Comparison to the fumarate sensor DcuS indicates that the observed effects are specific for MtrB. As a summary, the stimulating effects obtained for MtrB and DcuS *in vitro* autophosphorylation activity are listed in Table 4.
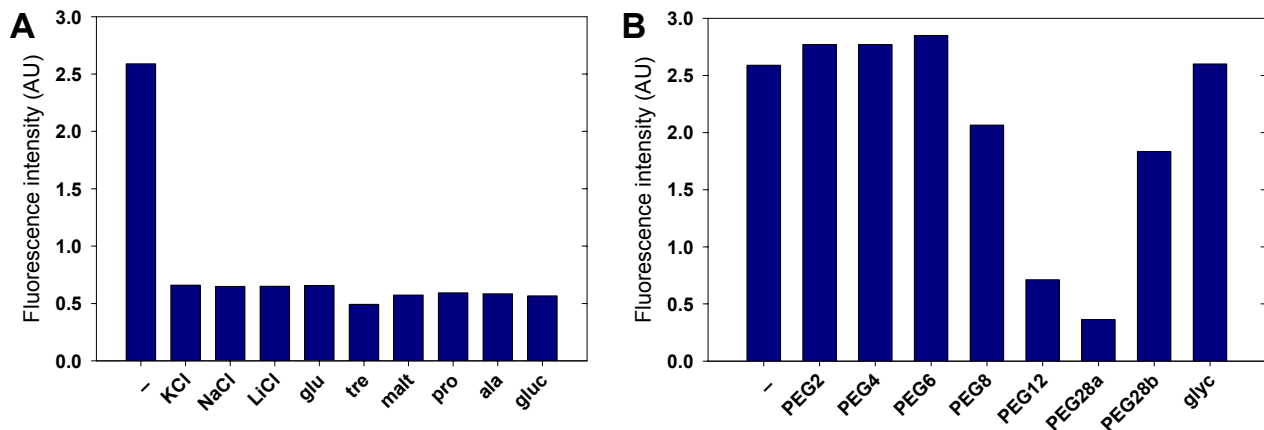
Fig. 33: High osmolarity-induced shrinkage of *E. coli* polar lipid extract liposomes. Shown are the fluorescence signals (arbitrary units, AU) resulting from calcein-loaded liposomes diluted in buffer without (**-**) or with osmolytes. **A** The osmotic upshift was imposed with 150 mM **KCl**, **NaCl**, **LiCl**, and Na-glutamate (**glu**), or with 300 mM trehalose (**tre**), maltose (**malt**), proline (**pro**), alanine (**ala**), and glucose (**gluc**), respectively. **B** The osmotic upshift was imposed with 300 mM polyethylene glycols of different molecular sizes (**PEG 2** to **28a**) or 150 mM PEG 28 (**PEG 28b**), respectively. As comparison, liposomes were incubated in presence of 300 mM glycerol (**glyc**).

Interestingly, osmolytes which were shown to induce liposome shrinkage at approximate osmolarities between 150 and 300 mosm were also shown to significantly stimulate autokinase activity of reconstituted MtrB. Furthermore, the membrane-permeant agents glycerol, urea, and PEG 2 were without influence. In contrast, PEG 4 and 6 turned out to fail to induce liposome-shrinkage, but had an activating effect on MtrB autophosphorylation.

It has to be noted that the results concerning MtrB stimulation described so far were achieved after proteoliposomes were treated by extrusion. The subsequently added osmolytes were only present in the exterior of the membrane systems, which results in liposome shrinkage induced by membrane-impermeant osmolytes. As a control, all osmolytes (despite PEGs) were examined after three cycles of freezing and thawing in presence of these substances, which is expected to result in equal concentrations in lumen and exterior. Consequently, liposome shrinkage should not occur. Interestingly, the MtrB activation by membrane-permeant osmolytes was not altered when proteoliposomes were differently treated. This contradicts the hypothesis that MtrB stimulation by membrane-impermeant osmolytes occurs as a consequence of liposome shrinkage. The monitored substances, including PEGs, can also be grouped by their dehydrating effect on protein surfaces, independent of their membrane-permeance. A more complete dehydration of the MtrB surface by high molecular weight PEGs and other osmolytes, which are more effectively excluded from the protein surface compared to PEG 2, urea and glycerol, is a possible explanation for activation of MtrB autophosphorylation.

Tab. 4: Summary of the effects of various osmolytes on the autophosphorylation activity of reconstituted MtrB-Strep in comparison to (His)$_6$-DcuS. The MtrB and DcuS stimulation profiles observed in presence of the listed compounds and a basal level of 20 mM KCl are summarized. The factors between basal activity and stimulation were calculated and grouped as weak (factors 1.5-2.5, **(+)**), medium (factors 2-4, **+**), strong (factors 3-7, **++**), and very strong (factors 6-10, **+++**) when osmolytes were used with an approximate osmolarity of 600 mosm. Polyethylene glycols (PEGs) were present at concentrations of 150 or 300 mosm. These were related to KCl at the approximately the same osmolarities. A lack of stimulation is also indicated (factors <1.3, **-**).

Type	Compound	MtrB	DcuS
amino acids / compatible solutes			
	Na-glutamate	**+++**	**-**
	alanine	**++**	**-**
	lysine-Cl	**++**	**-**
	proline	**++**	**-**
	glycine betaine	**++**	**-**
sugars			
	trehalose	**++**	**(+)**
	glucose	**++**	**-**
	sucrose	**++**	**(+)**
	fructose	**++**	**(+)**
	maltose	**++**	**(+)**
	maltotriose	**++**	**(+)**
	maltoheptaose (300 mM)	**+**	**n.d.**
PEGs			
	2 (membrane-permeant)	**-**	**n.d.**
	4 (membrane-permeant)	**+**	**n.d.**
	6 (membrane-permeant)	**++**	**-**
	8 (partially impermeant)	**++**	**n.d.**
	12 (impermeant)	**++**	**-**
	28 (impermeat)	**+++**	**-**
	urea (membrane-permeant)	**-**	**n.d.**
	glycerol (membrane-permeant)	**-**	**-**
salts			
	NH$_4$Cl	**+++**	**++**
	KCl	**+++**	**++**
	RbCl	**++**	**++**
	NaCl	**+**	**+**
	LiCl	**-**	**-**

3.4   Investigations on the sensing domain of the histidine kinase MtrB

The experiments described above strongly indicate that MtrB acts as an osmosensor. This led to the question, which domain of the protein is required for stimulus perception, e. g. the extracytoplasmic loop, the transmembrane domains, or the cytoplasmic part of MtrB (compare Fig. 34). Proteolysis using carboxypeptidase Y showed that the reconstitution of MtrB-Strep into *E. coli* lipid liposomes resulted in a unidirectional inside-out orientation (compare section 3.2.4.3), exposing the cytoplasmic kinase core domain of MtrB to the extraliposomal space. Whereas in the experiments using proteoliposomes after extrusion the stimulating compounds were only accessible to the cytoplamsic part of MtrB, the treatment by freezing and thawing is thought to result in an equal concentration in lumen and exterior. The observation that the stimulation pattern of the histidine kinase was unaffected by the different preparations of proteoliposomes already indicated that the sensing domain is not located within the external loop. To investigate in detail which domain of the sensor kinase is involved in the sensory function of MtrB, different truncated forms of the MtrB-Strep protein were constructed.

As mentioned, the sensor kinase MtrB is predicted to contain two transmembrane helices (compare section 3.1), which enclose an extended periplasmic domain of 144 amino acids (Fig. 34). Typically, the sensory domain of two-component system histidine kinases is located in the extracytoplasmic loop. In particular, this is the case in ligand-binding histidine kinases which sense external conditions as e. g. the presence of carbon sources or other nutrients, such as the fumarate sensor DcuS of *E. coli* (Kneuper *et al*., 2005). However, there are also examples of sensor histidine kinases available, in which the signal perception is located within the cytoplasmic domain. The K^+-sensor KdpD of the *E. coli* KdpDE system has been shown to be able to sense low K^+ concentrations after truncation of all four transmembrane domains (Heermann *et al*., 2003). More recent analyses showed that the sensing domain of KdpD is located within the cytoplasmic C-terminal part of the protein (Rothenbücher *et al*., 2006).
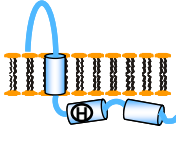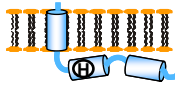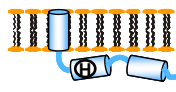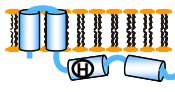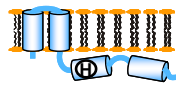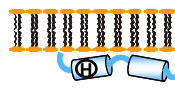
For the detailed investigation, which domain of MtrB is responsible for its sensory function,

Fig. 34: Topology model of membrane-incorporated MtrB.

various N-terminal sub-domains of the sensor were truncated, including the first (N-terminal) transmembrane (TM) helix, the first TM domain and the periplasmic loop, both TM helices including the loop, and only the periplasmic domain leaving both TM helices intact (compare Tab. 5). For the *in vitro* analyses of the autokinase activity of truncated MtrB sensor derivatives the above-described proteoliposome system was chosen.

3.4.1 Construction, isolation and/or reconstitution of various truncated forms of MtrB-Strep

For the construction of various N-terminally truncated derivatives of MtrB-Strep (see Tab. 5), the encoding genes were PCR amplified and ligated in frame with the sequence encoding a Strep-tag using the expression vector pASK-IBA3, resulting in a C-terminal Strep-tag of the respective recombinant proteins. The detailed construction of the expression vectors for the MtrB-Strep derivatives is described in the appendix (section 7.3). The heterologous synthesis of the truncated proteins was carried out as described for MtrB-Strep (see section 3.1.2), with the exception that synthesis of MtrBΔ25 and -Δ190 was induced using 200 µg/L AHT. Determination of the synthesis profiles by means of immunoblot analyses demonstrated that MtrBΔ190, -ΔL124 and -ΔL134 showed synthesis levels remarkably higher compared to full-length MtrB-Strep, whereas using MtrBΔ25 and -Δ154, heterologous synthesis resulted in protein amounts significantly lower compared to those obtained for MtrB-Strep. For MtrBΔ163, immunoblot analysis showed hardly detectable protein signals. Consequently, this construct was not used for purification and subsequent reconstitution.

Tab. 5: Construction of truncated forms of MtrB-Strep.

MtrBΔ25	MtrBΔ154	MtrBΔ163	MtrBΔ L134	MtrBΔ L124	MtrBΔ190
✂ 1st TM	✂ 1st TM ✂ loop	✂ 1st TM ✂ loop	✂ loop	✂ loop	✂ 1st TM ✂ loop ✂ 2nd TM

Isolation of the soluble MtrBΔ190 protein using *E. coli* DH5α*mcr*/pASK-IBA3/*mtrB*Δ190 was performed as described in section 2.5.8. After elution of MtrBΔ190, the protein was dialyzed against 50 mM Tris, 10 % glycerol, 1mM DTT, pH (HCl) = 8.0. Figure 35A illustrates a resulting elution fraction after SDS-PAGE. As in case of native MtrB-Strep, the heterologous expression of MtrBΔ190 resulted in degradation of the 34 kDa protein, which was verified by comparison to immunoblot analysis (Fig. 35A). The purification of the truncated sensor was successful and resulted in a total yield of 1.4 mg per 1.6 L of cell culture.

The MtrB derivatives MtrBΔ25, -Δ154, -ΔL124, and -ΔL134, which were all predicted to be membrane-integrated, were isolated as described for MtrB-Strep (section 3.1.5.1). Purification of MtrBΔ25 and -Δ154 (compare Fig. 35B, C) resulted in very low amounts of the proteins: using 4.8 L of *E. coli* DH5α*mcr* expression culture each, 220 µg of MtrBΔ25 and 170 µg of MtrBΔ154 were isolated in comparison to approximately 1.3 mg of full-length MtrB-Strep. Furthermore immunoblot analyses of the same fractions (data not shown) revealed that degradation fragments of the 52 and 38 kDa proteins were co-purified. Nevertheless, all resulting elution fractions of the two MtrB-Strep derivatives each were pooled and concentrated prior to reconstitution.

In contrast, the total yields of MtrBΔL124 and -ΔL134 after affinity chromatography turned out to be higher compared to MtrB-Strep. From 3.2 L of *E. coli* DH5α*mcr* expression culture each, 1.2 and 1.3 mg of total protein could be obtained. SDS-PAGE of the elution fractions after purification reveals major double bands in case of MtrBΔL124 (Fig. 35D) and a strong single band in case of MtrBΔL134 (Fig. 35E). The upper major band obtained for MtrBΔL124 as well as the single major band of MtrBΔL134 correspond to the predicted molecular masses of 41 and 40 kDa, respectively.

Reconstitution of the proteins into *E. coli* liposomes was performed as described for full-length MtrB-Strep in section 3.1.5.2. Immunoblot blot analyses showed that all truncated MtrB derivatives, as well as degradation fragments, were liposome-associated, and furthermore, that the double bands shown in case of MtrBΔPD124 were indeed caused by degradation of the protein (Fig. 35). The reconstitution was successful and resulted in proteoliposomes containing truncated MtrB-derivatives with final concentrations of approximately 1 µg/µL.
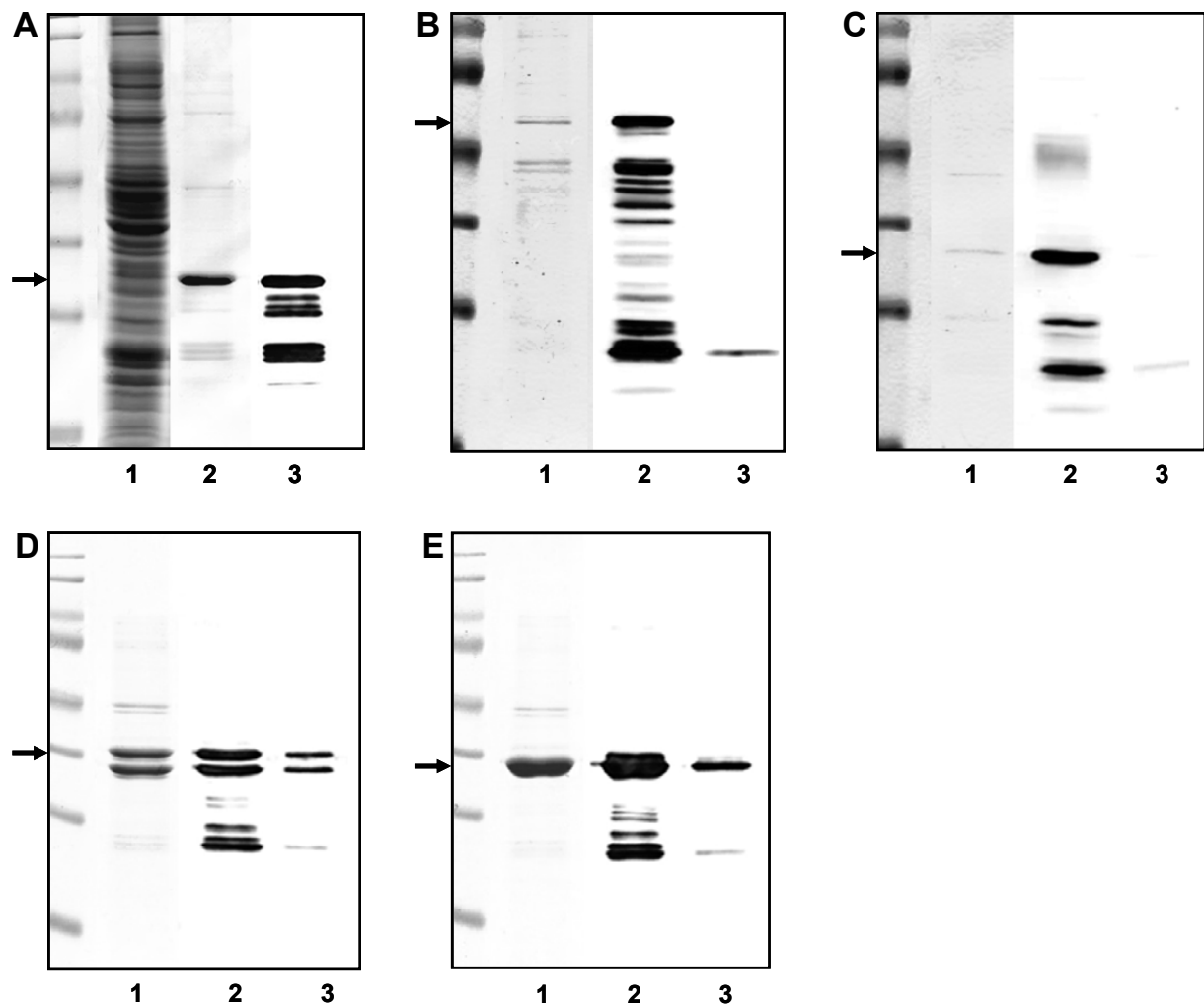
Fig. 35: Affinity purification and/or reconstitution of truncated MtrB-Strep derivatives into
***E. coli* liposomes. A** Isolation of MtrBΔ190 by means of StreptagII/StrepTactin affinity
chromatography. Shown are the flow through (**1**), and an elution fraction after SDS-PAGE (**2**) and
subsequent Western analyses (**3**). **B** - **E** Isolation and reconstitution of MtrBΔ25 (**B**), -Δ154 (**C**), -
ΔL124 (**D**), and -ΔL134 (**E**). Shown are the elution fractions after SDS-PAGE (**1**), as well as the
proteoliposome- (**2**) and the supernatant fractions after the first washing step (**3**) subsequent to
Western blot analyses. The arrows indicate non-degraded truncates MtrB-derivatives.

3.4.2 *In vitro* autokinase activity and/or sensing properties of various truncated forms of MtrB-Strep

3.4.2.1 *In vitro* autokinase activity of MtrBΔ190

The truncated MtrBΔ190 protein solely consists of the cytoplasmic part of the sensor histidine
kinase. Yamamoto *et al.* (2005) were able to show that 25 truncated histidine kinases of
E. coli consisting of their cytoplasmic part only, still exhibited autophosphorylation activity
after purification. However, this soluble part may be membrane-associated *in vivo*.

Consequently, the *in vitro* autokinase activity of this truncated protein was tested in two ways, in the presence or absence of *E. coli* liposomes. For this purpose, liposomes were formed by extrusion and subsequently mixed with MtrBΔ190 resulting in a lipid : protein ratio of 20 : 1. Autophosphorylation of the MtrB-Strep derivative was monitored in the presence of KCl concentrations varying from 0.025 to 1 M. The signal corresponding to MtrBΔ190 could neither in absence nor in presence of liposomes be made visible using radiolabeled ATP (data not shown). Therefore, it could be shown that the soluble part of MtrB-Strep does not exhibit autokinase activity *in vitro*. Together with the observation that solubilized MtrB-Strep did also fail to autophosphorylate *in vitro* (section 3.2.5), these findings indicate that *C. glutamicum* MtrB requires membrane incorporation for its autokinase activity.

3.4.2.2 *In vitro* autokinase activity of MtrBΔ25 and -Δ154

The reconstituted MtrB derivatives lacking the N-terminal membrane-spanning domain and/or additionally the periplasmic loop, MtrBΔ25 and -Δ154, still possess one transmembrane helix. The activity of the two truncated proteins was determined in presence of various osmolytes, which have been shown to stimulate full-length MtrB-Strep. Interestingly, none of the two examined truncated sensor kinases exhibited *in vitro* autophosphorylation activity (data not shown). Thus, truncation of the N-terminal trans-membrane domain of MtrB-Strep resulted in a loss of *in vitro* autophosphorylation activity of the sensor kinase. Also when *E. coli* DK8 inverted membrane vesicles enriched with MtrBΔ25 or -Δ154 were used, no autophosphorylation activity of the truncated proteins was detected (data not shown). As mentioned in section 3.1.2, heterologous synthesis of MtrB-Strep resulted in the isolation of N-terminally degraded forms of the kinase. The results described here are in contradiction with the observation that these degradation fragments, at least with a molecular mass of 40 kDa and higher, were shown to still exhibit *in vitro* autokinase activity in dependence of various osmolytes (compare section 3.3).

3.4.2.3 *In vitro* autokinase activity of MtrBΔL124 and -ΔL134 in presence of various osmolytes

In contrast to the previously described truncated derivatives of MtrB-Strep, MtrBΔL124 and -ΔL134 still contain both membrane-spanning domains. In these two constructs, the periplasmic loop was almost completely truncated, leaving 20 and 10 amino acids, respectively, between the predicted transmembrane domains. Autokinase activity was determined in presence of various osmolytes using a final concentration of 300 mM each for 20 minutes at 30 °C. Both truncated forms of the sensor kinase turned out to still exhibit *in vitro* autophosphorylation activity. As previously shown for full-length MtrB-Strep, MtrBΔL124

and -ΔL134 were significantly stimulated by 300 mM of glutamate, proline, glycine betaine, and lysine. The double bands in case of MtrBΔL124 turned out to show identical activity patterns. Consequently, for quantification, the major single band corresponding to intact MtrBΔL134 and the major double bands of MtrBΔL124 were considered. Figure 36 shows that the two MtrB-Strep derivatives exhibit a virtually identical autophosphorylation pattern.
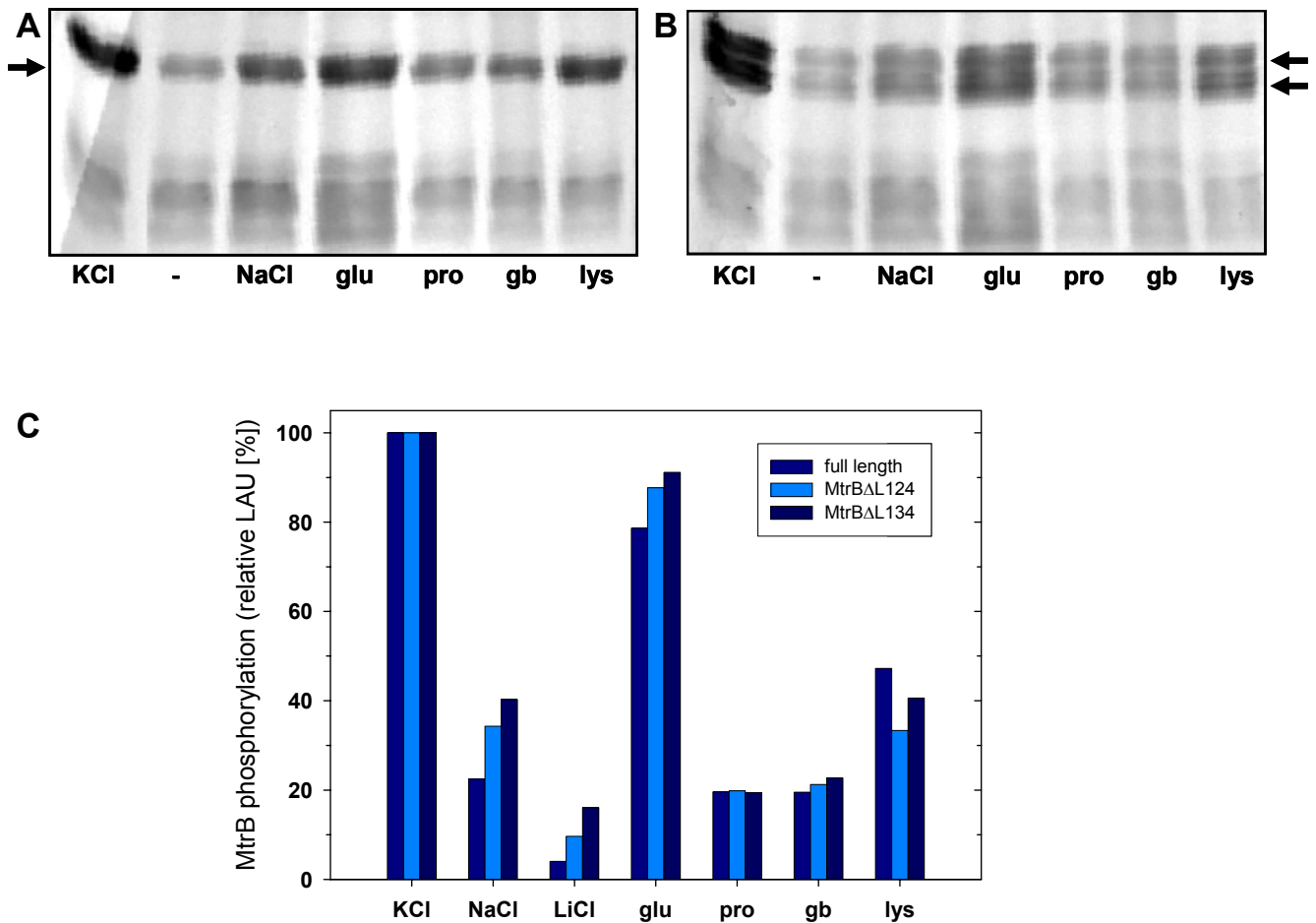
Fig. 36: Comparison of the influence of various osmolytes on MtrB-ΔL134 and -ΔL124. Proteoliposomes were prepared by three cycles of freezing and thawing in phosphorylation buffer (50 mM Tris, 1 mM DTT, 10 mM MgCl$_2$, 20 mM KCl, pH (HCl) = 8.0). **A** and **B** Phosphorylation images of MtrBΔL134 (**A**) and -ΔL124 (**B**) in absence (**-**) or presence of 300 mM **KCl**, **NaCl**, Na-glutamate (**glu**), proline (**pro**), glycine betaine (**gb**), and lysine-Cl (**lys**). **C** Quantification of the signals corresponding to non-degraded (arrow) MtrBΔL134 or to the two main protein signals (arrows) of MtrBΔL124. The signal intensities in presence of KCl were set 100 %. As comparison, quantified phosphorylation signals of full length MtrB-Strep in presence of 300 mM of the same osmolytes were blotted. The intensities of signals obtained in the absence of additional osmolytes (marked with **-** in Fig. 36 **A** and **B**) were subtracted.

As shown above for MtrB-Strep, MtrBΔL124 and -ΔL134 were strongly stimulated in presence of Na-glutamate. Addition of proline, lysine, and glycine betaine also resulted in increased phosphorylation signal intensities, but to somewhat lower extent. These compounds were added in final osmolarities of approximately 300 mosm compared to 600 mosm of KCl, NaCl, and Na-glutamate. Consequently, the resulting phosphorylation signals obtained in presence of the latter solutes were stronger in comparison to the non-ionic substances. However, full-length MtrB-Strep was stimulated to similar extent in presence of the same concentrations of these compounds (Fig. 36C), proving that the nearly complete loss of the extracytoplasmic loop did not affect the stimulation behavior of the sensor kinase. These studies revealed that the sensory function of MtrB is not located within the extracytoplasmic loop. The domain of MtrB, which is responsible for stimulus detection, is suggested to be located within the cytoplasmic part or the transmembrane domains of histidine kinase.

3.5   Influence of the membrane composition on the *in vitro* stimulation of MtrB activity

The membrane-spanning secondary uptake carrier BetP, which acts as an osmosensor in *C. glutamicum*, was recently shown to be influenced by the composition of its membrane surrounding. BetP exhibited an altered osmotic stimulation of betaine uptake in *E. coli* cells compared to the physiological surroundings in the *C. glutamicum* membrane (Peter *et al.*, 1996). These two bacteria differ in their membrane composition. Whereas the cytoplasmic membrane of *E. coli* is mainly composed of phosphatidylethanolamin (PE, 80 %), and furthermore of phosphatidyl glycerol (PG, 15 %), and diphosphatidyl glycerol (DPG, 5 %, Prasad, 1996), the *C. glutamicum* membrane mainly (70 to 90 %) consists of PG (Hoischen and Krämer, 1990). In contrast to PE, PG is negatively charged, resulting in a mainly negatively charged surface of the cytoplasmic membrane of *C. glutamicum*. It was previously shown, that the content of PG in the liposome membrane determined the sensitivity of the reconstituted secondary uptake carrier BetP towards hyperosmotic stress (Rübenhagen *et al.*, 2000).

Here, the osmotic stimulation of reconstituted MtrB was examined in liposomes of different membrane composition. Recently, a more detailed analysis of the fatty acid composition of the different phospholipid species in the *C. glutamicum* membrane revealed that PG is mainly esterified with 18:1 and 16:1 fatty acids (N. Özcan, personal communication). The MtrB autophosphorylation activity profile in a more *C. glutamicum*-like membrane surrounding was investigated by fusion of proteoliposomes made from *E. coli* polar lipid

extract with 33 % synthetic POPG (1-Palmitoyl-2-Oleoyl-*sn*-Glycero-3-[Phospho-*rac*-(1-glycerol)]. In order to obtain a total lipid : protein ratio of approximately 20 : 1, MtrB-Strep was first reconstituted into *E. coli* lipid liposomes with a lipid : protein ration of 13 : 1. Subsequently, these proteoliposomes were mixed with synthetic POPG resulting in 33 % final POPG content, extruded and frozen in liquid nitrogen. Prior to use, the proteoliposomes were slowly thawed and extruded again. As a control, proteoliposomes were fused adding *E. coli* polar lipid extract lipids. The MtrB autokinase activity in the varying liposome preparations was analyzed in presence of various osmolytes (approximately 600 mosm) for 20 minutes at 30 °C. These studies revealed that in both proteoliposome preparations MtrB autokinase activity was stimulated by the monitored osmolytes (Fig. 37 A-C). This stimulation was significantly stronger in the more *C. glutamicum*-like membrane surrounding including 33 % POPG compared to pure *E. coli* lipid liposomes. The addition of glucose, trehalose, alanine, and glycine betaine led to phosphorylation signals comparable to those in presence of KCl (Fig. 37B, C). Furthermore, MtrB stimulation was stronger in presence of all compounds, including KCl. Hence, MtrB *in vitro* activity depends on the membrane composition. When POPG was present in the proteoliposome system, the osmolytes stimulated MtrB to significantly higher extent compared to pure *E. coli* lipid.

The autokinase activity of MtrB incorporated in POPG containing proteoliposomes under the influence of various osmolytes was further analyzed in presence and absence of 20 mM KCl. Figure 37 (D, E) shows that the phosphorylation signals were hardly detectable, when KCl was absent. Compared to pure *E. coli* lipid proteoliposomes (Fig. 29), the difference of MtrB activity in presence compared to the absence of KCl seemed to be more drastic.

The presented data show, that the stimulation profile of MtrB depends on the membrane composition. This effect has to be addressed in more detail in future studies; using fusion with POPG it could not be determined in detail, whether the altered fatty acid composition had an influence, too.
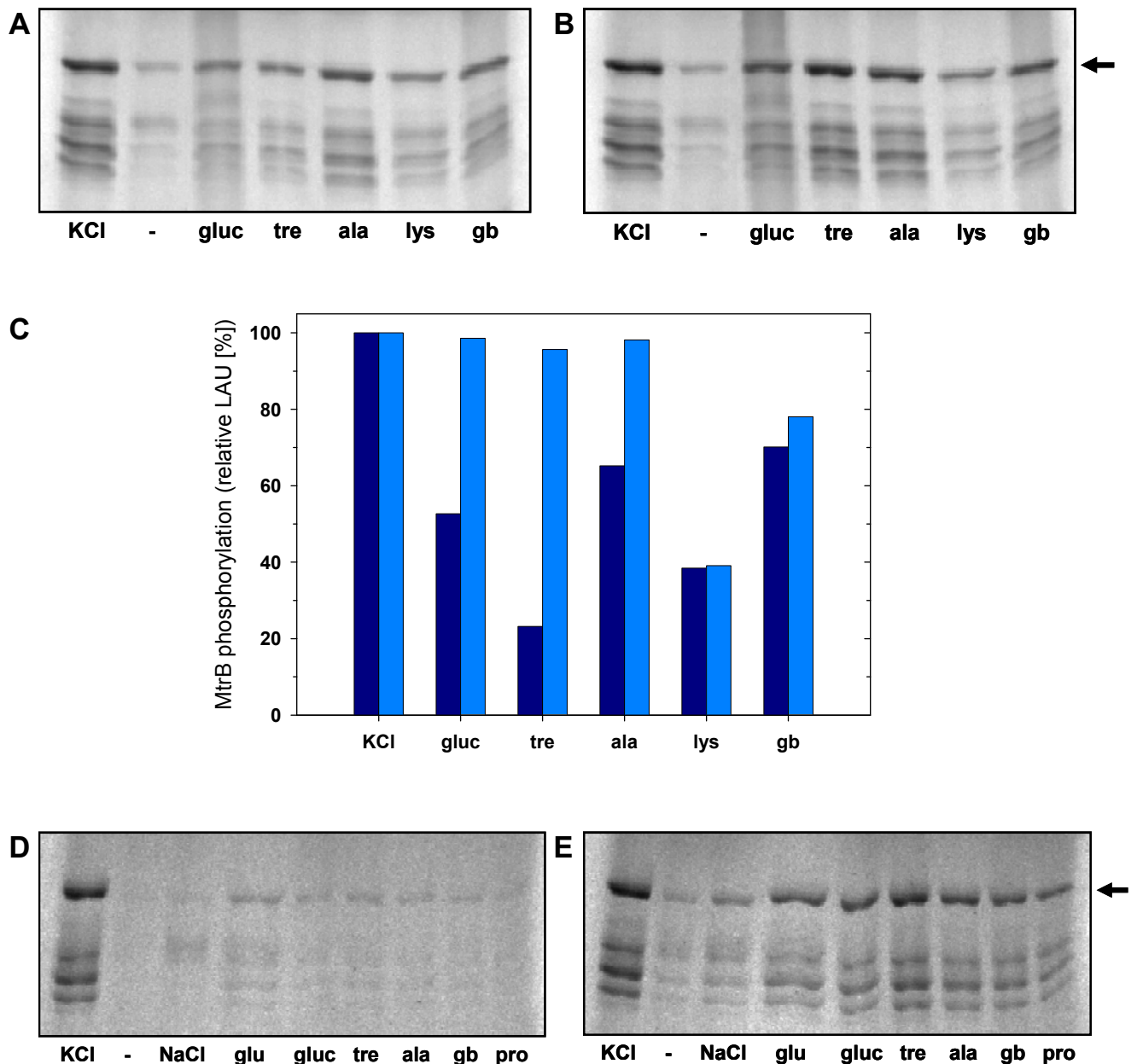
Fig. 37: Influence of an altered membrane composition on the autophosphorylation activity of reconstituted MtrB-Strep. Following extrusion of proteoliposomes, autokinase activity of MtrB-Strep was analyzed in phosphorylation buffer (50 mM Tris, 1 mM DTT, 10 mM $MgCl_2$, 20 mM KCl, pH (HCl) = 8.0). **A** and **B** MtrB-enriched *E. coli* proteoliposomes were fused to 1/3 *E. coli* polar lipid extract lipid (**A**) or synthetic POPG (**B**). The autophosphorylation activity of MtrB was determined in absence (**-**) or presence of 300 mM **KCl** and lysine-Cl (**lys**), or 600 mM glucose (**gluc**), trehalose (**tre**), alanine (**ala**), and glycine betaine (**gb**), respectively, in buffer supplemented with 20 mM KCl. **C** Phosphorylation signals shown in 37A and B corresponding to intact MtrB-Strep (arrows) in proteoliposomes fused to 1/3 *E. coli* lipid (dark blue) or POPG (light blue) were quantified. The signal intensity in presence of KCl was set 100 %. **D** and **E** Influence of various osmolytes in absence (**D**) or presence of 20 mm KCl (**E**) on MtrB-Strep in proteoliposomes fused to 1/3 POPG. The reaction was performed in buffer supplemented with 300 mM **KCl**, **NaCl**, and Na-glutamate (**glu**), or 600 mM glucose (**gluc**), trehalose (**tre**), alanine (**ala**), glycine betaine (**gb**), and proline (**pro**), respectively. As control, autophosphorylation was measured in the absence of any osmolyte (**-**). The arrow indicates phosphorylation signals corresponding to intact MtrB-Strep.

3.6   Investigation of the stimuli sensed by MtrB with focus on chill stress-related signals

Besides osmoregulation, MtrBA could be shown to be involved in the chill-stress response of *C. glutamicum*. Analyses of the expression of genes encoding the BCCT carriers BetP, LcoP and EctP in *C. glutamicum* WT and the *mtrAB* deficient mutant were performed using RNA hybridization experiments. These revealed that MtrBA mediates the expression regulation of *betP* and *lcoP* not only in response to hyperosmotic conditions, but also after exposure to chill stress (Özcan, 2003, compare section 1.5).

Regarding the osmostress response of *C. glutamicum*, the MtrBA-mediated expression regulation of *betP*, *lcoP* and a gene encoding a third secondary uptake carrier for compatible solutes, *proP*, could be shown (Möker *et al*., 2004). Consequently, it was of high interest, whether the *proP* gene is also induced in response to chill-stress in dependence of this two-component system. Furthermore, as a control, the results obtained concerning the expression of *betP* and *lcoP* at 30°C and 15°C in relation to the cultivation time (Özcan, 2003) had to be reproduced in relation to both, the cultivation time as well as the growth phase.

3.6.1 Expression regulation of *proP, betP*, and *lcoP* in response to chill stress conditions

In order to examine the influence of chill stress on the expression of *proP*, *betP*, and *lcoP*, *C. glutamicum* WT and $\Delta mtrAB$ cells were cultivated as described in section 2.2.2. Cells were adjusted to CgXII minimal medium and cultivated until the exponential phase (OD_{600} = 6 to 7) was reached. Subsequently, the cultures were divided, centrifuged at 30 °C and diluted into pre-tempered CgXII medium for further cultivation at either 30 or 15 °C. The growth phase of *C. glutamicum* cells at 15 °C was approximately reduced to one half in comparison to cultivation at 30 °C (Fig. 38). To achieve both, a comparison of gene expression at similar growth phases as well as similar time points after the change of temperature, the samples were taken before and 2, 4, 6, and 20 h after exposure to 15 °C, while the control cells grown at 30 °C were collected before and 1, 2, 3, 4, 5, 6 and 20 h after the division of the CgXII cultures. Figure 39 shows the resulting expression profiles of *proP*, *betP* and *lcoP* in *C. glutamicum* WT and $\Delta mtrAB$ cells before and after chill-stress exposure by cultivation at 15 °C (Fig. 39, right panels). As a control, the mRNA levels after continuous cultivation at 30 °C are shown (Fig. 39, left panels). All three genes exhibited increased transcript amounts after exposure to chill stress in *C. glutamicum* WT, when compared at identical growth stages. In the $\Delta mtrAB$ mutant, the transcription was significantly decreased or below the detection limit. Similar patterns were observed when the samples were taken at identical
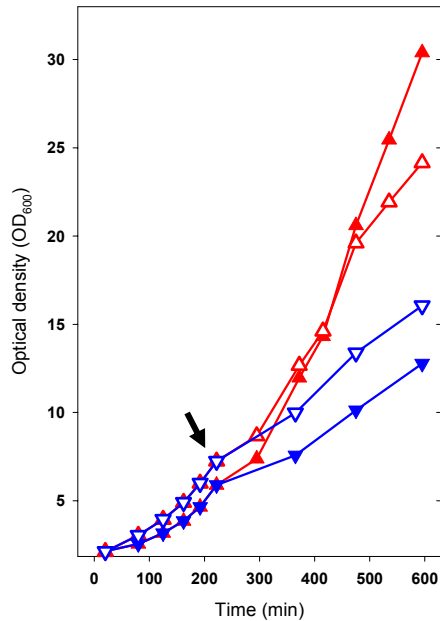
Fig. 38: Cultivation experiments with *C. glutamicum* WT (closed triangles) and Δ*mtrAB* (open triangles) at different temperatures. Cells were exposed to chill stress (blue) or continuously cultivated at 30 °C (red). The arrow indicates the time point of exposure to different temperatures.

cultivation times (data not shown). The comparison to the transcript levels of the control mRNA, *gapDH*, shows that almost similar total RNA amounts were blotted (Fig. 39). Consequently, exposure to 15 °C resulted in induction of the three genes *betP*, *lcoP*, and *proP*, which all encode secondary uptake carriers for compatible solutes, in *C. glutamicum* WT. However, the induction achieved by chill stress was to some extent lower compared to that observed after osmotic stress (compare Fig. 5). The reduced levels of mRNA in the *mtrAB*-deficient strain strongly indicate that the chill-stress induced transcription of these genes is mediated by the MtrBA two-component system. In addition, the results described before using identical incubation times (Özcan, 2003) were reproduced for identical growth phases as well. Since the genes controlled by the MtrBA two-component system were induced after exposure to both, osmotic- as well as chill stress, the sensor kinase MtrB is likely to exhibit the ability for chill sensing in addition to its osmosensory function. In order to examine the direct influence of low temperatures on MtrB activity, *in vitro* phosphorylation assays were performed.

Fig. 39: Influence of chill stress conditions on the expression profiles of *proP*, *betP*, and *lcoP*. Total RNA was isolated from *C. glutamicum* WT (**wt**) and Δ*mtrAB* (Δ) cells before (**T_0**) and after cultivation at 30 °C (left panels, marked with red) in comparison to 15 °C (right panels, marked with blue). Samples were taken at identical growth phases (OD_{600} = **8** to **14**), or incubation time points (data not shown). As control, *gapDH* expression was monitored identically.

3.6.2 Influence of chill on the *in vitro* autokinase activity of MtrB

For investigation of chill effects, MtrB was analyzed *in vitro* using the proteoliposome system described above. Proteoliposomes were prepared by extrusion and autophosphorylation activity of 2 µg reconstituted MtrB-Strep was monitored at 10, 15, and 30 °C. Samples were taken at different time points and the reaction was followed for 20 minutes. Strikingly, the autokinase activity of reconstituted MtrB turned out to be strongly stimulated after exposure to low temperatures (Fig. 40). Highest activity levels were obtained at 15 °C. In case of 10 °C, MtrB was also significantly stimulated.
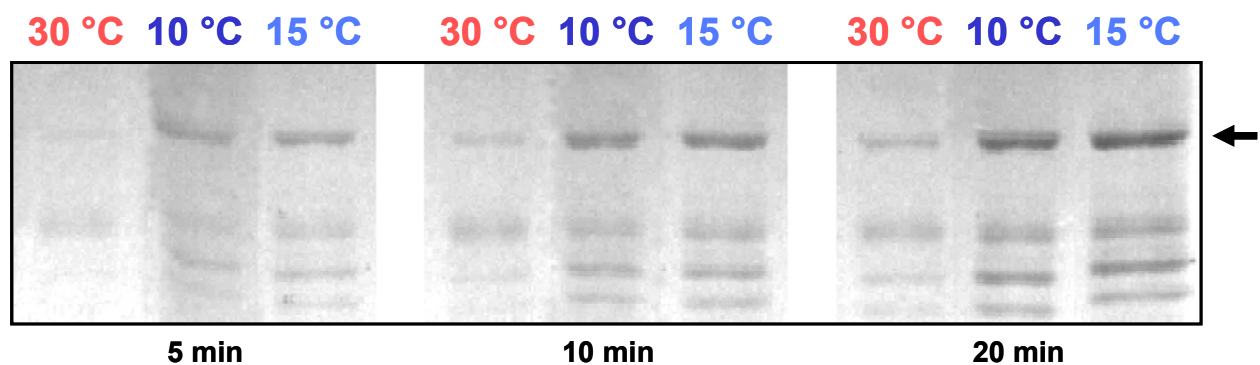
Fig. 40: Influence of chill on the autokinase activity of reconstituted MtrB-Strep. Subsequent to extrusion, the autophosphorylation reaction was followed in phosphorylation buffer (50 mM Tris, 1 mM DTT, 10 mM MgCl₂, 20 mM KCl) over 20 minutes at **30**, **10**, and **15 °C**. The arrow indicates phosphorylation signals corresponding to intact MtrB-Strep. The quantification of the phosphorylation image using signals corresponding to intact MtrB (arrow) is shown in Fig. 41 B.

This temperature-dependent autophosphorylation profile was observed after 5, 10, and 20 minutes reaction time. However, quantification of the MtrB phosphorylation signals demonstrates that the strongest chill-mediated stimulation was obtained within the initial 5 minutes of the reaction (Fig. 40, 41B, see Tab. 6). This chill-induced stimulation of MtrB activity was also observed, when inverted membrane vesicles, as well as the Strep-MtrB derivative were used (data not shown).

As a control whether chill stimulation is specific for MtrB, the autophosphorylation activity of the reconstituted fumarate sensor DcuS was determined under identical conditions. The resulting autoradiogram (Fig. 41) demonstrates that, after 5 to 10 minutes reaction time, no significant increase in phosphorylation signal intensity was observed at 10 or 15 °C. When the reaction was performed for 20 minutes, an increase in DcuS autophosphorylation could be measured at 15 °C, but clearly to a lower extent compared to that of MtrB (Fig. 41B, C).
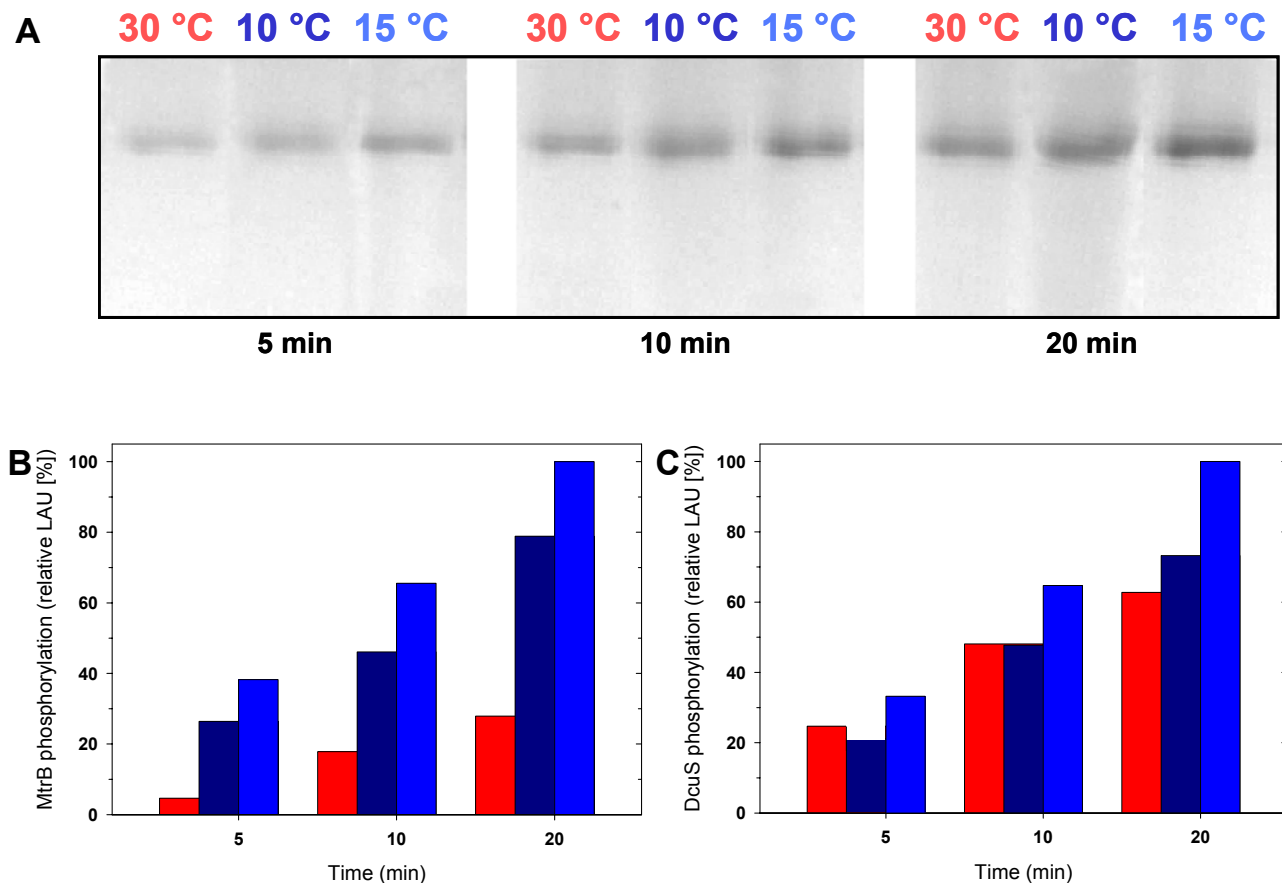
Fig. 41: Influence of chill on the autokinase activity of reconstituted MtrB in comparison to DcuS. The autophosphorylation reaction was followed over 20 minutes at 30, 10, and 15 °C. **A** Autophosphorylation image after incubation of reconstituted $(His)_6$-DcuS at **30**, **10**, and **15 °C**. **B** and **C** Quantification of the phosphorylation signals corresponding to intact MtrB-Strep (**B**) or $(His)_6$-DcuS (**C**) at **30** (left panels, red), **10** (mid panels, dark blue), or **15 °C** (right panels, blue). The signal intensities after 20 minutes autophosphorylation at 15 °C were set 100 %.

The calculation of the factors of increase in autophosphorylation activity measured at 15 and 10 °C in comparison to 30 °C is summarized in Table 6. The most striking differences were obtained after 5 minutes of autophosphorylation. Exposure to 10 and 15 °C resulted in a 3-5 and 7-8 fold increased phosphorylation signal intensity of MtrB, whereas DcuS showed a 1.3 to 1.8 fold increased radioactivity when exposed to 15 °C. When stimulation was monitored for 20 minutes, MtrB showed an average 3 and 4 fold increase in radioactivity at 10 and 15 °C, whereas for DcuS, the signal intensity was increased by factors averaging 1.3 and 1.6. The *in vitro* chill-induced stimulation of MtrB activity at 15 °C was observed to an extent comparable to that achieved for osmostress-related stimuli (compare Tab. 4). Thus, MtrB was shown to be stimulated *in vitro* by chill stress related signals in addition to its osmosensing function. The comparison with the fumarate sensor DcuS showed that this

response is specific for MtrB. Consequently, MtrB seems act as a sensor for chill stress in addition to its osmosensory function in *C. glutamicum*.

Tab. 6: The factors of increased signal intensity of MtrB and DcuS phosphorylation signals at 10 and 15 °C in comparison to 30 °C were calculated. Listed are these factors obtained after 5, 10, or 20 minutes of autophosphorylation at low temperature. The experiments summarized here were performed at least twice and the average factors are shown.

Incubation time (min)	MtrB		DcuS	
	10 °C	15 °C	10 °C	15 °C
5	3-5	7-8	0.9-1.1	1.3-1.8
10	2-3	3.5-4	1-1.3	1.4
20	3-4	3.5-4-5	1.2-1.5	1.6

The ability to sense both, signals related to osmotic as well as chill stress, has also been reported for the compatible solute uptake carrier BetP (compare section 1.3). However, in case of BetP, an *in vitro* chill stimulation of protein activity could only be achieved in a *C. glutamicum* membrane surrounding (Özcan, personal communication). Furthermore, as shown in section 3.5, fusion of MtrB enriched *E. coli* liposomes with 33 % POPG resulted in stronger stimulation by various osmolytes. This lead to the question whether the chill stimulation of the MtrB activity may also be influenced by an altered membrane composition of the liposome system. For this reason, MtrB autophosphorylation activity in proteoliposomes was, after fusion with 33 % POPG (compare section 3.5), determined under conditions identical to those used for pure *E. coli* lipid proteoliposomes (compare Fig. 40). In contrast to the stimulation obtained by the presence of osmolytes, the altered membrane composition did not result in stronger stimulation of MtrB autophosphorylation by low temperatures (Fig. 42). The sensor kinase showed increased basal activity levels after fusion to 33 % POPG at 30 °C. However, the extent of chill-mediated stimulation was somewhat lower compared to that obtained in pure *E. coli* lipid proteoliposomes.
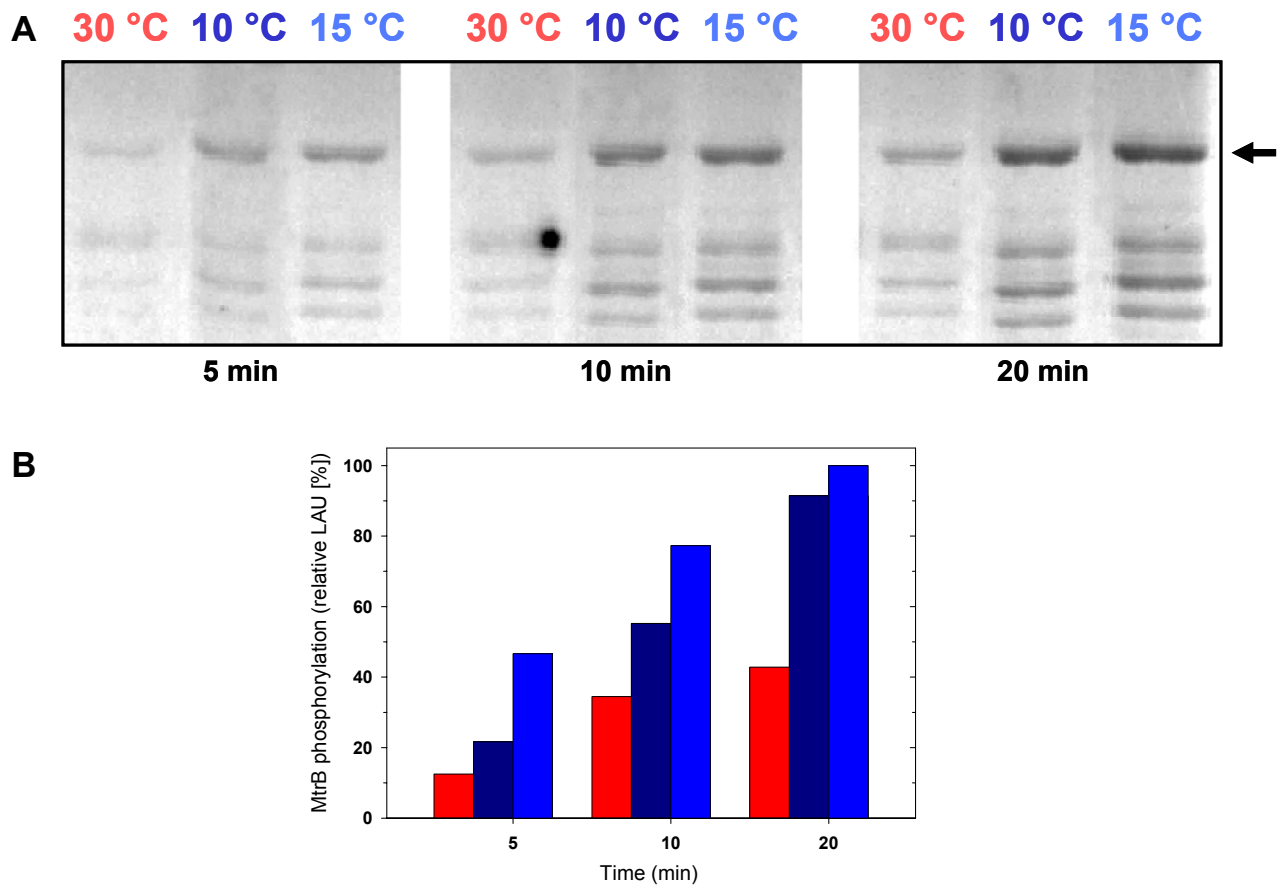
Fig. 42: Influence of an altered membrane composition on the chill-mediated stimulation of autophosphorylation activity of reconstituted MtrB-Strep. Following extrusion, the autophosphorylation reaction was followed over 20 minutes at **30**, **10**, and **15 °C** using MtrB-enriched proteoliposomes after fusion to 33 % POPG. Autophosphorylation of MtrB-Strep at **30** (red, left panels), **10** (dark blue, mid panels), and **15 °C** (blue, right panels) was analyzed as phosphorimages (**A**) or after quantification of the phosphorylation signals corresponding to intact MtrB-Strep indicated by the arrow (**B**). The signal intensity (LAU) after 20 minutes autophosphorylation at 15 °C was set 100 %.

4.   Discussion

The phosphorelay signal transduction mediated by two-component systems is a common feature of bacteria responding to environmental signals like stress situations. The MtrBA two-component signal transduction system, composed of the membrane-bound sensor histidine kinase MtrB and its cognate cytoplasmic response regulator MtrA, is highly conserved within the *Corynebacterium* and *Mycobacterium* species. This indicates that it plays an important role in the physiology of these organisms. *In vivo* analysis of the MtrB-MtrA system revealed its influence on genes involved in at least three different physiological functions in *C. glutamicum*, (I) osmoprotection, (II) chill stress response, and (III) cell wall metabolism (Möker *et al.*, 2004; Özcan, 2003). In the beginning of this work it was not known, whether MtrBA-mediated gene regulation is carried out directly or via an accessory protein. It was recently shown, that MtrA binds to the promoter regions of genes involved in all three physiological functions (Reihlen, 2006; Brocker and Bott, in preparation). Thus, the induction of *proP* and *betP*, as well as the repression of *mepA* and *nlpD*, are directly regulated by this two-component system, and an involvement of additional factors could be ruled out. Regarding the sensing mechanism of the histidine kinase, at least two scenarios are possible. (I) Either stimuli related to one of these functions are detected acting as measure for the three different purposes, or (II) MtrB is able to detect a set of different stimuli. These stimuli would likely be connected to the three above-mentioned physiological functions.

A number of two-component systems involved either in the chill stress response, osmoprotection, or cell wall metabolism were described earlier (Aguilar *et al.*, 2001; Polarek *et al.*, 1992; Mizuno *et al.*, 1988; Raivio *et al.*, 1999; Mascher *et al.*, 2004). Regarding the two-component system-mediated regulation of genes involved in both functions, osmostress-response and cell wall metabolism, an example was recently described. The VraSR system of *Staphylococcus aureus* was proposed to be a positive regulator of cell wall peptidoglycan synthesis (Kuroda *et al.*, 2003). Transcriptome analyses proposed that VraSR is furthermore involved in the transcription regulation of *proP*, encoding a compatible solute transporter. However, in contrast to MtrBA, the direct target genes of this system are still unknown.

In vivo experiments revealed that the expression regulation of genes involved in osmo- and chill stress protection is mediated by MtrBA in response to specific environmental stimuli, namely increased osmolarity and low temperature. This indicates that the histidine kinase MtrB acts as a sensor for stimuli related to both environmental conditions, osmo- as well as chill stress. In contrast, the conditions which lead to the regulation of cell wall-related genes are unknown. In this study, the signals triggering stimulation of MtrB autokinase activity were investigated in detail by use of *in vitro* phosphorylation systems.

4.1 Development and characterization of *in vitro* MtrB and MtrA phosphorylation assays

When microorganisms are exposed to osmotic- or chill stress, a set of cellular parameters changes simultaneously. Consequently, the direct physico-chemical stimuli, which are sensed by MtrB and hence initiate the two-component system signal transduction, cannot be identified using a whole cell approach. In order to discriminate between the different parameters, it was necessary to investigate the sensory properties of MtrBA *in vitro*. This required the development of artificially reduced membrane systems enriched with the membrane-bound sensor histidine kinase MtrB, namely proteoliposomes or inverted membrane vesicles. Before addressing the primary MtrB stimulating signals, it was necessary to prove that the *in vitro* systems exhibited all properties proposed for the two-component system signal transduction in the living cell. These included the autokinase activity of membrane-bound MtrB, the phosphoryl group transfer to soluble MtrA, and the dephosphorylation of MtrA-P.

Inverted membrane vesicles were prepared from MtrB synthesizing *E. coli* DK8 cells. In this case, the membrane-bound sensor kinase is integrated into the cytoplasmic membrane by the *E. coli* cell machinery, which might provide correct integration. However, in this system *E. coli* membrane proteins are also present. The proteoliposome system provides a more reduced complexity. For this purpose, MtrB had to be isolated and reconstituted into preformed liposomes made from *E. coli* polar lipid extract. This system guarantees that all monitored effects are related to MtrB, since no additional proteins are present. Proteoliposomes were used for the detailed analysis of a number of membrane-bound sensor proteins, i. e. the compatible solute uptake carriers BetP of *C. glutamicum*, and ProP of *E. coli* involved in osmoregulation, as well as the two-component system histidine kinases KdpD, EnvZ, and DcuS of *E: coli*, or PhoQ of *S. typhimurium*. Thus, proteoliposomes seemed to be a suitable system for the *in vitro* characterization of MtrB.

For the heterologous synthesis in *E. coli* and isolation of the sensor kinase, two recombinant MtrB derivatives were chosen, carrying either a C- ("MtrB-Strep") or an N-terminal ("Strep-MtrB") fusion to a Strep-tag. The possibility that the tag affects MtrB activity and/or stimulation should be ruled out by use of the two MtrB derivatives. It is highly unlikely, that a Strep-tag at the C-terminus would affect a protein in a similar way as an N-terminal fusion. Using both proteins, partial degradation occurred during expression in the heterologous host *E. coli*. Various cultivation and induction conditions failed to improve protein stability. However, the MtrB-derivatives were found in the membrane fraction of *E. coli*, and could be purified by affinity chromatography. Some of the degradation fragments were co-purified, indicating that they still carried a C- or N-terminal Strep-tag. These fragments in the elution

fractions could not be separated by gel filtration from intact proteins, which is presumably due to the integration of the membrane proteins into detergent vesicles. However, the main part (~ 80 %) of the elution fractions exhibited a molecular mass expected for intact MtrB (56 kDa). When the respective protein band was excised and analyzed by Edmann sequencing, it could be verified that this band indeed represents the full-length MtrB-Strep protein. The Strep-MtrB derivative carries an N-terminal Strep-tag, thus only those fragments were co-purified, which exhibited degradation from the C-terminus. Since Edmann analyses addresses the N-terminus of a protein, this construct was not sequenced. However, the main part of the Strep-MtrB elution fraction was composed of a protein with a molecular weight identical to that of MtrB-Strep. Therefore, it can be concluded that this fraction is also mainly composed of intact MtrB protein. Both derivatives were used for the preparation of inverted membrane vesicles and the reconstitution of isolated MtrB into *E. coli* liposomes.

For the isolation of the soluble response regulator, the *mtrA* gene was fused to the sequence encoding a C-terminal $(His)_{10}$-tag. In contrast to the membrane-spanning MtrB, the heterologous synthesis of the cytoplasmic response regulator MtrA yielded higher protein quantities without degradation products.

Autophosphorylation of MtrB was measured as *in vitro* activity in presence of radiolabeled ATP ($[\gamma^{33}P]ATP$). Using inverted membrane vesicles, both, MtrB-Strep and Strep-MtrB, exhibited autokinase activity, indicating that the sensor was functionally integrated into the *E. coli* cytoplasmic membrane. In contrast, when used in its solubilized state after purification, MtrB could not autophosphorylate. The autokinase activity was restored after reconstitution of the solubilized protein into *E. coli* liposomes, thus indicating that the membrane environment is a prerequisite for *in vitro* activity of MtrB. Since autophosphorylation requires transphosphorylation between the monomers of dimeric sensor histidine kinases, it is feasible that in case of MtrB the membrane surrounding favors the correct dimeric state, which might be lost when solubilized in detergent.

To date, the few sensor histidine kinases that were reported to be investigated in a proteoliposome system are KdpD, EnvZ, DcuS of *E. coli*, and PhoQ of *S. typhimurium*. As in case of MtrB, KdpD and DcuS lost activity in their solubilized state, which was regained after reconstitution (Jung *et al*., 1997; Janausch *et al*., 2002). For EnvZ and PhoQ four and two times higher activity levels were reported after reconstitution into liposomes or in membrane vesicles, respectively, in comparison to the solubilized protein (Jung *et al*., 2001; Sanowar and Le Moual, 2005). However, the activity of solubilized PhoQ was observed only if the measurement was performed directly after solubilization out of membrane vesicles. The autokinase function of the solubilized protein was lost following purification by Ni-NTA chromatography, and could be regained only after reconstitution. Taken together, the loss of

activity of two-component system histidine kinases in the solubilized state was reported for a number of two-component systems.

MtrB was shown to autophosphorylate in both membrane systems. For MtrB-Strep autokinase activity after reconstitution, a K_m value for ATP of 0.3 mM was determined (see Fig. 14). In *C. glutamicum* cells, the physiological ATP level averages 4-5 mM, thus significantly exceeding this K_m value (Krämer and Lambert, 1990). Assuming that the kinetics of reconstituted MtrB reflect the *in vivo* situation, ATP would be present in saturating levels for the MtrB autophosphorylation reaction in the whole cell, and would therefore not provide a regulatory signal. The autophosphorylation of reconstituted MtrB turned out to increase with the reaction time and was virtually linear for the first 30 minutes (see Fig. 13). The kinetics shown here are more or less similar to those reported for DcuS, which exhibits a K_m value for ATP of 0.16 mM and an approximate linearity of increasing phosphorylation for the first 25 minutes (Janausch *et al*., 2002). In contrast, reconstituted EnvZ showed rapid autophosphorylation in presence of ATP, reaching a maximal concentration of EnvZ-P after approximately 5 minutes already (Jung *et al*., 2001).

When purified MtrA-(His)$_{10}$ was added with a fourfold molar excess to reconstituted MtrB after autophosphorylation, the phosphoryl group was rapidly transferred to the response regulator. The MtrA phosphorylation reached an apparent steady state already after one minute (see Fig. 15). The observation, that the MtrB-MtrA phosphorelay was significantly faster than the autophosphorylation of MtrB is consistent with the fact that the transfer of the phosphoryl group to response regulators generally occurs more rapid as compared to the autophosphorylation of sensor histidine kinases (Stock *et al*., 2000). The latter reaction is the rate-limiting step of the two-component system signal transduction.

The lifetime of phosphorylated response regulators can vary between seconds and hours depending on the system. The signal transduction is turned off by dephosphorylation of the activated response regulator, for which a variety of phosphatases were reported. The inactivation of this protein can for example be catalyzed by a separate bacterial phosphatase, the combined action of the histidine kinase, the response regulator, and an accessory protein, or a phosphatase activity of the sensor kinase (Comeau *et al*., 1985; Ninfa *et al*., 1995; Blat and Eisenbach, 1994).

For the MtrBA phosphorelay it could be shown, that MtrA-P is comparatively stable. When incubated for 60 minutes, approximately 60-70 % of phosphorylated MtrA was still detectable. The slow dephosphorylation is probably caused by an intrinsic activity, which has been reported to be the reason for the limited lifetime of many response regulators (Hess *et al*., 1988). Membrane-bound MtrB could be shown to specifically mediate the dephosphorylation of MtrA-P (see Fig. 16). The phosphatase activity of the histidine kinase turned out to depend on the presence of ADP. In the absence of ADP, only intrinsic

dephosphorylation of MtrA-P was detected. In contrast, ADP did not affect MtrA-P stability, when the histidine kinase was not added. In this test assay, ATP was absent to clearly discriminate between autokinase- and phosphatase activity of MtrB. This situation does not reflect that in the whole cell. In future studies, it will be addressed, whether the ATP/ADP ratio is of importance for a possible switch between the two enzymatic activities. The ADP-induced phosphatase activity shown here for MtrB was described recently for other reconstituted sensor kinases, e. g. PhoQ and EnvZ (Sanowar and Le Moual, 2005, Igo *et al.*, 1989).

In order to describe the *in vitro* activity of MtrB in detail, the orientation of the reconstituted histidine kinase within the liposomes was important. Reconstitution of membrane proteins into liposomes can principally result in a random or unidirectional in-side-out or right-side-out orientation. Especially in case of osmosensors it is important to determine which domain of the protein is localized in the lumen or exterior of liposomes. The knowledge about the orientation of the reconstituted sensor protein is the prerequisite to define which stimulus, e. g. internal ionic strength versus external ionic strength, is received.

The observation, that the phosphoryl group was transferred from MtrB in intact liposomes to externally added MtrA showed that the kinase core domain of the sensor was accessible to the response regulator, thus already indicating an inside-out orientation. The orientation of reconstituted MtrB-Strep was experimentally determined by site-specific proteolysis addressing the C-terminus. For this purpose, the accessibility of the C-terminal cytoplasmic part of MtrB towards carboxypeptidase Y in intact proteoliposomes was compared to those ruptured in presence of detergent (0.1 % Triton-X-100). C-terminal proteolysis occurred in both cases to comparable extent (see Fig. 19), which could be reproduced with various proteoliposome preparations. Thus, it was proven, that MtrB exhibits a unidirectional in-side-out orientation after reconstitution.

This result was at a first glance contradicted by the observation that MtrB exhibited increased autophosphorylation signals, when $MgCl_2$ was added in increasing concentrations varying from 0.02 to 10 mM (see Fig. 17). Mg^{2+} and other divalent cations have been reported to permeabilize liposomes and proteoliposomes made from *E. coli* total lipid extract (Liu *et al.*, 1997) in concentrations of 5 mM and lower. Thus, the increased MtrB activity could be a consequence of increased accessibility of the kinase core domain to ATP and would then indicate that MtrB exhibits mainly a right-side-out orientation in proteoliposomes. Since these findings were in contradiction to those obtained by site-specific proteolysis, it was analyzed whether $MgCl_2$ indeed causes permeabilization of liposomes. It turned out that $MgCl_2$ in concentrations varying between 0.02 and 10 mM completely failed to permeabilize the *E. coli* polar lipid extract liposomes used in this study (see Fig. 18). This was in agreement to independent investigations (Sanowar and Le Moual, 2005), which also revealed that

liposomes made from *E. coli* polar lipid extract turned out to be intact after incubation in presence of 10 mM Mg^{2+}, Ca^{2+}, or Mn^{2+} for up to 150 minutes. Consequently, the increased MtrB phosphorylation observed in presence of high $MgCl_2$ concentrations is not likely to be caused by permeabilization of the proteoliposome system. A right-side-out orientation of the sensor kinase after reconstitution is thus highly unlikely. The question remained, why MtrB showed increased phosphorylation levels in presence of $MgCl_2$. ATP was only present in low concentration (0.22 µM) in the phosphorylation assays. Thus, 20 µM $MgCl_2$ were sufficient for the supplied ATP to form the Mg^{2+}-complex, which is the prerequisite for the ATP-dependent autokinase activity. The reason for the MtrB activating effect of $MgCl_2$ remains unsolved. However, *in vitro* analyses of all reported sensor kinases were generally performed in presence of high (10-20 mM) concentrations of this ion (Jung *et al.*, 2000; Jung *et al.*, 2001; Janausch *et al.*, 2002; Sanowar and Le Moual, 2005). Taken together, the results of this study suggest that reconstitution of MtrB results in a unidirectional inside-out orientation, exposing the cytoplasmic part of the histidine kinase to the exterior of proteoliposomes. This orientation was also reported for all reconstituted sensor histidine kinases, as KdpD, DcuS, and PhoQ (Jung *et al.*, 1997; Janausch *et al.*, 2002; Sanowar and Le Moual, 2005). It may be argued that the extended cytoplasmic domain, which constitutes the main part of this protein class, causes this unidirectional orientation.

With proteoliposomes, a suitable *in vitro* system was established to study the biochemical properties of MtrB in detail. Inverted membrane vesicles served to corroborate the results obtained with proteoliposomes, using an additional *in vitro* phosphorylation assay. The use of the two different derivatives, Strep-MtrB and MtrB-Strep, respectively, verifies that the reactions monitored *in vitro* are not affected by the presence of the Strep-tag. The sensing properties of MtrB could be analyzed by a systematic variation of physico-chemical parameters related to osmotic- and chill stress with the described MtrB activity assays.

4.2   Sensing properties of MtrB in dependence of osmotic stress

A first glance of the osmostress-related stimuli which are sensed by MtrB was achieved by *in vivo* analysis. RNA hybridization experiments addressing the expression of the genes *proP*, *betP*, and *lcoP*, encoding secondary uptake carriers for compatible solutes, as well as *mscL*, coding for a mechanosensitive channel, were performed before and after a hyperosmotic shift. MtrBA turned out to mediate the induction of the carrier genes, as well as the repression of the mechanosensitive channel gene, in response to hyperosmotic stress. This was first observed upon NaCl addition, imposing an osmotic shock (Möker *et al.*, 2004). To discriminate, whether NaCl is essential for the high osmolarity-induced expression regulation, the experiment was repeated with trehalose. This substance cannot be taken up by

C. glutamicum (Tropis *et al*., 2005), and thus provides an increased extracellular osmolarity, independent of the external ionic strength. The resulting osmotic gradient causes water efflux, thus additionally the intracellular conditions, including the osmolarity, ionic strength, or membrane state, are altered. The use of trehalose imposing the hyperosmotic shock altered the expression of the MtrBA target genes in the same way as NaCl (see Figures. 5, 21). Thus, MtrB *in vivo* does not seem to sense NaCl, or an increased external ionic strength, specifically.

In bacteria, at least two types of osmosensors were found. On one hand, transport systems can exhibit osmosensory properties, which are directly regulated at the level of activity. On the other hand, osmosensors can mediate the transcriptional regulation of osmoregulated transport systems and thus act at the level of expression. However, these transcriptional regulators themselves are regulated at the level of activity. The latter case can be accomplished by two-component systems, as seems to be the case for MtrBA.

Several cellular physico-chemical parameters change in case of environmental osmotic stress conditions, and are thus discussed as possible stimuli for osmosensors (see section 1.6). The osmotic activation of MtrB may be triggered by a variety of parameters including a change in cell turgor, membrane effects like a mechanical deformation of the membrane and altered protein-lipid interactions, a change in the external or internal osmolarity, changes in the hydration state of MtrB as a consequence of altered internal or external osmolarity, changes in the cytoplasmic ion concentration or ionic strength, or changes in the concentration of specific compounds interacting directly with the sensor kinase.

The described *in vitro* systems do not allow the variation of turgor pressure, however, in case of the well described osmosensors BetP of *C. glutamicum*, ProP and KdpD of *E. coli*, or OpuA of *Lactococcus lactis*, the cell turgor as signal triggering protein activity was shown to be an unlikely stimulus (Morbach and Krämer, 2002; Culham *et al*., 2003; Jung *et al*., 2000; Poolman *et al*., 2002).

In order to analyze which stimulus is used by MtrB to detect hyperosmotic stress, the *in vitro* effect of various possible osmostress-related signals was tested. First, a variation of monovalent ions was performed, to discriminate between the influence of ionic strength or specific ion effects. Various monovalent salts, especially KCl, RbCl, and NH_4Cl, turned out to strongly activate autokinase activity of MtrB-Step, and Strep-MtrB, respectively, both in membrane vesicles and proteoliposomes. NaCl had a weak activating effect, whereas LiCl completely failed to affect MtrB activity (see Fig. 22). Thus, it was not Cl^- mediating this activation, but rather cations, with varying intensities.

In case of membrane-bound osmosensors, a number of proteins have been reported to sense intracellular monovalent ions specifically, or the internal ionic strength in general. Especially for compatible solute uptake carriers, it could be shown that changes in the

internal cellular conditions are measured. For example the Na^+/betaine carrier BetP of *C. glutamicum* was reported to specifically sense internal K^+ (or Rb^+ and Cs^+, Rübenhagen *et al.*, 2001; Schiller *et al.*, 2004a), whereas the H^+/compatible solute symporter ProP of *E. coli* was postulated to be stimulated not only by internal cations, but additionally by cytoplasmic macromolecules (Racher *et al.*, 2001; Culham *et al.*, 2003). In case of the reconstituted ABC transporter OpuA of *L. lactis* an activation by increased internal ionic strength, which is thought to result in perturbations in the ionic interactions between protein and the surrounding membrane system, was proposed (van der Heide *et al.*, 2001).

In contrast, the sensing of internal conditions by two-component systems was clearly shown only for the histidine kinase KdpD of *E. coli*. The KdpDE system regulates the transcription of the *kdpFABC* operon, encoding the high affinity K^+ uptake ATPase KdpFABC (Polarek *et al.*, 1992; Walderhaug *et al.*, 1992). This two-component system reacts to two distinct *in vivo* conditions: the *kdpFABC* expression is regulated in response to low K^+ concentrations as well as to an osmotic upshift. Analysis of KdpD in right-side-out membrane vesicles showed that the histidine kinase senses two sets of stimuli *in vitro*. Whereas internal K^+, already at a concentration of 1 mM, showed an inhibitory effect on KdpD activity, an increased internal ionic strength, imposed by NaCl, RbCl, or HEPES-Na, had an activating effect on this protein (Jung *et al.*, 2000). Also in *E. coli*, the EnvZ/OmpR two-component system was reported to regulate the transcription of *ompC* and *ompF*, encoding porins of the outer membrane, in dependence of the medium osmolality (Pratt and Silhavy, 1995). The sensor kinase of this system, EnvZ was, after reconstitution, stimulated by the monovalent ions K^+, Rb^+, NH_4^+, and Na^+, with highest autokinase activity levels in presence of K^+.

Thus, a salt-dependent stimulation of MtrB seemed to be a reasonable signal for osmotic stress. The surprising similarity between BetP and MtrB, both being stimulated by K^+, led to the question, whether an increased K^+ concentration in the cytoplasm serves as general signal for *C. glutamicum* cells indicating hyperosmotic stress. However, at that state of this work, it was not yet shown, whether MtrBA directly mediates the expression regulation of the postulated target genes encoding osmoregulation systems. It was therefore necessary to provide a test system in order to discriminate between specific and non-specific signals for the postulated osmosensor MtrB. For this purpose, the well-analyzed DcuS histidine kinase of *E. coli* was chosen, which does not seem to be involved in osmostress-response. The DcuS-DcuR two-component system mediates the expression regulation of genes encoding carriers and enzymes for the catabolism of externally supplied C_4-dicarboxylates in response to the presence of extracellular C_4-dicarboxylates, such as fumarate (Zientz *et al.*, 1998; Golby *et al.*, 1999; Janausch *et al.*, 2002). *In vitro* analyses using DcuS-enriched proteoliposomes showed that the histidine kinase specifically senses the presence of C_4-dicarboxylates like fumarate and succinate with its extracytoplasmic loop (Janausch *et al.*,

2002; Kneuper *et al*., 2005). Strikingly, the present study revealed that the reconstituted fumarate sensor was, similar to MtrB, strongly activated by KCl, RbCl, and NH$_4$Cl. Furthermore, also like in the case of MtrB, NaCl had weaker activating effects, whereas LiCl remained without influence (see Fig. 24). Consequently, this pattern of activation was almost identical to that of MtrB and of EnvZ (Jung *et al*., 2001) in proteoliposomes. Additional analyses of the K$^+$ effect revealed that a stimulation of DcuS activity by fumarate could only be obtained in presence of basal levels of KCl. For activation induced by the C$_4$-dicarboxylate, already low concentrations of KCl (20 mM) were sufficient. Very recently, data were obtained on another purified and reconstituted sensor histidine kinase, CpxA of the CpxAR two-component system, which is involved in the envelope stress response in *E. coli*. This protein was also shown to be activated *in vitro* by the presence of KCl (S. Hunke, personal communication).

The DcuSR system is most probably not involved in the osmoregulation of *E. coli*, which indicates that the activating effect of K$^+$ would be a feature of the *in vitro* systems. If K$^+$ indeed was a signal for two-component systems *in vivo*, their target genes would all be induced or repressed in response to hyperosmotic stress, since K$^+$ is intracellularly accumulated under these conditions. This was not the case for the DcuSR-mediated signal transduction. *In vivo* analyses revealed that the stimulation of DcuSR by fumarate resulted in the induction of the target genes, whereas osmotic upshifts imposed by external sorbitol, NaCl, or KCl did not influence expression of these genes (Unden, personal communication). Furthermore comparison with data derived from DNA micro- or macroarrays for *C. glutamicum* and *E. coli* after a hyperosmotic shock showed that the regulons of known two-component systems which are not involved in osmoprotection were not affected by internally increased K$^+$ concentrations (Ley, 2005; Weber and Jung, 2002). These findings suggest that the observed salt effects are characteristic for *in vitro* systems, independent of the *in vivo* sensory properties of the histidine kinases. Possibly physiological concentrations of K$^+$ and other monovalent ions have stabilizing effects on the native conformation of the sensor kinases and thus provide correct *in vitro* autokinase function. Consequently, we suggest that the *in vitro* stimulation of MtrB by salts may be non-specific. A further possibility would be a superposition of stimulating and non-specific effects of the monitored salts. This might be indicated by the observation that MtrB was found to be more sensitive towards KCl compared to DcuS. However, the results discussed here show that DcuS provides a suitable control system to verify, that stimuli, which are proposed in this study to be sensed by MtrB, are indeed specific for this sensor histidine kinase.

The *in vitro* investigation of MtrB autokinase activity in presence of a variation of osmolytes of different chemical nature showed that the sensor kinase was strongly stimulated by the presence of various sugars, compatible solutes, and amino acids (see Fig. 27-29). These

effects turned out to be dependent on the concentration of the compounds, and were obtained for the C- and N-terminally tagged MtrB derivatives. The same substances did not influence the *in vitro* activity of DcuS (see Fig. 47-49). Hence, the stimulation by various osmolytes is specific for the MtrB sensor kinase. This was further verified by the findings of Jung and colleagues (2001), who showed that reconstituted EnvZ was not activated by osmolytes other than salts, e. g. trehalose, sucrose, glycine betaine, or proline, even when monitored in presence of basal levels of KCl (50 mM), which were all shown to significantly stimulate MtrB activity.

Furthermore, the influence of sugars, amino acids, and compatible solutes on the MtrB-MtrA phosphotransfer reaction, which is catalyzed by the response regulator, was investigated *in vitro*. The resulting MtrA phosphorylation profile turned out to be increased in presence of the same osmolytes which were shown to stimulate MtrB autokinase activity. Thus, an additional intermediary regulation within the MtrB-MtrA phosphorelay could be ruled out.

Interestingly, an activating effect on MtrB autophosphorylation was found for nearly all monitored membrane-impermeant osmolytes. In contrast, the membrane-permeant compounds glycerol and urea had no effect on MtrB activity. When polyethylene glycols with increasing molecular sizes were used, the partly or completely non-permeant substances PEG 8, -12, and -28 were shown to significantly stimulate MtrB autokinase activity, whereas the membrane-permeable PEG 2 remained without influence. However, PEG 4 and -6 were shown to be membrane-permeant in this study, but nevertheless turned out to stimulate MtrB activity to somewhat lower extent (see Fig. 31). The named compounds do not only differ in their membrane-permeance, but furthermore in their effect on the hydration state of protein surfaces (see below). It turned out that PEGs had no effect on DcuS *in vitro* activity (see Fig. 50), thus proving that also the PEG-induced stimulation of activity is specific for MtrB.

Taken together, it could be shown, that MtrB was *in vitro* significantly stimulated by various osmolytes of different chemical nature, such as sugars, compatible solutes, amino acids, and high molecular weight PEGs. Using reconstituted DcuS as a control system, it could be verified that these effects were specific for MtrB. Regarding the high osmolarity-dependent stimulation of the sensor kinase, at least two hypotheses can be derived.

(I) The reported stimulation profile indicates that MtrB is activated by an increased osmolarity *per se*, and not by the presence of specific compounds, since it is very unlikely, that MtrB exhibits binding sites for such a broad variety of molecules. Increased osmolarity could affect protein conformation, resulting in activation of MtrB autophosphorylation. The decrease of water activity can in principle influence protein activity by a change of the hydration state of the system. This was reported for hexokinase (Parsegian *et al*., 1995), whose dissociation constant for glucose binding decreased with increasing osmotic pressure of the assay medium, when varied with either low or high molecular weight PEGs. The smaller effects of

low molecular weight PEGs were explained by their less effective steric exclusion from a cleft in the enzymatic surface. Similar to hexokinase, the surface hydration could regulate the activity of MtrB. The degree of dehydration could be solute-dependent. In several studies, glycerol has been shown to be less excluded from protein surfaces than other solutes such as sucrose and glycine betaine (Courtenay *et al*., 2000; Timasheff and Arakawa, 1989). This could explain the failure of glycerol to stimulate MtrB activity. Since the sensor kinase was shown to be integrated in a unidirectional in-side-out orientation, the soluble and main part of the protein was accessible to the sugars, compatible solutes, amino acids and PEGs. The soluble part of MtrB could become more hydrated and more completely activated with the above-mentioned osmolytes and with PEGs, which are more effectively excluded from the hydrophilic surface of the protein compared to glycerol, urea, or PEG 2, resulting in activation.

In case of the secondary transporter ProP, Racher *et al*. (2001) reported different effects of high and low molecular size PEGs on the osmotic activation. Similar to reconstituted MtrB, PEGs, starting from PEG 4 and thus membrane-permeable, activated ProP activity, however to lower extent than the high molecular size, impermeant PEGs. As also found for MtrB, PEG 2, urea, and glycerol failed to stimulate ProP activity. Culham and colleagues (2003) proposed that ProP responds to osmotically induced changes in cytoplasmic K^+ levels and the concentration of cytoplasmic macromolecules, resulting in so-called macromolecular crowding.

In case of MtrB, the observation that low molecular weight substances such as glucose were able to activate MtrB to a level comparable to that of maltotriose, maltoheptaose, and high molecular weight PEGs, indicates that MtrB is regulated rather by the hydration state of the protein, and not by macromolecular crowding.

This model is in accordance with the situation *in vivo*. When *C. glutamicum* cells are exposed to hyperosmotic stress, water efflux results in shrinkage of the cytoplasm. Consequently, the concentration of cytoplasmic compounds is increased. Additionally, the osmoregulated uptake carriers BetP, LcoP, EctP, and ProP are activated accumulating compatible solutes, which leads to an additional increase of the cytoplasmic concentration of osmolytes (Fig. 43). It is reasonable, that an osmosensor uses this increased intracellular osmolarity, perhaps via an altered hydration state of the protein surface, as activating signal indicating hyperosmotic stress.
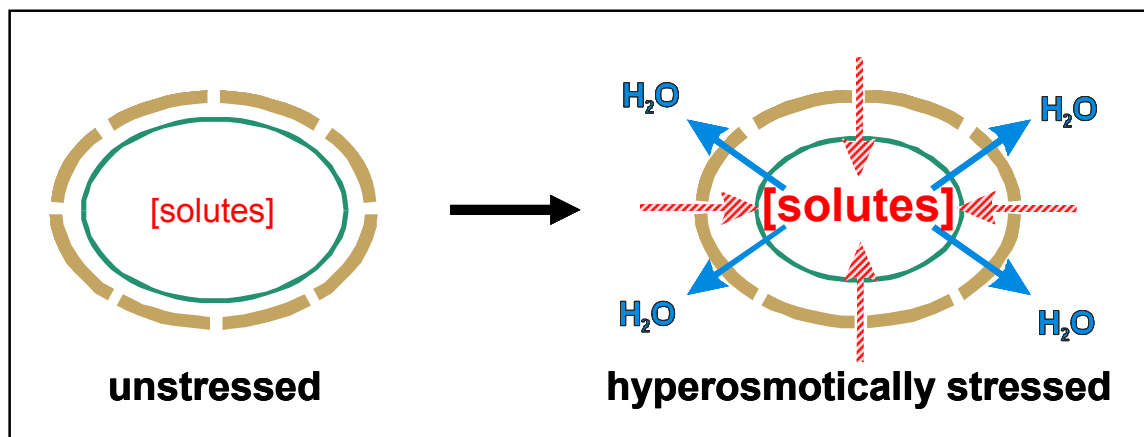
Fig. 43: Influence of hyperosmotic stress on *C. glutamicum* cells. When cells are exposed to hyperosmotic stress, the cytoplasm undergoes shrinkage and secondary carriers are activated mediating the uptake of compatible solutes. Both results in an increased concentration of cytoplasmic solutes; the internal osmolarity *per se* is increased.

(II) The second hypothesis is based on the observation of a correlation between membrane-permeance of the stimulating compound and stimulation of the sensor kinase MtrB. When integer membrane systems, such as proteoliposomes, membrane vesicles, or cells are exposed to high external osmolarity, lumenal water diffuses out until the osmotical gradient is balanced. This results in shrinkage of the membrane system, the shape changes and local variations in membrane structure such as lateral phase separation or changes in curvature strain can be the consequence. These membrane effects could change the protein conformation and thus activate MtrB autophosphorylation. Furthermore, altered interactions between the surrounding membrane and MtrB under these conditions could serve as an activating signal.

It has to be noted that, during MtrB activity assays, the *in vitro* membrane system was treated in two ways. (i) Proteoliposomes with a defined diameter were formed by extrusion, and the compounds of interest were subsequently added, thus being present in the exterior of the membrane system only. The high osmolarity-induced shrinkage of the liposomes treated this way was experimentally verified for the sugars, compatible solutes, and amino acids, which were shown to significantly stimulate MtrB activity. In contrast, glycerol and PEG 2 failed to induce shrinkage of the membrane system. These findings provided evidence for the hypothesis, that MtrB is able to sense an altered state of the membrane, resulting in activation at high osmolarity conditions. However, the low molecular size compounds PEG 4 and -6 also turned out to be membrane-permeant, but had a detectable stimulating effect on MtrB (see Fig. 33). Despite the fact that this stimulation occurred to

lower extent than with membrane-impermeant PEGs, this would, at a first glance, contradict this hypothesis. It was reported, that low molecular weight PEGs, such as PEG 4 and -6, diffuse relatively slowly across the liposomal membrane, resulting in a transient deformation of the bilayer (van der Heide *et al*., 2001). The system may have been in the activated state for a very short period, which could not be determined with the kinetic resolution of the volume measurements reported in this study. This would explain the observed weaker MtrB stimulation by PEG 4 and -6, which could be caused by a similar mechanistic basis as with the membrane-impermeant PEGs.

(ii) In a second series of experiments, the determination of MtrB stimulation was performed with an altered experimental set-up. First, the osmolytes (besides PEGs) were added to the proteoliposomes, and subsequently the samples were subjected to three cycles of freezing and thawing. This procedure is thought to result in an even concentration of all compounds in the liposomal lumen and the exterior. Thus, shrinkage of the liposome system should not occur as consequence of the presence of osmolytes. The stimulation profile of MtrB did not vary when proteoliposomes were treated differently. This contradicts the hypothesis that the stimulation of MtrB by membrane-impermeant osmolytes occurs as consequence of shrinkage of the membrane system. However, the final prove that the freezing and thawing procedure indeed results in an equal concentration in the lumen and exterior of the proteoliposomes used in this study is still missing. In future studies, it will be experimentally verified if MtrB activity is stimulated by the above-mentioned osmolytes when the liposome system is not exposed to shrinkage.

The second hypothesis of MtrB stimulation would be in accordance to the *in vivo* situation. *C. glutamicum* cells under hyperosmotic stress suffer water efflux out of the cytoplasm (see Fig. 43), thereby resulting in shrinkage of the cytoplasmic membrane. An altered state of the cytoplasmic membrane, or altered interactions between the membrane surrounding and MtrB, would serve as a suitable signal for MtrBA activation in response to hyperosmotic stress.

4.3 Sensing properties of MtrB in dependence of the membrane composition

Recently, it was observed that the compatible solute carrier BetP exhibited an altered sensitivity towards osmotic stress in the heterologous host *E. coli* compared to *C. glutamicum* cells (Peter *et al*., 1996). The threshold for osmotic activation was shifted to lower external osmolarities when BetP was heterologously synthesized in *E. coli*. It was concluded that this phenomenon could either be a result of the different turgor pressure

values in the Gram-positive *C. glutamicum* cells (approximately 20 atm) compared to the Gram-negative host *E. coli* (approximately 2 atm), or a consequence of the different membrane composition of the two organisms. Whereas the cytoplasmic membrane of *E. coli* is mainly composed of uncharged PE, the predominant lipid of the *C. glutamicum* membrane is negatively charged PG, resulting in a mainly negatively charged membrane surface (Prasad, 1996; Hoischen and Krämer, 1990). The systematic variation of the content of negatively charged phospholipids in the proteoliposome system revealed that the fraction of PG in the liposome membrane determined the sensitivity of BetP towards hyperosmotic stress (Rübenhagen *et al.,* 2000; Schiller *et al*., 2006).

In order to test whether the stimulation of MtrB depends on the lipid composition, the sensory properties of MtrB-Strep were analyzed in proteoliposomes enriched with *C. glutamicum*-like phospholipids. Since in this organism PG is mainly esterified with 18 : 1 and 16 : 1 fatty acids (Özcan, personal communication), synthetic POPG (1-Palmitoyl-2-Oleoyl-*sn*-Glycero-3-[Phospho-*rac*-(1-glycerol)], 16:0-18:1) was fused to proteoliposomes made of *E. coli* lipids. Comparison of the MtrB activity regulation in liposomes composed of 33 % synthetic POPG to those in pure *E. coli* lipid showed that the histidine kinase was more sensitive towards the presence of osmolytes in the POPG-enriched liposomes. Firstly, the MtrB activity stimulation in presence of KCl was significantly increased in comparison to pure *E. coli* lipid liposomes. Furthermore, the activating effect of the other osmolytes, which showed stimulation levels somewhat below KCl in pure *E. coli* liposomes, turned out to be as strong as in presence of KCl when POPG was present (see Fig. 37). This indicates that the membrane composition plays an important role in the sensing mechanism of MtrB. In case of BetP, it was recently proposed that the fraction of negative charges at the membrane surface, and not PG itself, is responsible for the altered K^+-dependent regulation pattern of the transport protein (Schiller *et al*., 2006).

For MtrB, it could be shown, that the sensor kinase was significantly more sensitive towards hyperosmotic stress in dependence of POPG in the membrane. However, it is not clear, whether the observed influence of the membrane was a consequence of an altered membrane composition or state in general, or whether this is due to effects of head groups or fatty acids of the lipids specifically. A discrimination between the influence of an altered fatty acid- or head group composition can be achieved by the analyses of the influence of further lipids, as e.g. DOPG, or DOPC/DOPE, either or not containing PG.

4.4   Sensing properties of MtrB in dependence of chill stress

Compatible solutes are known to protect proteins against denaturation under several stress conditions, like osmo-, heat-, or chill stress. In *C. glutamicum*, the two secondary uptake systems for compatible solutes BetP and LcoP, both osmoregulated in their activity, were shown to be furthermore regulated by chill at the level of activity. The strongest stimulation by low temperature was observed for BetP, whereas LcoP was activated to lower extent (Özcan *et al*., 2005). The *betP* and *lcoP* genes turned out to be transcriptionally regulated by MtrBA in response to chill stress (Özcan, 2003). In this study, it could be shown that a further gene coding for an osmoregulated transport system catalyzing the uptake of compatible solutes, *proP*, was induced in response to chill stress in dependence of MtrBA (see Fig. 39). Thus, the membrane-bound histidine kinase MtrB is likely to act as sensor for chill stress in addition to its osmosensor function. In case of chill stress conditions, various physiological parameters of a bacterial cell change and can principally serve as stimuli for proteins acting as chill sensors. These are (I) the physical state of the membrane (phase transition of membrane-bound lipids), (II) conformational changes in proteins, and (III) conformational changes in nucleic acids. An example for a two-component system mediating the chill stress response is given by DesK-DesR of *B. subtilis* (Aguilar *et al*., 1999, 2001), composed of the membrane-bound sensor kinase DesK and the cytoplasmic response regulator DesR. A temperature decrease-mediated change in the physical state of the membrane is believed to result in functional alteration of DesK, therefore initiating the signal transduction which leads to induction of the *des* gene. The resulting synthesis of a Δ5-lipid desaturase, catalyzing the desaturation of lipid fatty acids, is thought to mediate restoration of membrane fluidity.

The ability of MtrB to sense low temperature was closer analyzed *in vitro* by monitoring the activity of the histidine kinase at 10 and 15 °C in comparison to the physiological 30 °C, which provide optimal growth of *C. glutamicum* cells. The "normal" temperature profile of proteins would be a continuously increasing activity at increasing temperatures, according to the Arrhenius equation. Strikingly, MtrB reconstituted into *E. coli* liposomes was significantly activated by low temperature, with the highest activity around 15 °C. The strongest effects were observed, when MtrB was incubated for 5 minutes, which represented the initial phase of MtrB autophosphorylation, compared to 10 or 20 minutes (Fig. 40). The control system DcuS showed a weak stimulation at 10 and 15 °C, but to significantly lower extent (Fig. 41). The reason for a possibly non-specific weak activating effect of chill on a reconstituted sensor kinase is not clear. However, since DcuS was activated to significantly lower extent (1.3 to 1.8 fold increased activity at 15 °C, Tab. 6) in comparison to MtrB (4 to 8 fold increased activity at 15 °C, Tab.6), the chill stimulation of autokinase activity seems to be

rather specific for MtrB. The extent of chill-induced activation of MtrB at 15 °C was comparable to the stimulation by increased osmolarity.

For BetP it was reported that two different signal inputs are measured. The osmotic- and chill stimulation turned out to be independent and not additive (Özcan *et al*., 2005). However, a chill-dependent activation of this transporter could only be obtained in *C. glutamicum* cells, and not when synthesized in *E. coli* or reconstituted into *E. coli* liposomes. These findings are in accordance with changes in the physical properties of the membrane being a possible signal triggering chill stimulation of BetP. However, the participation of an additional factor in *C. glutamicum* cells cannot be excluded. Since BetP activation by low temperature could not be shown in proteoliposomes yet, the final prove that BetP itself acts as a sensor for chill is still missing.

Since MtrB showed chill-dependent stimulation in proteoliposomes, the requirement of an accessory protein for stimulus perception can be ruled out. The histidine kinase was thus shown to act itself as a sensor for chill. Furthermore, MtrB showed chill-induced stimulation in an *E. coli* membrane surrounding. The chill sensing property does therefore not seem to depend on a specific membrane composition. Interestingly, when proteoliposomes were fused to 33 % POPG, which resulted in an increased sensitivity towards osmotic stress, MtrB seemed to be stimulated to somewhat lower extent as compared to pure *E. coli* lipid liposomes. The different stimulation profiles in altered membrane surroundings suggest an influence of the membrane composition. Membrane fluidity is likely to be differently influenced by low temperature when altered membrane compositions are used. Thus, the physical state of the membrane seems to be a reasonable signal for MtrB resulting in activation at low temperature. However, a low temperature-induced change of protein conformation as activating signal cannot be ruled out. In contrast to BetP, it could not be differentiated yet, whether for activation by chill or by high osmolarity the same molecular mechanism is responsible, or if two independent input sites mediate stimulus perception. This has still to be addressed in future studies. The construction of a recombinant derivative of MtrB, which is defective in one of the two sensory functions only, as could be obtained for BetP (Schiller *et al*., 2004b; Özcan *et al*., 2005), would be an ideal approach.

4.5   Investigation of the sensing domain of MtrB

In two-component system histidine kinases the domain which provides the sensory function is typically located within the extracytoplasmic loop (Bourret *et al*., 1991), especially in case of ligand binding kinases, which sense extracelluar conditions, e. g. the presence of nutrients. This was reported for of the CitA sensor belonging to the CitAB two-component system of *Klebsiella pneumoniae*. For this sensor kinase a crystal structure of the

periplasmic loop in complex with its ligand citrate was obtained (Reinelt *et al.*, 2003). However, as mentioned above, a number of membrane-associated osmosensors were shown to sense intracellular conditions like the internal ionic strength or increased concentration of specific ions. Furthermore, for the two-component sensor kinase KdpD of *E. coli* it was reported that a truncated derivative lacking all four transmembrane domains was still able to sense low K^+ concentrations. It was thus suggested that the sensing domain is located in the cytoplasmic part of the protein (Heermann *et al.*, 2003). More recently, the analyses of the synthesis of various truncated derivatives of KdpD in a *kdpD* deficient *E. coli* strain revealed a more detailed location of the sensing domain, which turned out to be situated within the soluble C-terminal part of this protein (Rothenbücher *et al.*, 2006).

In this study, different truncated derivatives of MtrB-Strep were constructed to investigate the location of the sensing domain within this protein. MtrB contains two predicted membrane-spanning domains enclosing an extended extracytoplasmic loop of 144 amino acid residues, with a size comparable to that of DcuS or CitA. The N-terminal part of this protein contains only five intracellular amino acids, followed by the first trans-membrane domain. The main part of MtrB is composed of the soluble C-terminal domain comprising the catalytic sites. The most probable locations for a sensing domain within MtrB were the extracytoplasmic loop and the C-terminal soluble part, whereas the short N-terminal soluble part consisting of 5 amino acids only is less likely. Furthermore the membrane-spanning domains might be involved in the sensing mechanism. In order to determine the location of the sensing domain, the following truncations of MtrB-Strep were constructed. MtrBΔ190 consists of the soluble part of the histidine kinase (the N-terminal 190 amino acids are lacking). The derivatives referred to as MtrBΔ25 and -Δ154 still contain one membrane-spanning domain each, whereas the N-terminal trans-membrane domain, and/or the extracytoplasmic loop were truncated. In contrast, two proteins still contain both membrane-spanning domains; in case of MtrBΔL124 and -ΔL134 almost the complete extracytoplasmic loop was truncated, leaving only 20 or 10 amino acids, respectively.

It turned out that the isolated soluble part of MtrB completely lost its ability to autophosphorylate *in vitro*. To test the possibility, whether the cytoplasmic part may require membrane association, the experiment was repeated in presence of liposomes, which did not lead to MtrBΔ190 activity. In *E. coli*, 27 of 30 predicted two-component sensor histidine kinases were purified containing their cytoplasmic part only. Interestingly, out of these 27 truncated derivatives, 25 could be shown to autophosphorylate *in vitro* (Yamamoto *et al.*, 2005). Thus, these numerous truncated histidine kinases are likely able to still form dimers, which is the prerequisite for autophosphorylation. This led to the suggestion that in case of MtrB the loss of activity is not a consequence of failure to dimerize. Instead, it indicates that

integration into a membrane surrounding is the prerequisite for MtrB activity. This is in accordance to the observation that solubilized MtrB was also inactive. Probably the membrane integration is furthermore the prerequisite for signal input.

As mentioned above, synthesis of full-length MtrB-Strep (56 kDa) in the heterologous host *E. coli* resulted in partial degradation of the protein. Those fragments still carrying the C- (or N-) terminal Strep-tag were co-purified and reconstituted into liposomes. It turned out, that fragments with a molecular mass of approximately 40 kDa and higher still exhibited *in vitro* autokinase activity and furthermore sensory properties comparable to those of full-length MtrB-Strep. Their molecular masses indicated that these degradation fragments lack the N-terminal trans-membrane domain and/or parts of the periplasmic loop. Interestingly, those constructs carrying truncations of the N-terminal membrane-spanning domain and/or the extracytoplasmic loop, leaving one domain for membrane integration (MtrBΔ25 and -Δ154), were not able to autophosphorylate *in vitro*. This was found using both, *E. coli* cytoplasmic membranes and proteoliposomes. At least in case of MtrBΔ25, lacking the N-terminal 25 amino acids, the loss of activity was surprising. Since fragments caused by N-terminal degradation during heterologous synthesis of MtrB-Strep in *E. coli* with a molecular mass of approximately 40 kDa and higher were still active in autophosphorylation and sensing, this was also expected for MtrBΔ25 with a molecular mass of approximately 55 kDa. The reason for the loss of activity in case of MtrBΔ25 and not in case of some degradation fragments apparently smaller than this construct is not clear. However, the heterologous synthesis of the two truncated derivatives in *E. coli* was very inefficient. Possibly, heterologous expression resulted in synthesis of inactive protein. However, those degradation fragments with a molecular mass higher than 40 kDa indicate that the first (N-terminal) membrane-spanning domain is not essential for *in vitro* activity and sensory function of MtrB. Unfortunately, the amino acid sequence of the active degradation fragments of MtrB-Strep could not be determined by amino acid sequencing (Edmann degradation), presumably because the reaction was blocked.

Two derivatives of MtrB-Strep were constructed by truncation of the extracytoplasmic loop, leaving both trans-membrane domains intact. The external loop in these constructs contained only 10 or 20 amino acids, respectively. After reconstitution, both proteins exhibited autokinase activity. Furthermore, the two derivatives were stimulated in an identical manner compared to full-length MtrB-Strep (see Fig. 36). Thus, the truncation of almost the complete loop did not alter the sensing properties of MtrB-Strep *in vitro*. Consequently, the extracytoplasmic loop has no influence on the osmosensory function of MtrB.

Taken together, the sensing domain of the histidine kinase is suggested to be located either in the cytoplasmic part or, since degradation fragments most probably lacking the N-terminal

membrane segment were stimulated comparable to full-length MtrB, within the C-terminally located membrane-spanning domain. These data are in accordance with both hypotheses derived for the osmosensing mechanism of MtrB. (I) Either MtrB is able to sense increased osmolarity *per se*, for example by an altered hydration state of the protein. This would likely be mediated by the soluble part of the histidine kinase. (II) Or MtrB is able to detect alterations of the membrane state, for example high-osmolarity-induced shrinkage. This could be achieved by the membrane-spanning domain. Furthermore the measurement of interaction of the protein and membrane surrounding can be imagined to depend on both, the transmembrane domain and/ or the cytoplasmic part.

Future studies will address the location of the sensing domain in more detail. As probable candidates several parts of MtrB will be analyzed, including the above-mentioned C-terminal membrane-spanning domain. Regarding the soluble part of MtrB, several locations are possible candidates. Sequence alignments revealed that MtrB exhibits a cytoplasmic HAMP domain near the C-terminal trans-membrane segment. This domain is thought to exhibit important regulatory functions, e. g. as transmitting element between sensory input and output modules. This was proposed for the sensor histidine kinases NarX, NarQ, or CpxA of *E. coli* (Appleman *et al*., 2003). However, a sensory function of this domain can not be excluded. Consequently, this HAMP domain should be considered in future studies addressing the MtrB sensory site. Despite the fact that the parts of MtrB comprising the catalytic elements of the sensor have to be considered, the C-terminal tail of 23 amino acids, and a 45 amino acid including part located between the histidine kinase and the ATPase domain, are possible candidates to comprise the sensing domain of MtrB.

The *in vitro* analyses of the truncated derivatives of MtrB in this work already provided good characterizations of the sensor histidine kinase, proving that the sensory function of this protein is not located within the extracytoplasmic loop. For future studies, the fusion of the MtrBA target genes to reporter genes would be a suitable approach to verify the *in vitro* data obtained in this work by an *in vivo* approach. The results achieved by truncated derivatives of MtrB could then be verified by complementation studies using an *mtrB* deficient *C. glutamicum* mutant.

4.6   Models of MtrB stimulation

Taken together, the data presented here are in accordance with at least two models of MtrB stimulation in dependence of hyperosmotic- and chill stress (Fig. 44). When cells are osmotically adapted, MtrB is thought to be in its inactive state, resulting in low basal expression levels of *proP*, *betP*, and *lcoP*, as well as high basal *mscL* levels. In response to hyperosmotic stress, water efflux occurs leading to increased concentrations of the internal

compounds. Furthermore, the uptake carriers for compatible solutes are osmotically activated resulting in further increase of cytoplasmic solute concentrations.

A) The resulting internally increased osmolarity can lead to a conformational change of the soluble part of MtrB resulting in stimulation of autokinase activity (Fig. 44A). Since in case of sensor kinases one subunit of a dimer phosphorylates the histidine residue within the other subunit, the conformational change possibly results in an altered orientation of the two subunits to each other, thus activating autophosphorylation. A possible signal, which would explain activation by various different osmolytes, but not by PEG 2, glycerol, or urea, is the altered hydration state of the protein. A solute-dependent degree of dehydration of MtrB would be a reasonable signal, which can be sensed by the soluble part of the histidine kinase, indicating environmental hyperosmotic stress.

B) The loss of water as consequence of hyperosmotic stress is known to cause shrinkage of the cytoplasm of cells, resulting in an altered state of the membrane. This altered state of the cytoplasmic membrane may be sensed by MtrB as mechanical deformation of the membrane or altered protein-lipid interactions, resulting in stimulation of autokinase activity (Fig. 44B). For the detection of membrane alterations an involvement of the C-terminal transmembrane domain seems plausible. Since the treatment of proteoliposomes by freezing and thawing is thought to result in isoosmotic conditions between lumen and exterior, the *in vitro* stimulation of MtrB did probably not occur as consequence of liposome shrinkage. Sensing of hyperosmotic stress as an altered hydration state of MtrB may therefore be the more reasonable mechanism of MtrB activation. However, since the final proof whether indeed isoosmotic conditions were achieved in the activity assays is still missing, an activation of MtrB caused by membrane effects under environmental osmotic stress conditions cannot be ruled out.

The increased activity levels of MtrB result in increased phosphorylation of MtrA, which mediates the transcriptional activation of the compatible solute carrier encoding genes *betP*, *proP*, and *lcoP*, as well as the repression of the mechanosensitive channel gene *mscL*, thus providing long-term adaptation to osmotic stress.

When cells are exposed to chill stress, both, proteins as well as membrane systems, are thought to undergo a conformational change. A) MtrB autokinase activity might be stimulated as consequence of a chill-induced conformational change of the protein itself (Fig. 44A).

B) The signal could also be measured as alteration of the physical state of the cytoplasmic membrane after exposure to low temperature (Fig. 44B). Since an altered composition of the liposomal membrane resulted in an altered sensitivity of MtrB towards low temperature, sensing of a change in the physical state of the membrane by MtrB seems to be the more reasonable possibility. As in case of osmotic stress, environmental chill stress leads to increased MtrB autokinase activity resulting in the MtrA regulated transcriptional induction of

proP, *betP*, and *lcoP*. Increased synthesis of the chill response systems BetP and LcoP provide long-term adaptation. The sensing of high osmolarity and low temperature can occur as consequence of the same mechanism, as indicated in Fig. 44, or may be achieved by independent signal input sites.
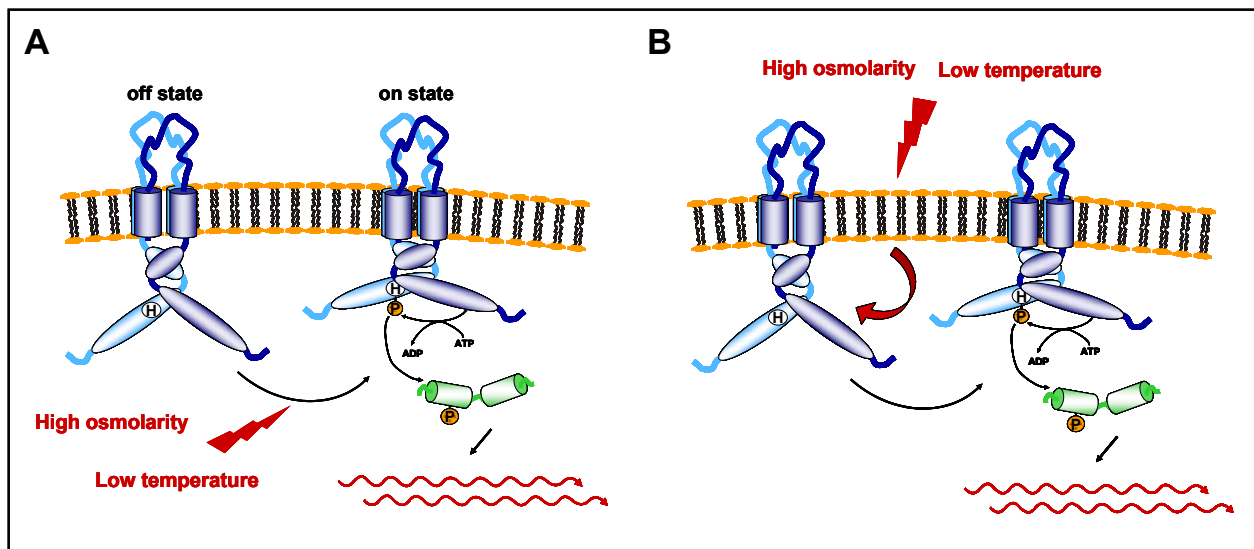
Fig. 44: Models of stimulus perception and signal transduction of the MtrBA system. External hyperosmotic- and chill stress result in internally increased osmolarity and low temperatures. **A** The signals can be measured internally by a conformational change of MtrB in response to intracellular increased osmolarity and decreased temperature. **B** Signal perception can be mediated by an altered physical state of the membrane under these conditions.

5.   Summary

The two-component system consisting of the membrane-bound sensor histidine kinase MtrB and its cognate cytoplasmic response regulator MtrA of *Corynebacterium glutamicum* was characterized in detail in this work. *In vivo* analysis previously showed that MtrBA mediates the expression regulation of genes involved in three different physiological functions in this bacterium, (I) osmoprotection, (II) chill stress response, and (III) cell wall metabolism. The osmo- and/or chill stress-related genes *proP*, *betP*, *lcoP*, and *mscL* were shown to be induced or repressed, respectively, in response to hyperosmotic stress and low temperature. In contrast, those conditions resulting in the repression of the genes which are thought to be involved in cell wall metabolism, *mepA*, *ppmA*, and *lpqB*, are still unknown. This work focused on the investigation of the direct stimuli which are sensed by the histidine kinase MtrB and therefore initiate the MtrB-MtrA signal transduction. For this purpose, *in vitro* phosphorylation assays were developed, namely *E. coli* inverted membrane vesicles and -proteoliposomes enriched with MtrB. Using these membrane systems, the basic properties of the two-component system phosphorelay could be detected. The sensor histidine kinase was shown to autophosphorylate, when reconstituted into *E. coli* liposomes, or when incorporated into the *E. coli* cytoplasmic membrane, thus proving that this enzyme was functionally integrated into the artificial membrane systems. The autokinase activity of MtrB exhibited a K_m value for ATP of 0.3 M. Using both membrane systems, the rapid transfer of the phosphoryl group from membrane-bound MtrB to the soluble response regulator could be shown. In case of MtrBA, the signal transduction pathway turned out to be shut down by a phosphatase activity of the sensor kinase, which catalyses the ADP-dependent dephosphorylation of MtrA-P. The orientation of MtrB after reconstitution could be determined by site-specific proteolysis, proving that the histidine kinase is membrane-incorporated with a unidirectional inside-out orientation.

Investigation of the direct stimuli, which are sensed by the histidine kinase MtrB, was realized by *in vitro* analysis of a systematic variation of signals related to osmotic- and chill stress using the described phosphorylation assays. The MtrB sensor kinase turned out to be significantly activated by the presence of various monovalent ions. In order to discriminate between specific and non-specific stimuli of autokinase activity, a test assay was developed by reconstitution of the sensor kinase DcuS belonging to the DcuSR system of *E: coli*, which was shown to sense external C_4-dicarboxylates, e. g. fumarate (Janausch *et al.*, 2002; Kneuper *et al.*, 2005). Interestingly, this protein was affected by the same monovalent ions in a pattern similar to MtrB. Since DcuS could be shown not to be involved in osmoregulation in *E. coli* (Unden, personal communication), it is proposed that physiological levels of

monovalent ions, especially K+, are required for proper *in vitro* functioning of sensor histidine kinases, independent from their *in vivo* sensory properties. The analysis of a variation of osmostress-related signals showed that MtrB activity is significantly stimulated by the presence of osmolytes, including sugars, amino acids, compatible solutes, and high molecular weight PEGs. The comparison to reconstituted DcuS proved that this activation is specific for MtrB. Analysis of chill stress-related conditions furthermore showed, that MtrB is *in vitro* significantly and specifically stimulated by exposure to low temperature, which was determined at 10 and 15 °C. Thus, the histidine kinase was shown to act as sensor for both, osmo- as well as chill stress. Variation of the lipid content by fusion of proteolipsomes to POPG showed that MtrB was significantly more sensitive towards high osmolarity in the altered membrane surrounding. This indicates, that the sensory function of the histidine kinase depends on the lipid composition of the surrounding membrane system.

In order to determine the sensing domain of MtrB, different truncated derivatives of the histidine kinase were constructed. In contrast to most sensor kinases, in which the sensory function is thought to reside within the extracytoplasmic loop, this external part of MtrB could be ruled out as the sensor domain.

The analysis described here are in accordance with two hypotheses for the sensing mechanism of MtrB. (I) Exposure to high osmolarity and/or chill stress conditions is sensed internally by the soluble part of MtrB, resulting in a conformational change of the protein. This leads to stimulation of autophosphorylation activity and thus initiates the signal transduction cascade. (II) The osmo- and/or chill stress conditions cause a change of the physical state of the membrane. This results in stimulation of MtrB activity mediated either by the transmembrane domain of MtrB, or as consequence of altered protein-membrane interactions. The sensing of high osmolarity and chill can thereby either be mediated by same mechanism, or by independent signal input sites.

6.   References

Abe, S., Takayama, K. I., and Kinoshita, S. (1967) Taxonomical studies on glutamic acid-producing bacteria. *J. Gen. Appl. Microbiol.* **13:** 279-301.

Aguilar, P. S., Lopez, P., and Mendoza, D. (1999) Transcriptional control of the low-temperature-inducible *des* gene, encoding the Δ5 desaturase of *Bacillus subtilis*. *J. Bacteriol.* **181:** 7028-7033.

Aguilar, P. S., Hernandez-Arriaga, A. M., Cybulski, L. E., Erazo, A. C., and Mendoza, D. (2001) Molecular basis of thermosensing: a two-component signal transduction thermometer in *Bacillus subtilis*. *EMBO J.* **20:** 1681-1691.

Alex, L. A., Borkovich, K. A., and Simon, M. I. (1996) Hyphal development in *Neurospora crassa*: involvement of a two-component histidine kinase. *Proc. Natl. Acad. Sci.* USA **93:** 3416-3421.

Ankri, S., Serebrijski, I., Reyes, O., and Leblon, G. (1996) Mutations in the *Corynebacterium glutamicum* proline biosynthesis pathway: a natural bypass of the *proA* step. *J. Bacteriol.* **178:** 4412-4419.

Bayles, D. O. and Wilkinson, B. J. (2000) Osmoprotectants and cryoprotectants of *Listeria monocytogenes. Letters in Applied Microbiol.* **30:** 23-27.

Berrier, C., Besnard, M., Ajouz, B., Coulombe, A., and Ghazi, A. (1996) Multiple mechanosensitive ion channels from *Escherichia coli*, activated at different thresholds of applied pressure. *J. Membr. Biol.* **151:** 175-187.

Berrier, C., Coulombe, A., Szabo, I., Zoratti, M., and Ghazi, A. (1992) Gadolinium ion inhibits loss of metabolites induced by osmotic shock and large stress-activated channels in bacteria. *Eur. J. Biochem.* **206:** 559-565.

Birnboim, H.C. and Doly, J. (1979) A rapid alkaline extraction procedure for screening recombinant plasmid DNA, *Nucleic Acids Res.* **7:** 1513-1523.

Blat, Y. and Eisenbach, M. (1994) Phosphorylation-dependent binding of the chemotaxis signal molecule CheY to its phosphatase, CheZ. *Biochemistry* **33:** 902-906.

Blum, M., Beier, H., and Gross, H. J. (1987) Improved silverstaining of plant proteins, RNA and DNA in polyacrylamid gels. *Electrophoresis* **8:** 93-99.

Booth, I. R., and Louis, P. (1999) Managing hypoosmotic stress: aquaporins and mechanosensitive channels in *Escherichia coli*. *Curr. Opin. Microbiol.* **2:** 166-169.

Bourret R. B., Borkovich K. A., and Simon M.I. (1991) Signal transduction pathways involving protein phosphorylation in prokaryotes. *Annu Rev Biochem.* **60:** 401–441.

Bradford, M.M. (1976) A rapid and sensitive method for the quantification of microgram quantities of protein using the principle of protein-dye binding. Anal. Biochem. **72:** 248-254.

Bremer, E. and Krämer, R. (2000) Coping with osmotic challenges: Osmoregulation through accumulation and release of compatible solutes in bacteria. In: Storz, G. und Hengge-Aronis, R. (Editoren) *Bacterial Stress Responses.* ASM Press, Washington D.C*., pp. 79-96.

Brocker, M. and Bott, M. (2006) Evidence for activator and repressor functions of the response regulator MtrA from *Corynebacterium glutamicum*. In preparation.

Caldas, T., Demont-Caulet, N., Ghazi, A., and Richarme, G. (1999) Thermoprotection by glycine betaine and choline. *Microbiology* **145:** 2543-2548.

Canovas, D., Fletcher, S. A., Hayashi, M., and Csonka, L. N. (2001) Role of threhalose in growth at high temperature of *Salmonella enterica* serovar *Typhimurium*. *J. Bacteriol* **183:** 3365-3371.

Chang, C., Kwok, S. F., Bleeker, A. B., and Meyerowitz, E. M. (1993) *Arabidopsis* ethylene-response gene ETR1: similarity of product to two-component regulators. *Science* **262:** 539-544.

Chung, C. T., Niemela, S. L., and Miller, R. H. (1989) One-step preparation of competent *Escherichia coli*: transformation and storage of bacterial cells in the same solution. *Proc. Natl. Acad. Sci*. USA **86:** 2172-2175.

Comeau, D. E., Ikenaka, K., Tsung, K., and Inouye, M. (1985) Primary characterization of the protein products of the *Escherichia coli ompB* locus: structure and regulation of synthesis of the OmpR and EnvZ proteins. *J. Bacteriol*. **164:** 578-584.

Courtenay, E. S., Capp, M. W., Anderson, C. F., and Record, M. T., Jr. (2000) Vapor pressure osmometry studies of osmolyte-protein interactions: implications for the action of osmoprotectants in vivo and for the interpretation of "osmotic stress" experiments in vitro. *Biochemistry*. **39:** 4455-4471.

Csonka, L. N. and Epstein, W. (1996) Osmoregulation. In: Neidhard, F.C. *et al*. (Eds), *Escherichia coli and Salmonella typhimurium. Cellular and molecular biology*. ASM Press, Washington D.C., pp 1210-1223.

Culham, D.E., Henderson, J., Crane, R.A., and Wood, J.M. (2003) Osmosensor ProP of *Escherichia coli* responds to the concentration, chemistry, and molecular size of osmolytes in the proteoliposome lumen. *Biochemistry* **42:** 410-420.

Derzelle, S., Hallet, B., Ferain, T., Delcour, J., and Hols, P. (2003) Improved adaptation to cold-shock, stationary-phase, and freezing stresses in *Lactobacillus plantarum* overproducing cold-shock proteins. *Applied and Environmetal Microbiol.* **69:** 4285-4290.

Deshnium, P., Gombos, Z., Nishiyama, Y., and Murata, N. (1997) The action *in vivo* of glycine betaine in enhancement of tolerance of *Synechococcus sp.* strain PCC 7942 to low temperature. *J. Bacteriol.* **179**: 339-344.

Diamant, S., Eliahu, N., Rosenthal, D., and Goloubinoff, P. (2001) Chemical chaperones regulate molecular chaperones *in vitro* an in cells under combined salt and heat stresses. *J. Biol. Chem.* **276:** 39586-39591**.**

Edman, P. (1950) Method for determination of the amino acid sequence in peptides. *Acta Chem. Scand*. **4:** 283-293.

Egger, L. A., Park, H., and Inouye, M. (1997) Signal transduction via the histidyl-aspartyl phospho-relay. *Gens to cells* **2:** 167-184.

Eikmanns, B. J., Kleinertz, E., Liebl, W., and Sahm, H. (1991) A familiy of *Corynebacterium glutamicum*/*Escherichia coli* shuttle vectors for cloning, controlled gene expression, and promoter probing. *Gene* **102:** 93-98.

Eikmanns, B. J., Thum-Schmitz, N., Eggeling, L., Ludtke, K. U., and Sahm, H. (1994) Nucleotide sequence, expression and transcriptional analysis of the *Corynebacterium glutamicum gltA* gene encoding citrate synthase. *Microbiology* **140:** 1817-1828.

Fletcher, S. A. and Csonka, L. N. (1995) Fine-structure analysis of the transcriptional silencer of the proU operon of *Salmonella typhimurium. J. Bacteriol*. **177:** 4508-4513.

Galinski, E. A. and Trüper, H. G. (1994) Microbial behavior in salt-stressed ecosystems. *FEMS Microbiol. Rev*. **39:** 73-78.

Golby, P., Davies, S., Kelly, J. R., Guest, J. R., and Andrews, S. C. (1999) Identification and characterization of a two-component sensor-kinase and response-regulator system (DcuS-DcuR) controlling gene expression in response to C4-dicarboxylates in Escherichia coli. *J. Bacteriol.* **181:** 1238–1248

Grant, S. G. N., Jessee, J., Bloom, F. R., and Hanahan, D. (1990) Differential plasmid rescue from transgenic mouse DNAs into *Escherichia coli* methylation-restriction mutants. *Proc. Natl. Acad*., USA, **87:** 4645-4649.

Grebe, T. W. and Stock, J. B. (1999) The histidine protein kinase superfamily. *Adv. Microbial. Phys.* **41:** 139-227.

Hakenbeck R. and Stock, J. B. (1996) Analysis of two-component signal transduction systems involved in transcriptional regulation. *Methods Enzymol*. **273:** 281-300.

Heermann, R., Fohrmann, A., Altendorf, K., and Jung, K. (2003) The transmembrane domains of the sensor kinase KdpD of *Escherichia coli* are not essential for sensing K$^+$ limitation. *Mol. Microbiol*. **47:** 839-848.

Hess, J. F., Oosawa, K., Kaplan, N., and Simon, M. I. (1988) Phosphorylation of three proteins in the signaling pathway of bacterial chemotaxis. Cell **53:** 79-87.

Hermann T. (2003) Industrial production of amino acids by coryneform bacteria. *J. Biotechnol.* **104:** 155-172

Hoischen, C. and Krämer, R. (1990) Membrane alteration is necessary but not sufficient for effective glutamate secretion in *Corynebacterium glutamicum*. *J. Bacteriol*. **172:** 3409-3416.

Igo, M. M., Ninfa, A. J., and Silhavy, T. J. (1989) A bacterial environmental sensor that functions as a protein kinase and stimulates transcriptional activation. *Genes Dev.* **3:** 598-605.

Igo, M. M., Ninfa, A. J., Stock, J. B., and Silhavy, T. J. (1989) Phosphorylation and dephosphorylation of a transcriptional activator by a transmembrane receptor. *Genes Dev.* **3:** 1725-1734.

Ikeda, M. and Nakagawa, S. (2003) The *Corynebacterium glutamicum* genome: features and impacts on biotechnological processes. *Appl. Microbiol. Biotechnol*. **62:** 99-109.

Janausch I. G., Garcia-Moreno I., and Unden G. (2002) Function of DcuS from *Escherichia coli* as a fumarate-stimulated histidine protein kinase in vitro. *J. Biol. Chem.* **277:** 39809-39814.

Janausch, I. G., Zientz, E., Tran, Q. H., Kröger, A., and Unden, G. (2002) C$_4$-dicarboxylate carriers and sensors in bacteria. *Biochim. Biophys. Acta* **1553:** 39–56.

Jung, K., Hamann, K., and Revermann, A. (2001) K$^+$ stimulates specifically the autokinase activity of purified and reconstituted EnvZ of *Escherichia coli*. *J. Biol. Chem.* **44:** 40896-40902.

Jung, K., Tjaden, B., and Altendorf, K. (1997) Purification, reconstitution, and characterization of KdpD, the turgor sensor of *Escherichia coli*. *J. Biol. Chem.* **272:** 10847-10852.

Jung, K., Veen, M., and Altendorf, K. (2000) K$^+$ and ionic strength directly influence the autophosphorylation activity of the putative turgor sensor KdpD of *Escherichia coli*. *J. Biol. Chem*. **51:** 40142-40147.

Kalinowski, J., Bathe, B., Bartels, D., Bischoff, N., Bott, M., Burkovski, A., *et al*. (2003) The complete *Corynebacterium glutamicum* ATCC 13032 genome sequence and its impact on the production of L-aspartate-derived amino acids and vitamins. *J. Biotechnol*. **104:** 5-25.

Kanamaru, K., Aiba, H., and Mizuno, T. (1990) Transmembrane signal transduction and osmoregulation in *Escherichia coli*. I. Analysis by site-directed mutagenesis of the amino acid residues involved in phosphotransfer between the two regulatory components, EnvZ and OmpR. *J. Biochem*. **108:** 483-487.

Kase, H. and Nakayama, K. (1972) Production of L-threonine by analog-resistant mutants *Agric. Biol. Chem*. **36:** 1611-1621.

Keilhauer, C., Eggeling, L., and Sahm, H. (1993) Isoleucine synthesis in *Corynebacterium glutamicum*: molecular analysis of the *ilvB-ilvN-ilvC* operon. *J. Bacteriol*. **175:** 5595-5603.

Kempf, B. and Bremer, E. (1998) Uptake and synthesis of compatible solutes as microbial stress responses to high-osmolality environments. *Arch. Microbiol.* **170:** 319-330.

Kinoshita, S., Udaka, S., and Shimono, M. (1957) Studies on the amino acid fermentation. Part I production of L-glutamic acid by various microorganisms. *J. Gen. Appl. Microbiol*. **3:** 193-205.

Klein, W., Weber M. H., and Marahiel M. A. (1999) Cold shock response of *Bacillus subtilis*: isoleucine-dependent switch in the fatty acid branching pattern for membrane adaptation to low temperatures. J. Bacteriol. **191:** 5341–5349.

Klionsky, D. J., Brusilow, W. S. A., and Simoni, R. D. (1984) *In vivo* evidence for the role of the ε subunit as an inhibitor of the proton-translocating ATPase of *Escherichia coli*. *J. Bacteriol*. **160:** 1055-1060.

Klumpp, S. and Krieglstein, J. (2002) Phosphorylation and dephosphorylation of histidine residues in proteins. *Eur. J. Biochem*. **269:** 1067-1071.

Kneuper, H., Janausch I. G., Vijayan V., Zweckstetter M., Bock, V., Griesinger, C., and Unden, G. **(2005)** The nature of the stimulus and of the fumarate binding site of the fumarate sensor DcuS of *Escherichia coli*. *J. Biol. Chem.* **280:** 20596–20603.

Ko, R., Smith, L. T., and Smith, G. M. (1994) Glycine betaine confers enhanced osmotolerance and cryotolerance on *Listeria monocytogenes*. *J. Bacteriol*. **176:** 426-431.

Kocan, M., Schaffer, S., Ishige T., Sorger-Hermann, U., Wendisch, V. F., and Bott, M. (2006) Two-component systems of *Corynebacterium glutamicum*: deletion analysis and involvement of the PhoS-PhoR system in the phosphate starvation response. *J. Bacteriol.* **188:** 724-732.

Krämer, R. and Lambert, C. (1990) Uptake of glutamate in *Corynebacterium glutamicum*. 2. Evidence for a primary active transport system. *Eur J Biochem.* **194:** 937-944.

Kuroda, M., Kuroda, H., Oshima, T., Takeuchi, F., Mori, H., and Hiramatsu, K. (2003) Two-component system VraSR positively modulates the regulation of cell-wall biosynthesis pathway in *Staphylococcus aureus*. *Mol. Microbiol.* **49:** 807-821.

Laemmli, U. K. (1970) Cleavage of structural proteins during assembly of bacteriophage T4. *Nature* **227:** 680-685.

Leuchtenberger, W. (1996) Amino acids-technical production and use. In: Rehm, H. und Reed, G. (Editoren). *Products of primary metabolism. Biotechnology*. VCH Weinheim, pp. 455-502.

Ley, O. A. (2001) Bedeutung der Prolin-Biosynthese bei der Osmoregulation von *Corynebacterium glutamicum*. Diploma thesis, Universität zu Köln.

Ley, O. A. (2005) Charakterisierung der Regulation des Prolinbiosyntheseweges in *Corynebacterium glutamicum.* PhD thesis, Universität zu Köln.

Liu, C. E., Liu, P.-Q., and Ferro-Luzzi Ames, G. (1997**)** Characterization of the Adenosine Triphosphate Activity of the Periplasmic Histidine Permease, a Traffic ATPase (ABC transporter). *J. Biol. Chem.* **35:** 21883-21891.

Lupas, A. and Stock, J. B. (1989) Phosphorylation of an N-terminal regulatory domain activates the CheB methylesterase in bacterial chemotaxis. *J. Biol. Chem.* **264:** 17337-17342.

Maeda, T., Wurgler-Murphy, S. M., and Saito, H. (1994) A two-component system that regulates an osmosensing MAP kinase cascade in yeast. *Nature* **369:** 242-245.

Makino, K., Shinagawa, H., Amemura, M., Kawamoto, T., Yamada, M., and Nakata, A. (1989) Signal transduction in the phosphate regulon of *Escherichia coli* involves phosphotransfer between PhoR and PhoB proteins. J. Mol. Biol. **210:** 551-559.

Malin, G. and Lapidot, A. (1996) Induction of synthesis of tetrahydropyrimidine derivatives on protein-nucleic acids interaction. Type II restriction endonucleases as a model system. *J. Biol. Chem.* **274:** 6920-6929.

Mansilla, M. C., Cybulski L. E., Albanesi D., and de Mendoza D. (2004) Control of membrane lipid fluidity by molecular thermosensors. J. Bacteriol. **186:** 6681–6688.

Mascher, T., Zimmer, S. L., Smith, T.-A., and Helmann, J. D. (2004) Antibiotic-Inducible Promoter Regulated by the Cell Envelope Stress-Sensing Two-Component System LiaRS of *Bacillus subtilis. Antimicrob. Agents Chemother*. **48:** 2888-2896.

Miller, K. J. and Wood, J. M. (1996) Osmoadaptaion by rhizosphere bacteria. *Annu. Rev. Microbiol*. **50:** 101-136.

Mizuno, T., Kato, M., Jo, Y.-L., and Mizushima, S. (1988) Interaction of OmpR, a positive regulator, with the osmoregulated *ompC* and *ompF* genes of *Escherichia coli*. *J. Biol. Chem*. **263:** 1008-1012.

Möker, N. (2002) Einfluss von Zwei-Komponenten-Systemen auf die Osmoregulation in *Corynebacterium glutamicum.* Diploma thesis. Universität zu Köln.

Möker, N., Brocker, M., Schaffer, S., Krämer, R., Morbach, S., and Bott, M. (2004) Deletion of the genes encoding the MtrA-MtrB two-component system of *Corynebacterium glutamicum* has a strong influence on cell morphology, antibiotics susceptibility and expression of genes involved in osmoprotection. *Mol. Microbiol*. **54:** 420-438.

Morbach, S. and Krämer. R. (**2002)** Body shaping under water stress: Osmosensing and osmoregulation of solute transport in bacteria. *ChemBioChem* **3:** 384-397.

Morris, C. E. (1990) Mechanosensitive ion channels. *J. Membr. Biol.* **113:** 93-107.

Mullis, K. B., Farone, F. A., Schar, S., Saiki, R., Horn, G., and Ehrlich, H. (1986) Specific amplification of DNA *in vitro*: the polymerase chain reaction. *Cold Spring Harbor Symp. Quant. Biol*. **51:** 263-273.

Nakashima, K., Sugiura, A., Kanamaru, K., and Mizuno, T. (1993) Signal transduction between the two regulatory components involved in the regulation of the *kdpABC* operon in *Escherichia coli*: phosphorylation-dependent functioning of the positive regulator, KdpE. *Mol. Microbiol.* **7:** 109-16.

Neuhaus, K., Francis, K. P., Rapposch, S., Görg, A., and Scherer, S. (1999) Pathogenic *Yersina* species carry a novel, cold-inducible major cold shock protein tandem gene duplication producing both bicistronic and monocystronic mRNA. *J. Bacteriol*. **181:** 6449-6455

Ninfa, A. J., Atkinson, M. R., Kamberov, E. S., Feng, J., and Ninfa, E. G. (1995) Control of nitrogen assimilation by the NRI-NRII two-component system of enteric bacteria. In: Hoch, J.A. und Silhavy, T.J. (Editoren) *Two-Component Signal Transduction.* ASM Press, Washington D.C., pp. 67-88.

Nixon, B. T, Ronson, C. W., and Ausubel, F. M. (1986) Two-component regulatory systems responsive to environmental stimuli share strongly conserved domains with nitrogen assimilation regulatory genes *ntrB* and *ntrC. Proc. Natl. Acad. Sci. USA* **83:** 7850-7854.

Nolden, L. (2001) Mechanismen der Stickstoff-Kontrolle in *Corynebacterium glutamicum*. Dissertation, Universität zu Köln.

Nottebrock, D., Meyer, U., Krämer, R., and Morbach, S. (2003) Molecular and biochemical characterization of mechanosensitive channels in *Corynebacterium glutamicum*. *FEMS Microbiol. Lett*. **218:** 305-309.

Ota, I. M. and Varshavsky, A. (1993) A yeast protein similar to bacterial two-component regulators. *Science* **262:** 566-569.

Özcan, N. (2003) Kälteadaptation osmoregulierter Transportsysteme in *Corynebacterium glutamicum.* Diploma thesis, Universität zu Köln.

Özcan, N., Krämer, R., and Morbach, S. (2005) Chill activation of compatible solute transporters in *Corynebacterium glutamicum* at the level of transport activity. *J. Bacteriol.* **187:** 4752-4759.

Parsegian, V. A., Rand, R. P., and Raun, D. C. (1995) Macromolecules and water: probing with osmotic stress. *Methods Enzymol* **259:** 43-94.

Peter, H., Bader, A., Burkovski, A., Lambert, C., and Krämer, R. (1997) Isolation of the *putP* gene from *Corynebacterium glutamicum* and characterization of a low-affinity uptake system for compatible solutes. *Arch. Microbiol*. **168:** 143-151.

Peter, H., Burkovski, A., and Krämer, R. (1996) Isolation, characterization and expression of the *Corynebacterium glutamicum betP* gene, encoding the transport system for the compatible solute glycine betaine. *J. Bacteriol.* **178:** 5229-5234.

Peter, H., Burkovski, A., and Krämer, R. (1998) Osmosensing by N- and C-terminal extensions of the glycine betaine uptake system BetP of *Corynebacterium glutamicum*. *J. Biol. Chem*. **273:** 2567-2574.

Polarek, J. W., Williams, G., and Epstein, W. (1992) The products of the *kdpDE* operon are required for expression of the Kdp ATPase of *Escherichia coli. J. Bacteriol.* **174:** 2145-2151.

Poolman, B., Blount, P., Folgering, J. H. A., Friesen, R. H. E., Moe, P. C., and van der Heide, T. (2002) How do membrane proteins sense water stress? *Mol Microbiol.* **44:** 889-902.

Prasad, R. (1996) Manual on membrane lipids, Springer Verlag, Heidelberg. Germany.

Pratt, LA and Silhavy, TJ. (1995) Identification of base pairs important for OmpR-DNA interaction. *Mol. Microbiol*. **17:** 565-73

Racher, K. I., Culham, D. E., and Wood, J. M. (2001) Requirements for osmosensing and osmotic activation of transporter ProP from *Escherichia coli. Biochemistry*. **40:** 7324-7333.

Raivio, T. L., Popkin, D. L., and Silhavy, T. J. (1999) The Cpx envelope stress response is controlled by amplification and feedback inhibition. *J. Bacteriol*. **181:** 5263-72.

Rajashekar, C. B., Zhou, H., Marcum, K. B., and Prakash, O. (1999) Glycine betaine accumulation and induction of cold tolerancce in strawberry (*Fragaria X ananassa* Duch.) plants. *Plant Science* **148:** 175-183.

Reihlen, P. (2006) Bedeutung des Zwei-Komponenten-Systems MtrAB bei der Osmoregulation von *Corynebacterium glutamicum.* Diploma thesis, Universität zu Köln.

Reinelt, S., Hofmann,E., Gerharz, T., Bott, M., and Madden D. R. (2003) The structure of the periplasmic ligand-binding domain of the sensor kinase CitA reveals the first extracellular PAS Domain. *J. Biol.Chem* **278:** 39189-39196.

Rigaud, J. L., Pitard, B., and Levy, D. (1995) Reconstitution of membrane proteins into liposomes: application to energy-transducing membrane proteins. *Biochim. Biophys. Acta* **1231:** 223-246.

Rönsch, H., Krämer, R., and Morbach, S. (2003) Impact of osmotic stress on volume regulation, cytoplasmic solute composition and lysine production in *Corynebacterium glutamicum* MH20-22B. *J. Biotechnol*. **104:** 87-97.

Rothenbucher, M. C., Facey, S. J., Kiefer, D., Kossmann, M., and Kuhn, A. (2006) The cytoplasmic C-terminal domain of *the Escherichia coli* KdpD protein functions as a K+ Sensor. *J. Bacteriol*. **188:** 1950-1958.

Rübenhagen R., Morbach S., and Krämer R. (2001) The osmoreactive betaine carrier BetP from *Corynebacterium glutamicum* is a sensor for cytoplasmic K+. *EMBO J*. **20:** 5412-5420.

Rübenhagen, R., Rönsch, H., Jungs, H., Krämer, R., and Morbach, S. (2000) Osmosensor and osmoregulator properties of the betaine carrier BetP from *Corynebaterium glutamicum* in proteoliposomes. *J. Biol.Chem* **275:** 735-741.

Ruffert, S., Berrier, C., Krämer, R., and Ghazi, A. (1999) Identification of mechanosensitive ion channels in the cytoplasmic membrane of *Corynebacterium glutamicum*. *J. Bacteriol*. **181:** 1673-1676.

Sambrook, J., Fritsch, E. F., and Maniatis, T. (1989) Molecular cloning: A laboratorymanual (2nd ed.). *Cold Spring Habor Laboratory Press*, New York, USA.

Sanowar, S. and Le Moual, H. (2005) Functional reconstitution of the *Salmonella typhimurium* PhoQ histidine kinase sensor in proteoliposomes. *J. Biochem*. **390:** 769-776.

Schaffner, W. and Weissmann, C. (1973) A rapid sensitive, and specific method for the determination of protein in dilute solution. *Anal. Biochem*. **56:** 502-514.

Schiller, D., Krämer, R., and Morbach, S. (2004a) Cation specificity of osmosensing by the betaine carrier BetP of *Corynebacterium glutamicum*. *FEBS Lett*. **563:** 108-12.

Schiller, D., Ott, V., Krämer, R., and Morbach, S. (2006) Influence of membrane composition on osmosensing by the betaine carrier BetP from *Corynebacterium glutamicum*. *J Biol Chem*. **281:** 7737-7746.

Schiller, D., Rübenhagen, R., Krämer, R., and Morbach, S. (2004b) The C-terminal domain of the betaine carrier BetP of *Corynebacterium glutamicum* is directly involved in Sensing K^{+} as an osmotic stimulus, *Biochemistry* **43:** 5583-5591.

Schuster, S. S., Noegel, A. A., Oehme, F., Gerisch, G., and Simon, M. I. (1996) The hybrid histidine kinase DokA is part of the osmotic response system of *Dictyostelium*. *EMBO J*. **15:** 3880-3889.

Skerra, A. (1994) Use of the tetracycline promoter for the tightly regulated production of a murine antibody fragment in *Escherichia coli*. *Gene* **151:** 131-135.

Steger, R., Weinand, M., Krämer, R., and Morbach, S. (2004) LcoP, an osmoregulated betaine/ectoine uptake system from *Corynebacterium glutamicum*. *FEBS Lett*. **573:** 155-160.

Stock, A. M., Robinson, V. L., and Goudreau, P. N. (2000) Two-component signal transduction. *Annu. Rev. Genet.* **26:** 71-112.

Stock, J.B., Stock, M.G., and Mottonen, J.M. (1990) Signal transduction in bacteria. *Nature* **344:** 395-400.

Sukharev, S. I., Blount, P., and Kung, C. (1997) Mechanosensitive channels of *Escherichia coli*: the MscL gene, protein, and activities. *Ann. Rev. Physiol*. **59:** 633-657.

Timasheff, S. N. and Arakawa, T. (1989) In *Protein Structure: A practical approach* (Creighton, T. E., Ed.) pp 331-345, IRL Press, Oxford.

Tropis, M., Meniche, X., Wolf, A., Gebhardt, H., Strelkov, S., Chami, D., Schomburg, D., Krämer, R., Morbach, S., and Daffé, M. (2005) The crucial role of trehalose and structurally related oligosaccharides in the biosynthesis and transfer of mycolic acids in *Corynebacterineae*. *J. Biol. Chem*. **280:** 26573-26585.

van der Heide, T., Stuart, M. C., and Poolman, B. (2001) On the osmotic signal and osmosensing mechanism of an ABC transport system for glycine betaine. *EMBO J.* **20:** 7022-7032.

Via, L. E., Curcic, R., Mudd, M. H., Dhandayuthapani, S., Ulmer, R. J., and Deretic, V. (1996) Elements of signal transduction in *Mycobacterium tuberculosis*: In vitro phosphorylation and in vivo expression of the response regulator MtrA. *J. Bacteriol.* **178:** 3314-3321.

Walderhaug, M. O., Polarek, J. W., Voelkner, P., Daniel, J. M., Hesse, J. E., Altendorf, K., and Epstein, W. (1992) Kdp D and KdpE, proteins that control expression of the *kdpABC* operon, are members of the two-component sensor-effector class of regulators. *J. Bacteriol.* **174:** 2152-2159.

Weber, A. and Jung, K. (2002) Profiling early osmostress-dependent gene expression in *Escherichia coli* using DNA Macroarrays. *J. Bacteriol* **184:** 5502-5507.

Weber, M. H. W., Klein W., Müller L., Niess U. M., and Marahiel M.. (2001) Role of the *Bacillus subtilis* fatty acid desaturase in membrane adaptation during cold shock. Mol. Microbiol. **39:**1321–1329.

Weber, H. W. and Marahiel, M. A. (2002) Coping with the cold: the cold shock response in the Gram-positive soil bacterium *Bacillus subtilis*. *Philos Trans R Soc Lond B Biol Sci.* **357:** 895-907.

Weiss, V. and Magasanik, B. (1988) Phosphorylation of nitrogen regulator I (NRI) of *Escherichia coli*. Proc. Natl. Acad. Sci. USA **85:** 8919-8923.

Whatmore, A. M. and Reed, R. H. (1990) Determination of turgor pressure in *Bacillus subtilis*: a possible role of K^+ in turgor regulation. *J. Gen. Microbiol*. **136:** 2521-2526.

Wood, J. M. (1999) Osmosensing in bacteria: signals and membrane based sensors. *Microbiol. Mol. Biol. Rev*. **63:** 230-262.

Wolf, A., Krämer, R., and Morbach, S. (2003) Three pathways for trehalose metabolism in *Corynebacterium glutamicum* ATCC13032 and their significance in response to osmotic stress. *Mol. Microbiol*. **49:** 1119-1134.

Wright, G. D., Holman, T. R., and Walsh, C. T. (1993) Purification and characterization of VanR and the cytosolic domain of VanS: a two-component regulatory system required for vancomycin resistance in *Enterococcus faecium* BM4147. *Biochemistry* **32:** 5057-5063.

Xing, W. and Rajashekar C. B. (2001) Glycine betaine involvement in freezing tolerance and water stress in *Arabidopsis thaliana*. *Environ Exp. Bot.* **46:** 21-28.

Yamamoto K., Hirao K., Oshima T., Aiba H., Utsumi, R., and Ishihama, A. (2005) Functional characterization *in vitro* of all two-component signal transduction systems from *Escherichia coli*. *J. Biol. Chem*. **280:** 1448-56.

Yancey, P. H. (1994) Compatible and counteracting solutes. In: Strange, K. (Editor) *Cellular and molecular physiology of cell volume regulation. CRC Press, Boca Raton*, pp. 81-109.

Zahrt, T. C. and Deretic, V. (2000) An essential two-component signal transduction system in *Mycobacterium tuberculosis. J. Bacteriol.* **182:** 3832-3838.

Zientz, E., Bongaerts, J., and Unden, G. (1998) Fumarate regulation of gene expression in Escherichia coli by the DcuSR (dcuSR genes) two-component regulatory system. *J. Bacteriol.* **180:** 5421–5425.

7.   Appendix

7.1   Influence of MtrB-MtrA on the expression of the open reading frames 3447, 1449, and 1435

In the following, the expression of the open reading frames (orfs) located directly upstream of *proP* (orf 3447), *betP* (orf 1449), and *mscL* (orf 1435) mentioned in section 1.5 is shown. RNA hybridization experiments were performed using total RNA isolated from *C. glutamicum* wt and -Δ*mtrAB* cells. The transcription of orf 3447, 1449, and 3447 was analyzed in response to a hyperosmotic shift from 0.3 to 2.2 osm/kg.
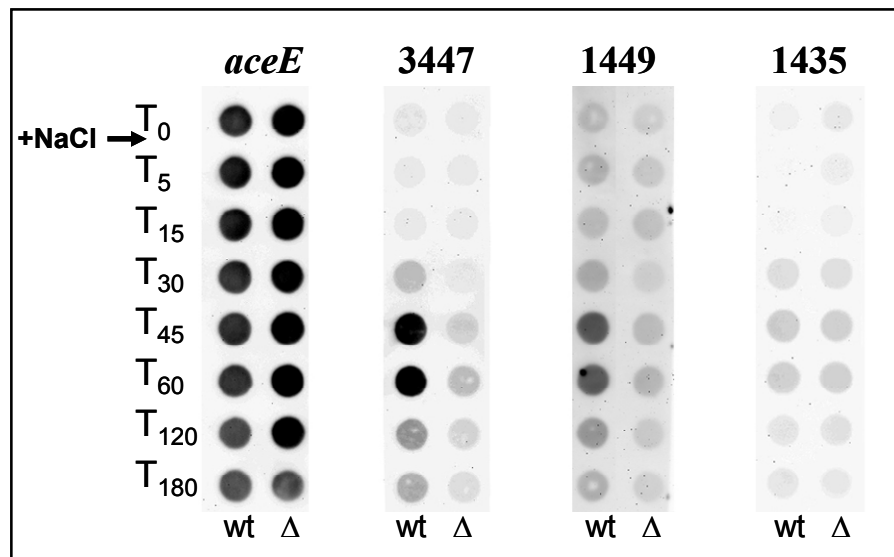
Fig. 45: Expression pattern of the open reading frames 3447, 1449, and 1435 in response to an increased medium osmolarity. Shown are the transcript amounts of the open reading frames upstream of *proP* (**3447**), *betP* (**1449**) and *mscL* (**1435**) in *C. glutamicum* wildtype (**wt**) and -Δ*mtrAB* (Δ). Total RNA was isolated from cells grown before (T_0) and 5 to 180 minutes (T_5 to T_{180}) after an osmotic upshift from 0.3 osm to 2.2 osm. Controls concerning the approximate total RNA amounts were achieved via *aceE* probe.

7.2   Transcriptional organization of *proP*, *betP*, and *mscL*

The characterization of the genomic organization of the osmostress-related genes in *C. glutamicum* related to in section 1.5 was performed using total RNA of *C. glutamicum* wt before and 30 or 60 minutes after an osmotic upshift (0.3 to 2.2 osm/kg). Figure 46 (left panel) shows the resulting transcript sizes for each gene analyzed. The transcript lengths obtained are summarized in Table 7. The comparison with the lengths expected for mono- and polycistronic mRNA transcripts (Tab. 7), which could be calculated from the transcription

start sites (Möker *et al.*, 2004), indicates, that all three genes were mainly monocistronically transcribed. In case of *proP* and *betP,* weak bands corresponding to the expected sizes of polycistronic mRNA were also found (Fig. 46, left panel).

Tab. 7: Calculated and with Northern Hybridization obtained sizes of the mono- and polycistronic transcripts of *proP*, *mscL* and *betP*.

	proP	*mscL*	*betP*
Calculated sizes			
Monocistronic mRNA	1660 b	440 b	1790 b
Polycistronic mRNA	≥2600 b	≥1140 b	2800 b
Resulting sizes	1400 b	≤ 500 b	1800 b
	1600 b	800 b	2800 b
	2600 b		
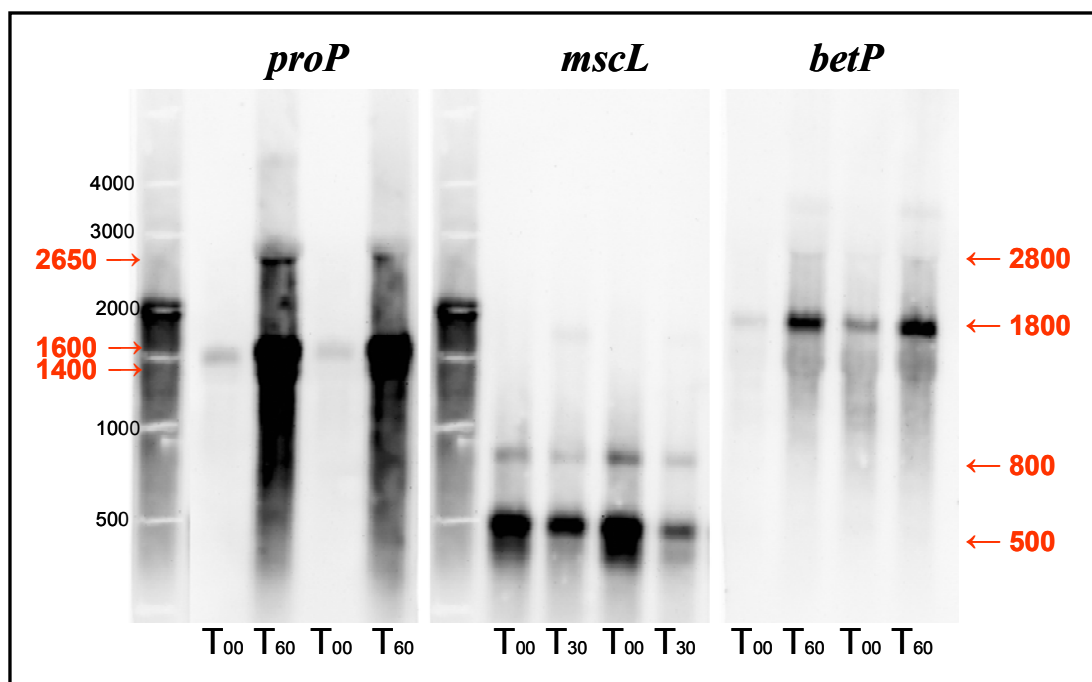
Fig. 46: Transcript sizes of *proP*, *mscL*, and *betP*. Shown are the transcript sizes of *proP*, *mscL* and *betP* in *C. glutamicum* wt obtained by Northern Hybridization. Total RNA was isolated from cells grown before (T_{00}) and 60 (T_{60}) minutes after an osmotic upshift from 0.3 to 2.2 osm/kg.

7.3   Construction of plasmids

In the following, the construction of the plasmids listed in Table 2 (section 2.1.2) is described. For the PCR amplification chromosomal DNA from *C. glutamicum*, or, if indicated, plasmids were used as template. The primers used for the construction are listed in 5´- to 3´- end direction. Those bases printed boldly correspond to the restriction sites of the appropriate forward or reverse primer.

pASK-IBA3-mtrB-strep

For the construction of this expression vector the *mtrB* gene from *C. glutamicum* was amplified by PCR using the primers **GAC CGC GGT C**TC GGC TCC ATC TTC ACC (forward), and **G ACC ATG GTC** CTG CTG CTC CCC TTC CC (reverse). After restriction using PshAI, the PCR product was ligated into the PshAI restricted pASK-IBA3 vector (IBA GmbH, Göttingen), resulting in a 3´-end fusion to the DNA sequence encoding the Strep-tag. The correct orientation and sequence of the *mtrB-strep* gene was verified by sequencing.

pASK-IBA7-strep-mtrB

For the construction of this expression vector the *mtrB* gene from *C. glutamicum* was amplified by PCR using the primers **GAC CGC GGT C**TC GGC TCC ATC TTC ACC (forward), and **G ACC ATG GTC** TCA CTG CTG CTC CCC TTC (reverse). After restriction using PshAI, the PCR product was ligated into the PshAI restricted pASK-IBA7 vector (IBA GmbH, Göttingen), resulting in a 5´-end fusion to to the DNA sequence encoding the Strep-tag. The correct orientation and sequence of the *strep-mtrB* gene was verified by sequencing.

pASK-IBA3-mtrBΔ25

This plasmid is an expression vector for the synthesis of N-terminally truncated MtrB protein, lacking the first 25 amino acids. The *mtrB*Δ25 gene was amplified by PCR using the primers CCC GGG GA**C CGC GG**T CAA CGG TTG GTG GAT CAG (forward), and CAC TTC ACA GGT CAA GC (reverse), with the plasmid pASK-IBA3-mtrB-strep serving as template. After restriction using SacII and HindIII, the PCR product was ligated into the SacII and HindIII restricted pASK-IBA3 vector (IBA GmbH, Göttingen), resulting in a 3´-end fusion to the DNA sequence encoding the Strep-tag. The correct orientation and sequence of the *mtrB*Δ25 gene was verified by sequencing.

pASK-IBA3-mtrBΔ154

This plasmid is an expression vector for the synthesis of N-terminally truncated MtrB protein, lacking the first 154 amino acids. The *mtrBΔ154* gene was amplified by PCR using the primers CCC GGG GA**C CGC GG**T GTG TTC TCC ATG GAA AGC (forward), and CAC TTC ACA GGT CAA GC (reverse), with the plasmid pASK-IBA3-mtrB-strep serving as template. After restriction using SacII and HindIII, the PCR product was ligated into the SacII and HindIII restricted pASK-IBA3 vector (IBA GmbH, Göttingen), resulting in a 3´-end fusion to the DNA sequence encoding the Strep-tag. The correct orientation and sequence of the *mtrBΔ154* gene was verified by sequencing.

pASK-IBA3-mtrBΔ163

This plasmid is an expression vector for the synthesis of N-terminally truncated MtrB protein, lacking the first 163 amino acids. The *mtrBΔ163* gene was amplified by PCR using the primers CCC GGG GA**C CGC GG**T TCT CTT GCT CTC ATG CG (forward), and CAC TTC ACA GGT CAA GC (reverse), with the plasmid pASK-IBA3-mtrB-strep serving as template. After restriction using SacII and HindIII, the PCR product was ligated into the SacII and HindIII restricted pASK-IBA3 vector (IBA GmbH, Göttingen), resulting in a 3´-end fusion to the DNA sequence encoding the Strep-tag. The correct orientation and sequence of the *mtrBΔ163* gene was verified by sequencing.

pASK-IBA3-mtrBΔ190

This plasmid is an expression vector for the synthesis of N-terminally truncated MtrB protein, lacking the first 190 amino acids. The *mtrBΔ190* gene was amplified by PCR using the primers CCC GGG GA**C CGC GG**T ACC CAA CAG GTC ACC GC (forward), and CAC TTC ACA GGT CAA GC (reverse), with the plasmid pASK-IBA3-mtrB-strep serving as template. After restriction using SacII and HindIII, the PCR product was ligated into the SacII and HindIII restricted pASK-IBA3 vector (IBA GmbH, Göttingen), resulting in a 3´-end fusion to the DNA sequence encoding the Strep-tag. The correct orientation and sequence of the *mtrBΔ190* gene was verified by sequencing.

pASK-IBA3-mtrBΔL124

This plasmid is an expression vector for the synthesis of truncated MtrB protein, lacking 124 amino acids of the periplasmic loop. For the construction, the linear pASK-IBA3-*mtrB-strep* plasmid lacking the respective bases was amplified by PCR using the primers CTT GCT CTC ATG CGA GG (forward), and ATC CAC CAA CCG TTG GG (reverse), with the plasmid pASK-IBA3-mtrB-strep serving as template. After removal of the 3´-end A overhang and

subsequent phosphorylation, the PCR product was re-ligated. Subsequently, the *mtrB*ΔL124 gene was obtained by restriction using SacII and HindIII, and ligated into the SacII and HindIII restricted pASK-IBA3 vector (IBA GmbH, Göttingen), resulting in a 3´-end fusion to the DNA sequence encoding the Strep-tag. The correct orientation and sequence of the *mtrB*ΔL124 gene was verified by sequencing.

pASK-IBA3-mtrBΔL134

This plasmid is an expression vector for the synthesis of truncated MtrB protein, lacking 134 amino acids of the periplasmic loop. For the construction, the linear pASK-IBA3-mtrB-strep plasmid lacking the respective bases was amplified by PCR using the primers AGC GAC GAA TCC TCT CTT G (forward), and AAT ATC GAT TTT CTG ATC CAC (reverse), with the plasmid pASK-IBA3-mtrB-strep serving as template. After removal of the 3´end A overhang and subsequent phosphorylation, the PCR product was re-ligated. Subsequently, the *mtrB*ΔL134 gene was obtained by restriction using SacII and HindIII, and ligated into the SacII and HindIII restricted pASK-IBA3 vector (IBA GmbH, Göttingen), resulting in a 3´-end fusion to the DNA sequence encoding the Strep-tag. The correct orientation and sequence of the *mtrB*ΔL134 gene was verified by sequencing.

pASK-IBA7-strep-mtrA

For the construction of this expression vector the *mtrA* gene from *C. glutamicum* was amplified by PCR using the primers GAA GGG CGC C**GA GAC C**GC ATG TCA CAG AAA ATT CTC GTG (forward), and GT TAG ATA TCA **GAG ACC** TTA ATC GTT GTG GCC AGT TTT G (reverse). After restriction using BsaI, the PCR product was ligated into the BsaI restricted pASK-IBA7 vector (IBA GmbH, Göttingen), resulting in a 5´-end fusion to the DNA sequence encoding the Strep-tag. The correct orientation and sequence of the *strep-mtrA* gene was verified by sequencing.

pDrive1435

For the construction of this vector, a 0.51 kb fragment of the orf 1435 (upstream of *mscL*) from *C. glutamicum* was amplified by PCR using the primers GAT TGC AGG ACT GCT GAT G (forward), and GAG CGA TTG TGC TGC AAC (reverse). Subsequently, the fragment was directly ligated into linear pDrive with a U overhang at each 3´-end (Qiagen, Hilden).

pDrive1449

For the construction of this vector, a 0.47 kb fragment of the orf 1449 (upstream of *proP*) from *C. glutamicum* was amplified by PCR using the primers GTA GCT GCG GAG GAT AC

(forward), and GAC AGT TCA CGG CAC AC (reverse). Subsequently, the fragment was directly ligated into linear pDrive with a U overhang at each 3´-end (Qiagen, Hilden).

pDrive3447

For the construction of this vector, a 0.48 kb fragment of the orf 3447 (upstream of *betP*) from *C. glutamicum* was amplified by PCR using the primers GCG CAG GCG ACT GAT TC (forward), and GAG CGC TTC AAT CAT CCG (reverse). Subsequently, the fragment was directly ligated into linear pDrive with a U overhang at each 3´-end (Qiagen, Hilden).

6.4   Oligonucleotides

The oligonucleotides used in this work are summarized in Table 8

Tab. 8: Oligonucleotides used in this study.

Oligonukleotide	Sequence (5'-3')	Reference
lpqB-sense	GTGAGTAAAATTTCGACGAAAC	Möker *et al*, 2004
lpqB-anti sense	CCCGGGTAATACGACTCACTATAGGGCGTTCGTTCCGCATTCG	Möker *et al*, 2004
mepA-sense	ATGCTAAACATCGCACGC	Möker *et al*, 2004
mepA-anti sense	CCCGGGTAATACGACTCACTATAGGGCCATAGCCGGATGCTG	Möker *et al*, 2004
mscL-sense	ATGCTTAAAGGTTTTAGAGATTTC	This work
mscL-anti sense	CTACTGAAGGCGCTTTTGCTCC	This work
mtrA-sense	ATGTCACAGAAAATTCTC	Möker *et al*, 2004
mtrA-anti sense	TAATACGACTCACTATAGGGCGTTTGACGGTGTGTG	Möker *et al*, 2004
mtrAB-sense	CTATAAACTAATCCCAATTAGC	This work
mtrAB-anti sense	CAGAGTGGTCACAGACAG	This work
mtrB-sense	ATGATCCTTTTGGGGC	Möker *et al*, 2004
mtrB-anti sense	TAATACGACTCACTATAGGGGTTCCGATGATGAGCG	Möker *et al*, 2004

Oligonukleotide	Sequence (5'-3')	Reference
ppmA-sense	ATGAGCACCATAGAAGAGC	Möker *et al*, 2004
ppmA-anti sense	CCCGGGTAATACGACTCACTATAGGGCG CAGGGTTCCGATG	Möker *et al*, 2004
RT-sense-1436	CAGTGGAATCAGGCTAGGTAAAG	This work
RT-sense-3449	GTACTTCGTGATGAGCCAC	This work
RT-sense-mscL	CAGCACCTCCTACGATTC	This work
RT-antisense-proP	TTTGAGCGAATCGGGCTC	This work

7.4 Influence of MtrB-stimulants on the autophosphorylation activity of reconstituted (His)$_6$-DcuS

The sensor kinase MtrB has been shown to be stimulated by various osmolytes (section 3.3). It was necessary to analyze, whether these effects are specific for MtrB. For that reason, using identical conditions, the influence of the same osmolytes on the *E. coli* fumarate sensor DcuS in proteoliposomes was investigated.

7.4.1 Determination of the DcuS autokinase activity in presence of various amino acids and compatible solutes

The stimulation profile of the sensor histidine kinase MtrB in proteoliposomes obtained by various amino acids and compatible solutes was investigated in the presence of 20 mM KCl (Fig. 27, section 3.3.4.1). The autophosphorylation activity profile of DcuS using identical conditions after quantification of the autophosphorylation signals using PcBAS version 2.09 is shown in Fig 47.
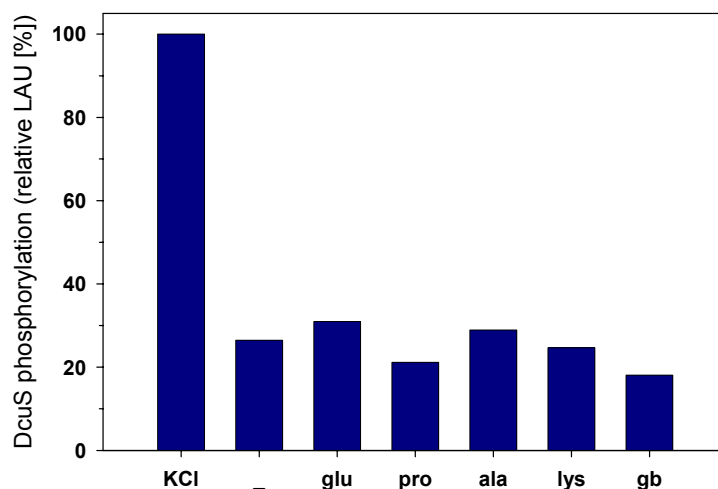
Fig. 47: Influence of various amino acids and compatible solutes on the autophosphorylation activity of reconstituted DcuS. Proteoliposomes enriched with MtrB-Strep were incubated in absence (-) or presence of 300 mM **KCl** and Isine-Cl (**lys**), or 600 mM Na-glutamate (**glu**), proline (**pro**), alanine (**ala**), and glycine betaine (**gb**), respectively. The DcuS autophosphorylation signals (light arbitrary units, LAU) were quantified using PcBAS version 2.09c. The signal intensity in presence of KCl was set 100 %.

7.4.2 Determination of the DcuS autokinase activity in presence of various sugars

The stimulation profile of the sensor histidine kinase MtrB in proteoliposomes obtained by various sugars was investigated in the presence of 20 mM KCl (Fig. 28, section 3.3.4.2). The autophosphorylation activity profile of DcuS using identical conditions is shown in Figure 48.
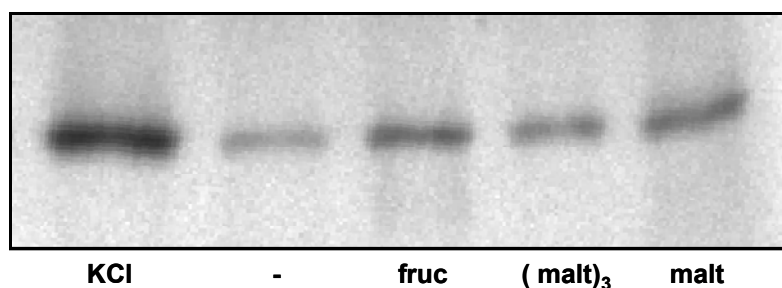
Fig. 48: Influence of various sugars on the autokinase activity of reconstituted DcuS. Autoradiogram after incubation of (His)$_6$-DcuS in the absence (-) or presence of 300 mM **KCl**, or 600 mM, fructose (**fruc**), maltose (**malt**), and maltotriose (**(malt)$_3$**). The reactions were performed in buffer supplemented with 20 mM KCl.

7.4.3 Influence of various solutes on the DcuS autokinase activity in presence or absence of 20 mM KCl

The stimulation profile of the sensor histidine kinase MtrB in proteoliposomes obtained by various amino acids and compatible solutes was investigated in the absence as well as the presence of 20 mM KCl (Fig. 29). The autophosphorylation activity profile of DcuS using identical conditions is shown in Figure 49.
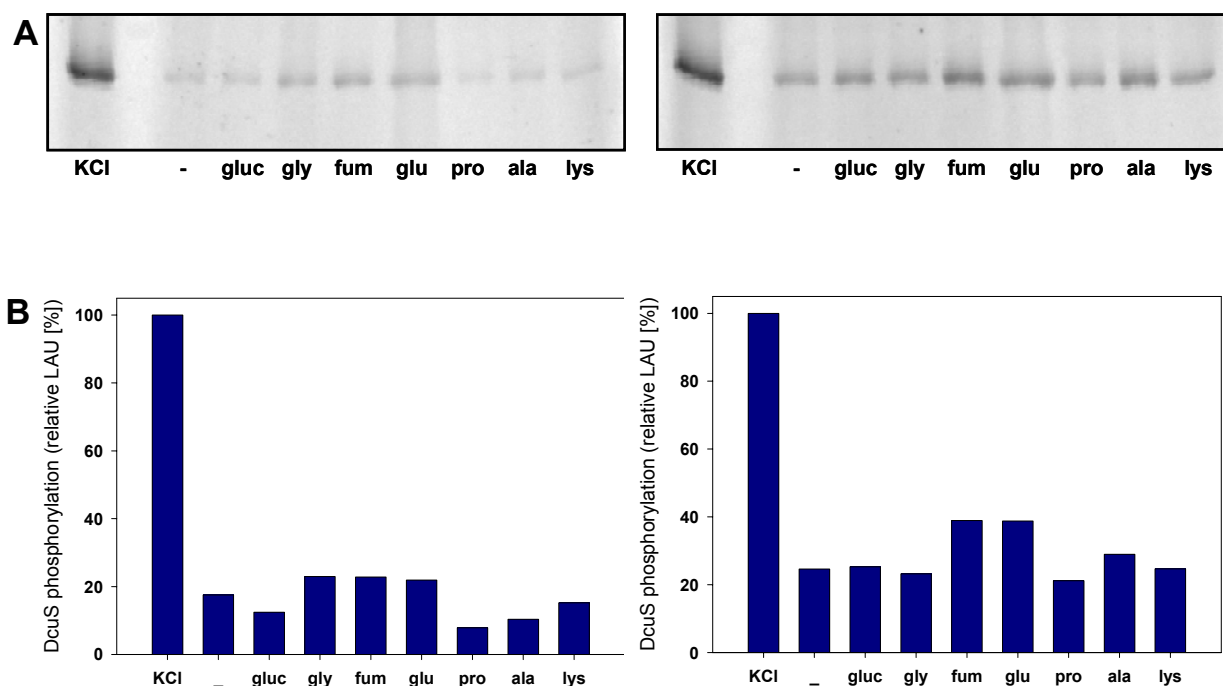
Fig. 49: Influence of various solutes on the autophokinase activity of reconstituted DcuS in presence or absence of 20 mM KCl. A Phosphorylation images after incubation of $(His)_6$-DcuS in the absence (**-**) or presence of 300 mM **KCl**, Na-glutamate (**glu**), and lysine-Cl (**lys**),600 mM glucose (**gluc**), glycerol (**gly**), proline (**pro**), and alanine (**ala**), or 20 mM fumarate (**fum**), respectively. The reactions were performed without (left panel) or with additional 20 mM KCl (right panel). **B** Quantification of the phosphorylation signals corresponding to $(His)_6$-DcuS using PcBAS version 2.09c. The signal intensities in presence of 300 mM KCl were set 100 %.

7.4.4 Analyses of the MtrB autokinase activity in presence of polyethylene glycols (PEGs) with various molecular sizes

The stimulation profile of the sensor histidine kinase MtrB in proteoliposomes obtained by polyethylene glycols (PEGs) of various molecular sizes was investigated in the presence of 20 mM KCl (Fig. 31). The autophosphorylation activity profile of DcuS using identical conditions is shown in Figure 50.
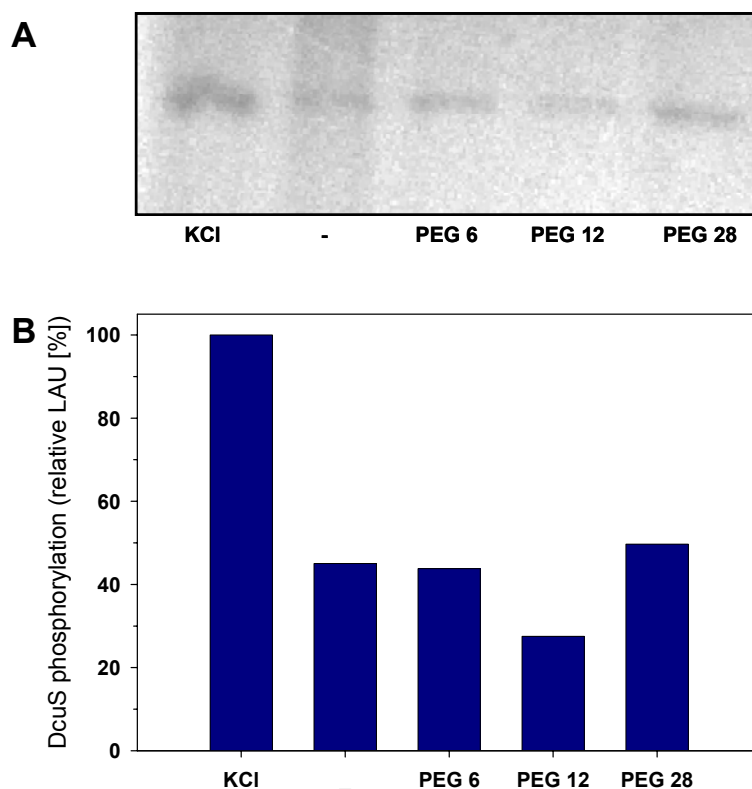
Fig. 50: Influence of polyethylene glycols (PEGs) with various molecular sizes on the autophosphorylation activity of reconstituted DcuS. Proteoliposomes enriched with (His)$_6$-DcuS were incubated in absence (**-**) or presence of 75 mM **KC**l, or 150 mM **PEG 6**, -**12**, and -**28**, respectively. The reactions were performed in buffer supplemented with 20 mM KCl and 20 µM MgCl$_2$. **A** Autoradiogram after SDS-PAGE. **B** Quantification of the signals (light arbitrary units, LAU) corresponding to (His)$_6$-DcuS using PcBAS version 2.09c. The signal intensity in presence of KCl was set 100 %.

Danksagung

Erklärung

Ich versichere, dass ich die von mir vorgelegte Dissertation selbständig angefertigt, die benutzten Quellen und Hilfsmittel vollständig angegeben und die Stellen der Arbeit - einschließlich Tabellen, Karten und Abbildungen -, die anderen Werken im Wortlaut oder dem Sinn nach entnommen sind, in jedem Einzelfall als Entlehnung kenntlich gemacht habe; dass diese Dissertation noch keiner anderen Fakultät oder Universität zur Prüfung vorgelegen hat; dass sie - abgesehen von unten angegebenen Teilpublikationen - noch nicht veröffentlicht worden ist sowie, dass ich eine solche Veröffentlichung vor Abschluss des Promotionsverfahrens nicht vornehmen werde. Die Bestimmungen dieser Promotionsordnung sind mir bekannt. Die von mir vorgelegte Dissertation ist von Prof. Dr. R. Krämer am Institut für Biochemie der Mathematisch-Naturwissenschaftlichen Fakultät der Universität zu Köln betreut worden.

Teilpublikation:

Möker, N., Brocker, M., Schaffer, S., Krämer, R., Morbach, S., and Bott, M. (2004) Deletion of the genes encoding the MtrA-MtrB two-component system of *Corynebacterium glutamicum* has a strong influence on cell morphology, antibiotics susceptibility and expression of genes involved in osmoprotection. *Mol. Microbiol*. **54:** 420-438.

Ich versichere, dass ich alle Angaben wahrheitsgemäß nach bestem Wissen und Gewissen gemacht habe und verpflichte mich, jedmögliche, die obigen Angaben betreffende Veränderung dem Dekanat unverzüglich mitzuteilen.

Datum: Köln, Mai 2006   Unterschrift:

Lebenslauf

Persönliche Angaben:

Name:	Nina Möker
Geburtsdatum, -ort:	17.08.1976, Berlin
Anschrift:	Wissmannstrasse 31, 50823 Köln
Staatsangehörigkeit:	deutsch

Schulbildung:

1983 – 1987	Grundschule Overath
1987 – 1993	Paul-Klee-Gymnasium, Overath
1994 – 1997	Königin-Luise-Schule, Köln Abschluss: Abitur

Auslandsaufenthalt:

1993 – 1994	Cerdon College, Merrylands, NSW, Australien

Hochschulbildung:

1997 – 2002	Studium der Biologie, Universität zu Köln Abschluss: Diplom
2003 – 2006	Promotion als assoziiertes Mitglied der *International Max-Planck Research School* am Institut für Biochemie der Universität zu Köln Arbeitsgruppe Herr Prof. Dr. R. Krämer

Fortbildungen:

Juni – August 1997	Beschäftigung in der Arbeitsgruppe *Potato Genome Analysis*, Max-Planck Institut für Züchtungsforschung, Köln
1999 – 2000	Beschäftigung in der Pressestelle des Westdeutschen Rundfunks, Köln
Juli 2001	Praktikum am Institut für Biologische Informations-verarbeitung 1, Forschungszentrum Jülich